AD NUMBER

AD859806

LIMITATION CHANGES

TO:

Approved for public release; distribution is unlimited.

FROM:

**Distribution authorized to U.S. Gov't. agencies and their contractors;
Administrative/Operational Use; JUN 1959. Other requests shall be referred to Army Aviation Materiel Labs., Fort Eustis, VA.**

AUTHORITY

USAAMRL ltr 18 Jun 1971

AD

USAAVLABS TECHNICAL REPORT 69-8

ISOLATION OF HELICOPTER ROTOR-INDUCED VIBRATIONS USING ACTIVE ELEMENTS

By

P. C. Calcaterra
D. W. Schubert

June 1969

U. S. ARMY AVIATION MATERIEL LABORATORIES
FORT EUSTIS, VIRGINIA

CONTRACT DA 44-177-AMC-472(T)
BARRY CONTROLS DIVISION
BARRY WRIGHT CORPORATION
WATERTOWN, MASSACHUSETTS

170

Disclaimers

The findings in this report are not to be construed as an official Department of the Army position unless so designated by other authorized documents.

When Government drawings, specifications, or other data are used for any purpose other than in connection with a definitely related Government procurement operation, the United States Government thereby incurs no responsibility nor any obligation whatsoever; and the fact that the Government may have formulated, furnished, or in any way supplied the said drawings, specifications, or other data is not to be regarded by implication or otherwise as in any manner licensing the holder or any other person or corporation, or conveying any rights or permission, to manufacture, use, or sell any patented invention that may in any way be related thereto.

Trade names cited in this report do not constitute an official endorsement or approval of the use of such commercial hardware or software.

Disposition Instructions

Destroy this report when no longer needed. Do not return it to the originator.

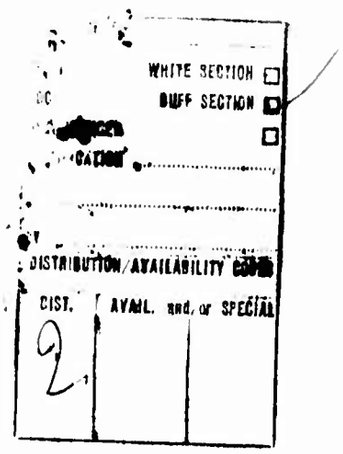

DEPARTMENT OF THE ARMY
HEADQUARTERS US ARMY AVIATION MATERIEL LABORATORIES
FORT EUSTIS, VIRGINIA 23604

This contract was initiated to investigate the feasibility of helicopter rotor isolation using active elements. Feasibility of rotor isolation was investigated for "statistical" single-rotor helicopters ranging in gross weight from 2,000 pounds to 80,000 pounds. An electrohydraulic isolator exhibiting narrow bandwidths of isolation at frequencies corresponding to the blade passage frequency and its second and third harmonics is proposed.

A conceptual design of the isolator installed in the OH-6A Light Observation Helicopter is presented. The proposed system incorporates a hydraulic cylinder interposed between the rotor and the transmission. The rotor shaft is splined and is assumed to have sufficient end play to permit relative vertical displacement between the rotor and fuselage and yet still have the capability of transmitting torque from the fuselage-mounted transmission to the rotor. It should be noted that the rotor shaft and mast are installed in the production OH-6A in such a manner that the mast carries all loads (lifting and bending moments) while the rotor shaft transmits torque to the rotor. The rotor isolator installed in the OH-6A, as conceived by Barry Controls, must assume these mast loads. For this study, however, such loads as mast moments and transverse shear loads are not considered. The isolators were assumed to be loaded in the vertical direction only.

On the basis of these simplifying assumptions, impressive vibration attenuation and displacement control are predicted for a range of helicopters with an associated weight penalty of approximately 4 to 6 percent of helicopter gross weight.

Task 1F125901A13903
Contract DA 44-177-AMC-472(T)
USAAVLABS Technical Report 69-8
June 1969

ISOLATION OF HELICOPTER ROTOR-INDUCED VIBRATIONS USING ACTIVE ELEMENTS

Report No. 128

By

P. C. Calcaterra
D. W. Schubert

Prepared by

Barry Controls Division
Barry Wright Corporation
Watertown, Massachusetts

for

U. S. ARMY AVIATION MATERIEL LABORATORIES
FORT EUSTIS, VIRGINIA

ABSTRACT

Results of an analytical investigation are presented which verify the feasibility of isolating helicopter fuselages from rotor-induced vertical vibratory forces while limiting the relative displacements during transient maneuvers and landing. Electrohydraulic elements are combined to provide better than 90 percent isolation at the critical rotor frequencies. System parameters are selected for single-rotor helicopters ranging in weight from 2,000 to 80,000 pounds. Results of the parametric study show the response of the electrohydraulic notch isolation systems to the various types of dynamic excitations in terms of rotor and fuselage transmitted accelerations, relative displacement between the rotor and fuselage, stability margin, power requirements, and estimated isolation system weight. System performance and requirements are evaluated as a function of helicopter weight, blade passage frequency, number of notches of isolation, stability, changes in fuselage weight and rotor speed, and maximum allowable relative displacement during landing. Recommendations are made regarding experimental verification of system performance, incorporation of approach into practical hardware, and isolation of combined vertical and in-plane rotor-induced vibrations.

FOREWORD

The investigation was conducted by the Barry Controls Division of Barry Wright Corporation of Watertown, Massachusetts, under Contract DA 44-177-AMC-472(T) sponsored by the U. S. Army Aviation Materiel Laboratories (USAAVLABS), Fort Eustis, Virginia. The program was under the technical direction of Mr. Joseph McGarvey, Contracting Officer's Representative.

Barry Controls' personnel were under the technical direction of Mr. Jerome E. Ruzicka. Mr. Peter C. Calcaterra was project engineer, and Mr. Dale W. Schubert was principal investigator. Dr. Frederick D. Ezekiel, of F. D. Ezekiel Company, Lexington, Massachusetts, was consultant in the area of fluid power control. Professor Norman D. Ham of the Aerospace and Aeronautics Department of the Massachusetts Institute of Technology, Cambridge, Massachusetts, was consultant in the area of helicopter dynamics. The task was begun in June 1966 and completed in February 1968.

Acknowledgement is hereby made of the helicopter excitation criterion used in this study and a statistical analysis of existing operational helicopters provided by Kaman Aircraft Division, Kaman Corporation, Bloomfield, Connecticut.

BLANK PAGE

TABLE OF CONTENTS

	Page
ABSTRACT	iii
FOREWORD	v
LIST OF ILLUSTRATIONS	ix
LIST OF TABLES	xiii
LIST OF SYMBOLS	xv
INTRODUCTION	1
SYSTEM ANALYSIS AND DEVELOPMENT	3
REQUIRED ISOLATION SYSTEM CHARACTERISTICS	3
PROPOSED SOLUTION	5
EVALUATION AND PERFORMANCE CRITERIA	7
DEVELOPMENT OF SYSTEM TRANSFER FUNCTIONS	9
Equivalent Integral Displacement Control	9
Wideband Active System Applied to Isolation of Rotor-Induced Forces	12
Ideal Single-Notch Isolator	15
Realizable Single-Notch Isolator	17
Multiple-Notch Isolator	22
System Closed-Loop Transfer Function	24
System Open-Loop Transfer Function	27
TRACKING OF ROTOR SPEED	28
NOTCH BANDWIDTH	29
VIBRATION RESPONSE AT THE NOTCH FREQUENCY	30
FINAL RELATIVE DISPLACEMENT DUE TO MANEUVER LOAD	33
ACTUATOR AREA FOR MINUMUM FLOW	34
FLOW AND POWER REQUIREMENTS	35
SELECTION OF COMPONENTS AND TYPICAL SYSTEM RESPONSE	37
CASE IDENTIFICATION	37
SELECTION OF COMPONENTS	39
Supply Pressure	39
Actuator Characteristics	42
Servovalve Characteristics	42
Transducer Characteristics	45
SELECTION OF FEEDBACK PARAMETERS	45
TYPICAL RESPONSE	51
Open-Loop Response	52
Response to Vibratory Excitations	53
Cruise Vibrations	54
Comparison of Two- and Three-Notch Systems	56
Response of System Designed for Criterion C	56
Ground Vibrations	57
Response to Flight Maneuvers	58
Response to Landing Shock	66

Page

DISCUSSION OF RESULTS 71
STATIC DEFLECTION 71
DYNAMIC RESPONSE 73
Vibratory Excitations 73
In-Flight Maneuvers 107
Landing Shock 120
FLOW AND POWER REQUIREMENTS 130
ISOLATION SYSTEM WEIGHT 134

RELIABILITY, FAIL-SAFE AND CRASH LOAD CONSIDERATIONS . 140
RELIABILITY AND MAINTAINABILITY 140
FAIL-SAFE REQUIREMENTS 141
Hydraulic Power Failure 141
Accelerometer Failure 141
Displacement Transducer Failure 142
Failure of Electronics in Acceleration Loop . . 142
Failure of Electronics in Displacement Loop . . 142
Failure of Electronics in the Frequency Tracking Network 142
Electronic Power Supply Failure 142
Servovalve Failure 143
CRASH LOAD CONSIDERATIONS 143

CONCLUSIONS 144

RECOMMENDATIONS 145

REFERENCES 146

APPENDIX, FREQUENCY TRACKING CIRCUITS 148

DISTRIBUTION 151

LIST OF ILLUSTRATIONS

Figure		Page
1	Relationship Between Levels of Rotor-Induced Forces at b/rev and its Harmonics, Normalized With Respect to the Level at b/rev	3
2	Relationship Between Rotor Speed and Gross Weight for Single-Rotor Helicopters	3
3	Block Diagram of Generalized Electrohydraulic Isolation System	5
4	Conceptual Diagram of Active Isolator Applied to Helicopter Rotor	6
5	Cruise Effectiveness for Fuselage and Rotor for Wideband Electrohydraulic Isolation System	14
6	Transient Relative Displacement for 3 g Maneuver and 10 ft/sec Landing Shock for Wideband Electrohydraulic Isolation System	14
7	Absolute and Relative Transmissibility of Ideal Notch System	16
8	Relationship Between the Maximum Relative Displacement and Bandwidth Ratio for a Unit Step Displacement Excitation of an Ideal Notch Isolation System	17
9	Relationship Between Realizable Notch Bandwidth and Notch Gain Function	19
10	Transmissibility of Realizable Notch	20
11	Relationship Between the Maximum Relative Displacement and the Bandwidth Ratio for a Unit Step Displacement Excitation of a Realizable Notch Isolator	21
12	Schematic Representation of Helicopter Rotor Isolation System	22
13	Block Diagram of Helicopter Rotor Isolation System	23
14	Magnitude and Phase Diagrams of the Open-Loop Transfer Function for 2,000-lb Helicopter, Two-Blade Rotor, Design Criterion A	52

Figure		Page
15	Magnitude and Phase Diagrams of the Open-Loop Transfer Function for 2,000-lb Helicopter, Four-Blade Rotor, Design Criterion A	52
16	Fuselage Effectiveness for 2,000-lb, Two-Blade Helicopter With Three-Notch Isolator During Cruise Vibrations (b/rev = 13.3 Hz)	53
17	Rotor Effectiveness for 2,000-lb, Two-Blade Helicopter With Three-Notch Isolator During Cruise Vibrations (b/rev = 13.3 Hz)	54
18	Fuselage and Rotor Effectiveness for 2,000-lb Helicopter With Three-Notch Isolator During Cruise Vibrations (Design Criterion B).	55
19	Fuselage and Rotor Effectiveness for 2,000-lb, Two-Blade Helicopter With Two-Notch Isolator During Cruise Vibrations for Nominal Helicopter Gross Weight (b/rev = 13.3 Hz)	56
20	Fuselage Effectiveness for 2,000-lb, Two-Blade Helicopter With Three-Notch Isolator During Ground Vibrations (b/rev = 13.3 Hz)	57
21	Rotor Effectiveness for 2,000-lb, Two-Blade Helicopter With Three-Notch Isolator During Ground Vibrations (b/rev = 13.3 Hz)	57
22	Analog Computer Block Diagram for Electrohydraulic System With Three Notches of Isolation	60
23	Typical Fuselage Acceleration Response for 2,000-lb Helicopter With Criterion B Isolation System Design Subjected to +3 g, 0.6 Second Rise-Time Maneuver . .	61
24	Typical Rotor Acceleration Response for 2,000-lb Helicopter With Criterion B Isolation System Design Subjected to +3 g, 0.6 Second Rise-Time Maneuver . .	62
25	Typical Relative Displacement Response for 2,000-lb Helicopter With Criterion B Isolation System Design Subjected to +3 g, 0.6 Second Rise-Time Maneuver . .	63
26	Characteristics of Relative Displacement Between Fuselage and Rotor Due to Transient Maneuver . . .	64

Figure		Page
27	Effect of +3 g Maneuver Load Rise-Time Duration on the Relative Response for 2,000-lb Helicopter With Two-Notch Criterion A Isolation System Design and Nominal Gross Weight	65
28	Typical Fuselage Acceleration Response for 2,000-lb Helicopter With Criterion B Isolation System Design Subjected to 10 ft/sec Landing Velocity Shock . . .	67
29	Typical Rotor Acceleration Response for 2,000-lb Helicopter With Criterion B Isolation System Design Subjected to 10 ft/sec Landing Velocity Shock . . .	68
30	Typical Relative Displacement Response for 2,000-lb Helicopter With Criterion B Isolation System Design Subjected to 10 ft/sec landing Velocity Shock . . .	69
31	Fuselage Acceleration, Rotor Acceleration and Relative Displacement Response for 2,000-lb, Two-Blade Helicopter With Two-Notch Criterion B Isolation System Design and Nominal Gross Weight Subjected to 5 ft/sec Landing Velocity Shock	70
32	Relationship Between Normalized Peak Relative Deflection and Blade Passage Frequency During Steady-State Vibration .	75
33	Relationship Between Notch Bandwidth [Equation (53)] and Blade Passage Frequency for Two- and Three-Notch Isolators Having Parameters Based on Criteria A, B and C .	76
34	Relationship Between Peak Relative Displacement During +3 g, 0.6 Second Maneuver, and Blade Passage Frequency for Two- and Three-Notch Isolators Having System Parameters Based on Criteria A, B and C	114
35	Relationship Between Peak Rotor Acceleration During the 10 ft/sec Landing Velocity Shock and Blade Passage Frequency for Two- and Three-Notch Isolators Having System Parameters Based on Criteria A, B and C . . .	122
36	Relationship Between Peak Fuselage Acceleration During the 10 ft/sec Landing Velocity Shock and Blade Passage Frequency for Two- and Three-Notch Isolators Having System Parameters Based on Criteria A, B and C . . .	123

Figure		Page
37	Relationship Between Instantaneous Peak Flow, Total Helicopter Gross Weight, and Blade Passage Frequency	131
38	Relationship Between Maximum Pump Flow, Helicopter Gross Weight, and Blade Passage Frequency	131
39	Relationship Between Maximum Pump Power, Helicopter Gross Weight, and Blade Passage Frequency	133
40	Conceptual Design For the Incorporation of Electro-hydraulic Isolation System in OH-6A Helicopter . . .	135
41	Relationship Between Estimated Isolation System Weight and Blade Passage Frequency	139
42	Active Electronic Notch Oscillator Circuit	148
43	Active Electronic Notch Oscillator Circuit With Frequency Tracking Element	149

LIST OF TABLES

Table		Page
I	Electrohydraulic Isolation System Design Criteria .	8
II	Variations in Rotor Speed	28
III	Summary of Predominant Excitation Frequencies .	38
IV	Case and Configuration Identification . . .	40
V	Summary of Actuator Characteristics. . . .	43
VI	Summary of Peak Flow Requirements and Servovalve Characteristics	44
VII	Summary of Acceleration Open-Loop Crossover Frequencies	46
VIII	Qualitative Summary of the Effect of Gains on System Response	48
IX	Summary of Servoamplifier Parameters for Two-Notch System	49
X	Summary of Servoamplifier Parameters for Three-Notch System	50
XI	Summary of System Pseudo Static Deflection . .	72
XII	Summary of Fuselage and Rotor Effectivenesses for Cruise Vibrations	77
XIII	Summary of Fuselage and Rotor Effectivenesses for Ground Vibrations	84
XIV	Summary of Fuselage and Rotor Normalized Accelerations for Cruise Vibrations	91
XV	Summary of Fuselage and Rotor Normalized Accelerations for Ground Vibrations	99
XVI	Summary of System Response to + 3g Acceleration, 0.6 sec Rise-Time Maneuver . .	108
XVII	Fuselage and Rotor Accelerations for Transient Conditions	115

Table		Page
XVIII	Summary of System Response to 10 ft/sec Velocity Landing Shock	124
XIX	Summary of Pump Flow and Power Requirements .	132
XX	Isolator Weight for OH-6A	136
XXI	Summary of Estimated Isolation System Weight .	138

LIST OF SYMBOLS

A	average actuator piston area, $in.^2$
A_1	upper actuator piston area, $in.^2$
A_2	lower actuator piston area, $in.^2$
b	number of blades, dimensionless
B_s	undercarriage damping coefficient, $\frac{lb\text{-}sec}{in.}$
C	capacitance, farads
C_a	acceleration flow gain, $\frac{in.^3/sec}{in./sec^2}$
C_d	relative displacement flow gain, $\frac{in.^3/sec}{in.}$
C_{dv}	relative velocity flow gain, $\frac{in.^3/sec}{in./sec}$
C_{id}	integral relative displacement flow gain, $\frac{in.^3/sec}{in.\text{-}sec}$
C_L	leakage coefficient of actuator piston, $\frac{in.^3/sec}{lb/in.^2}$
E	Laplace transform of open-loop command signal, $in.^3$
e_{in}	input voltage, volts
e_{out}	output voltage, volts
F	Laplace transform of rotor-induced force, lb-sec
F_N	sinusoidal rotor-induced force at the notch frequencies, lb
F_o	sustained rotor force, lb
F_1	sinusoidal rotor-induced force at b/rev, lb
f	rotor-induced force, lb
G	notch flow gain$=\frac{1}{\sqrt{3}} \frac{C_a}{A} \omega_n$, dimensionless
G_a	acceleration loop gain, dimensionless

G_c notch compensator transfer function, $\sum_{1}^{N} \frac{(N\omega_n)^2 K_N}{s^2 + (N\omega_n)^2}$, dimensionless

G_L transfer function of compensator for wideband isolator, dimensionless

G_{sv} transfer function of servovalve, $\frac{\omega^2_{sv}}{s^2 + 2\zeta_{sv}\omega_{sv} s + \omega^2_{sv}}$, dimensionless

g represents 385.98 in./sec^2

H open-loop transfer function, dimensionless

HP horsepower

j represents $\sqrt{-1}$

K spring stiffness of passive isolator, lb/in.

K_N gain of N^{th} notch circuit, dimensionless

K_s undercarriage stiffness, lb/in.

k gain of frequency detector, dimensionless

k_1 gain of first notch circuit, dimensionless

k_2 gain of second notch circuit, dimensionless

k_3 gain of third notch circuit, dimensionless

M represents $\frac{M_R}{M_R + M_F}$, dimensionless

M_F fuselage mass, $\frac{\text{lb-sec}^2}{\text{in.}}$

M_R rotor mass, $\frac{\text{lb-sec}^2}{\text{in.}}$

N number of notch circuits

P_1 pressure in upper actuator chamber, lb/in.^{2}

P_2 pressure in lower actuator chamber, lb/in.^{2}

P_d pressure drop across piston, lb/in.^{2}

P_s	supply pressure, lb/in.^{2}
P_v	pressure drop across servovalve land, lb/in.^{2}
Q	Laplace transform of servovalve flow, in.^{3}
$\hat{Q}$	peak flow, in.^{3}/sec
$\bar{Q}$	rectified average flow, gpm
Q_c	Laplace transform of flow command signal, in.^{3}
q	servovalve flow, in.^{3}/sec
R_f	notch circuit feedback resistor, ohms
R_i	notch circuit input resistor, ohms
R_v	notch circuit coupling resistor, ohms
s	Laplace operator, sec^{-1}
T	transmissibility, dimensionless
T_1	time of first peak response, sec
t	time, sec
t_o	rise time of ramp maneuver force, sec
U	Laplace transform of base displacement, in.-sec
u	base displacement, in.
V	actuator chamber volume, in.^{3}
W_F	fuselage weight, lb
W_R	rotor weight, lb
X	Laplace transform of rotor displacement, in.-sec
x	rotor displacement, in.
Y	Laplace transform of fuselage displacement, in.-sec
y	fuselage displacement, in.
α	constant, dimensionless

β	bulk modulus of hydraulic fluid, 200,000 lb/in.^{2}
Δ	Laplace transform of relative displacement between fuselage and rotor, in.-sec
δ	relative displacement between fuselage and rotor, in.
$\hat{\delta}$	peak relative velocity between fuselage and rotor, in./sec
$\delta(\infty)$	final relative displacement between fuselage and rotor due to sustained rotor force, in.
ζ_c	actuator fraction of critical damping, $\frac{1}{2}\frac{C_L}{A}\sqrt{\frac{2\beta MM_F}{V}}$
ζ_s	undercarriage fraction of critical damping, $\frac{1}{2}B_s\sqrt{\frac{1}{K_s(M_R+M_F)}}$
ζ_{sv}	servovalve fraction of critical damping
τ_1	time constant, sec
Ω	bandwidth ratio of ideal notch isolator, dimensionless
$\Omega_{0.5}$	bandwidth ratio of realizable notch isolator, dimensionless
ω	frequency, rad/sec
ω_1, ω_2	notch bandwidth frequencies for ideal notch, rad/sec
ω_b	blade passage frequency, rad/sec
ω_c	actuator natural frequency, $\sqrt{\frac{2\beta A^2}{VMM_F}}$, rad/sec
ω_H	tracking circuit high frequency limit, rad/sec
ω_L	tracking circuit low frequency limit, rad/sec
ω_n	natural frequency of first notch circuit, rad/sec
ω_s	undercarriage natural frequency, $\sqrt{\frac{K_s}{M_R+M_F}}$, rad/sec
ω_{sv}	servovalve natural frequency, rad/sec

INTRODUCTION

The importance of structural dynamics, vibration of the controls, and pilot fatigue in the development and use of rotor-powered aircraft is well recognized. The aerodynamic characteristics of a helicopter rotor in forward flight give rise to shear forces at the hub which are transmitted through the rotor shaft into the fuselage. The magnitude of these forces is a function of the rotor blade angle of attack and the velocity of the air stream entering the rotor plane. The frequency of the forces is a direct function of the rotor speed and number of blades, and generally coincides with frequencies which are particularly critical to the comfort and/or task performance capabilities of passengers and crew, respectively. As a result, helicopters and their crews must endure high levels of rotor-induced vibrations. Some helicopters are vibration limited and must operate at speeds below those they might otherwise achieve (Reference 1).

Considerable strides are being made to better understand the basic mechanism and the nature of rotor-induced forces in an attempt to minimize harmonic force excitations. Research in the area of vibration control, such as utilizing phase relationships between the various sources of rotor loads and introducing higher harmonic pitch control to reduce shaft loads (Reference 1), appears to hold future promise in reducing the level of force transmitted to the fuselage. However, immediate requirements exist to improve the vibration characteristics of helicopters.

Forces acting on the rotor due to blade dynamics are numerous and occur in the in-plane and vertical as well as in the torsional modes (Reference 2). However, the levels of vibratory excitation at the hub perpendicular to the plane of the rotor are generally an order of magnitude greater than those occurring along the plane of the rotor (References 3 and 4). Reduction of the former to acceptable levels would represent a significant step forward in the solution of helicopter vibration problems.

The investigation reported herein deals with the design feasibility of applying active or a combination of active/passive isolation techniques to reduce the vertical vibration transmitted from a helicopter rotor hub to the fuselage. A parametric study of electrohydraulic isolation systems is presented for helicopter weights ranging from 2,000 to 80,000 pounds. Selection of systems' design and parameters is based on analysis and evaluation of: (1) various shock and vibration techniques; (2) dynamic environment characteristics typically encountered during helicopter flight, maneuvers and landing; (3) relative deflections between rotor and fuselage; (4) peak rotor and fuselage transmitted accelerations; and (5) system stability. In the analyses and evaluation of the isolation systems, helicopters are represented by a model consisting of lumped rigid rotor and fuselage masses. The feasibility of providing better than 90 percent isolation of rotor-induced vertical forces at the blade passage frequency and second and third harmonics thereof is demonstrated, while limiting the relative deflection between rotor and fuselage during severe landing and transient maneuvers to levels compatible with helicopter control requirements.

Results are presented in terms of system stability, peak rotor and fuselage transmitted accelerations, maximum relative displacements between rotor and fuselage, flow and power requirements, weight considerations, reliability, and fail-safe criteria. A conceptual design is shown for the incorporation of the isolation system in the OH-6A helicopter. Recommendations are made regarding experimental verification of the analytical results and extension of the techniques to isolate combined vertical and in-plane rotor-induced forces.

SYSTEM ANALYSIS AND DEVELOPMENT

REQUIRED ISOLATION SYSTEM CHARACTERISTICS

Isolation of vertical rotor-induced excitations is extremely difficult due to the conflicting requirements of small displacements across the isolation system under imposed thrust loads and the stiffness values required for effective isolation of low frequency excitations. The vibratory forces have significant magnitudes at only the rotor shaft speed (1/rev) and at the fundamental and harmonics of the blade passage frequency (b/rev, 2b/rev, ---) where b is the number of blades. Moreover, analytical studies and experimental results indicate that the levels of excitation at higher harmonics of the blade passage frequency are small in comparison to b/rev (References 2 and 5). Figure 1 shows a comparison between the vibration levels at 1/rev, b/rev, and higher harmonics normalized with respect to the level at b/rev. The 1/rev vibration is induced by rotor imbalance and can be virtually eliminated by proper tracking of the blades. The b/rev excitation and its harmonics are due to the aerodynamics of existing rotary-wing aircraft and cannot presently be eliminated. Although the nominal rotor speed decreases with increasing helicopter gross weight as shown in Figure 2, larger helicopters utilize rotors having more blades than lighter helicopters. As a result, values of b/rev occur over a relatively narrow frequency range from 10 to 30 Hz regardless of helicopter weight (Reference 5).

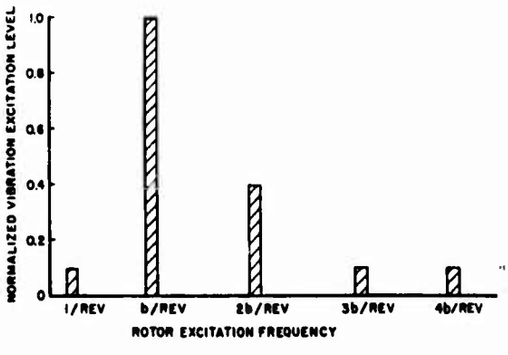

Figure 1. Relationship Between Levels of Rotor-Induced Forces at b/rev and its Harmonics, Normalized With Respect to the Level at b/rev.

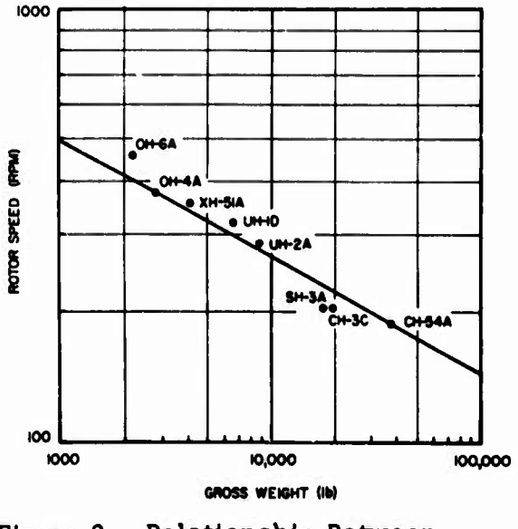

Figure 2. Relationship Between Rotor Speed and Gross Weight for Single-Rotor Helicopters.

A conventional passive isolator placed between the rotor and the fuselage would reduce the vertical vibratory force transmitted to the fuselage. However, due to the dynamics of the rotor-isolator-fuselage system and the low values of frequency associated with the excitation, effective isolation at b/rev would give rise to displacements between the rotor and fuselage which would be incompatible with helicopter control requirements, particularly under transient loads associated with maneuvering and landing. For example, if 70 percent isolation is to be provided at a blade passage frequency of 13.3 Hz, the natural frequency of a conventional isolation system should be approximately 2 Hz. For typical fuselage-to-rotor weight ratios of 8, the static deflection of such a system employing linear passive elements would be in excess of 20 inches. Under transient maneuvers, displacements would be multiples of 20, depending on the number of g's experienced. It is evident that such values of relative displacement are incompatible with helicopter control requirements.

Nonlinearities can be incorporated into the design of conventional passive isolators to limit displacements. However, snubbing would occur during a large portion of the time, particularly during transition flight and maneuvers when the levels of vibration excitation are most severe and sustained accelerations of several g's are experienced. The conventional passive isolation system, when snubbed into its nonlinear region by sustained acceleration transients, would offer a greatly reduced degree of isolation, and could even amplify the level of transmitted acceleration by raising the resonant frequency to values where significant excitation forces exist.

Several approaches have been studied in the past which incorporate various types of active elements in an attempt to provide vibration isolation of low-frequency rotor-induced excitation while limiting the transient relative displacements between the rotor and fuselage. Combinations of a passive stiff spring and force servo in parallel have been investigated (Reference 6), where the servocontrolled force would be tuned to attenuate the vibratory excitations at the blade passage frequency. A system consisting of a stiff spring, in parallel with a negative spring rate achieved by a special linkage, has been analyzed to obtain a low vertical natural frequency; a servomechanism is used to position the base of the stiff spring to maintain a constant vertical distance between the rotor and fuselage (Reference 7). An electropneumatic servocontrolled system utilizing an air cylinder as both the isolating medium and the energy source was investigated in conjunction with the Boeing Vertol 107 helicopter (Reference 8). None of these approaches, however, represent suitable solutions for the isolation of modern high performance helicopters, due primarily to the high levels of transient maneuver loads and the resulting large relative deflections between the fuselage and the rotor.

PROPOSED SOLUTION

In recent years, techniques have been developed to incorporate electro-hydraulic elements in the design of active isolation systems to provide both low frequency vibration isolation and displacement control (References 9 and 10). As shown in Figure 3, electrohydraulic isolation systems are servomechanisms consisting of response sensors, signal processors, and actuators. The sensors provide signals proportional to selected system response variables, and the signal processors modify and combine these signals to create a command signal. Actuators apply forces or induce motions in accordance with the command signals. The selected system response variables and the functions performed within the signal processor will determine the system response.

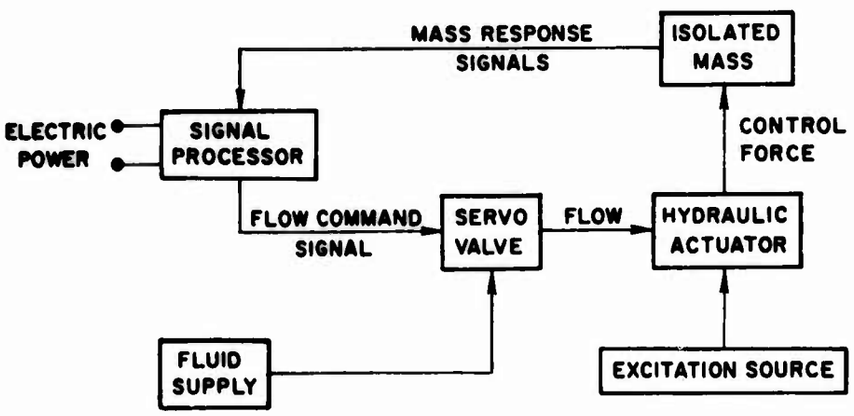

Figure 3. Block Diagram of Generalized Electrohydraulic Isolation System.

A wide variety of excitation and response sensors can be employed to provide feedback signals and form a closed-loop control system. For example, feedback signals can be developed which are functions of any observable response such as jerk, acceleration, velocity, displacement, differential pressure, and force. The signal processor may consist of electronic networks which perform amplification, attenuation, differentiation, integration, addition, multiplication, division and compensation functions. Because of the wide selection of feedback signals, loop gains, and signal processing networks, and the relative incompressibility of the hydraulic fluid, ultra-low frequency isolation can be provided by the electrohydraulic isolation system even during conditions of sustained acceleration, with zero static deflection, high speed of response and extreme flexibility in shaping the overall frequency response characteristics (Reference 11). Selection of system design is dictated by the specific requirements of a given application.

One such electrohydraulic isolation system has been constructed to evaluate the effect of vibration isolation on pilot performance during simulated low-level high-speed flight conditions (Reference 12). For this application the system resonant frequency is 0.45 Hz, and better than 80 percent isolation is provided for all frequencies above 5 Hz. The static deflection of a linear passive system of equivalent isolation performance would be over 4 feet whereas the static deflection of the electrohydraulic system is zero and, by use of nonlinear feedback, deflects only 2.1 inches in response to a 3 g acceleration step having a 0.1-second rise-time. Moreover, vibration isolation is provided during conditions of combined vibratory and 3 g sustained accelerations. The wideband vibration isolation characteristics and displacement control are attained by a combined active/passive isolation system, where active elements provide the desired response at low frequencies and during transient conditions, and the passive element provides isolation at high frequencies above the frequency band over which the active elements are operative. However, as will be shown, even this type of active isolator with nonlinear feedback is not suited to attenuate helicopter rotor-induced vibrations and meet the displacement requirements of less than 0.5 inch.

The highest levels of rotor-induced force excitations occur at the blade passage frequency and its harmonics, as shown in Figure 1. Ideally then, for this type of excitation the desired vibration isolation characteristics and displacement control are obtained by a system exhibiting zero stiffness at the critical excitation frequencies and very high stiffness at other frequencies. These performance characteristics can be approached by employing an electrohydraulic "notch-type" system exhibiting narrow bandwidths of isolation at frequencies corresponding to the blade passage frequency and its second and third harmonics. The proposed system, shown schematically in Figure 4, incorporates a hydraulic cylinder interposed between the rotor and transmission. The rotor shaft is splined and is assumed to have sufficient end play to permit relative vertical displacement between the rotor and fuselage and yet still have the capability of transmitting torque from the fuselage-mounted transmission to the rotor.

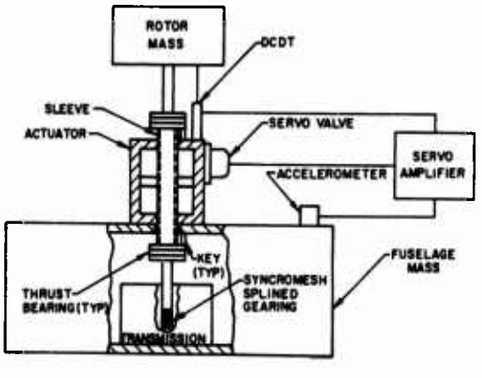

Figure 4. Conceptual Diagram of Active Isolator Applied to Helicopter Rotor.

EVALUATION AND PERFORMANCE CRITERIA

For the feasibility study, the engine, transmission, and fuselage are considered as a single lumped rigid mass. The rotor is also considered as a rigid mass. A ratio of fuselage to rotor mass of eight is assumed in all cases. This report considers single-rotor helicopters only, with the rotor drive shaft assumed to be aligned through the fuselage and rotor centers of gravity. In-plane rotor excitations and isolation from same are excluded for this study. On the basis of these simplifying assumptions, the results of the feasibility study demonstrate whether or not an isolation system could be designed to provide vibration protection from the more severe vertical rotor-induced forces, while limiting the relative displacements between rotor and fuselage to acceptable levels.

Two types of steady-state vibratory excitations are considered:

Cruise: Vertical sinusoidal forces applied to the rotor at shaft speed; blade passage frequency; and the 2nd, 3rd, and 4th harmonics of blade passage frequency. The relative magnitude of the excitations is shown in Figure 1.

Ground: Vertical sinusoidal forces applied to the rotor (as in the cruise condition) with the landing gear resting on the ground. Landing gears are assumed to have a stiffness to yield a natural frequency of 3 Hz, based on helicopter gross weight.

Two types of transient excitations are considered:

Maneuver: + 3.0 g and -0.5 g ramp accelerations with a rise-time of 0.6 second. Supplemental cases are investigated for ramp rise-times of 0.8 and 1.0 second to illustrate the effect of ramp rise-time.

Landing: Vertical velocity shocks of 5 and 10 ft/sec are investigated, where the representative value of landing gear natural frequency based on helicopter gross weight and undercarriage stiffness is considered to be 3 Hz.

The limiting design criterion for the study (established in the contract) was that the maximum relative displacement between rotor and fuselage under any excitation conditions must not exceed 0.5 inch. Although from the control point of view, this displacement may be considered excessive and impractical, the maximum values anticipated are expected to occur during the most severe landing conditions. For the steady-state flight condition as well as for the 3 g and - 0.5 g maneuvers, the relative displacement is to be kept to a minimum, well within the 0.5-inch value anticipated for landing. In all cases, of course, the design goal is to provide vibration isolation approaching 100 percent at the critical frequencies.

The vibration isolation performance of the system is evaluated in terms of fuselage (or rotor) effectiveness, where effectiveness is defined as the ratio or response for the unisolated rotor system to that for the isolated system. In each instance the response ratio is for the vertical acceleration at the same point in the aircraft. Vibratory forces are generated at the rotor hub due to blade dynamics and to the overall aerodynamic forces required to achieve the desired lift, forward speed, and maneuverability. If the same flight requirements are to be met, the level of these forces must be the same whether the rotor is isolated or not. However, the accelerations experienced by the rotor and fuselage would be different for the isolated and unisolated cases. Therefore, the evaluation of any isolation system applicable to helicopter fuselage protection from rotor-induced forces should be based on a comparison of accelerations transmitted to the fuselage (and experienced by the rotor) for the isolated and unisolated rotors. Effectiveness is selected since it directly compares the isolated system with an otherwise identical helicopter not having an isolation system. Effectiveness values greater than 1.0 indicate that isolation is provided, whereas values less than 1.0 indicate amplification.

Six configurations of the electrohydraulic "notch-type" isolator exhibiting narrow bandwidths of isolation at discrete frequencies are evaluated. These are two- and three-notch systems designed to the criteria shown in Table I.

TABLE I

ELECTROHYDRAULIC ISOLATION SYSTEM DESIGN CRITERIA

Criterion	Maximum Relative Displacement (inches)	Stability Gain Margin (db)	Minimum Effectiveness at 1/rev
A	0.5	20	0.7
B	0.2	20	0.7
C	0.2	> 20	0.7

Design Criterion A is based on the required maximum displacement specification. Design Criteria B and C were selected in an attempt to increase the displacement control capabilities of the active isolator. Systems based on different maximum relative displacement criteria are compared and evaluated based on their frequency response and stability. Finally, consideration is given to changes in performance with variations in rotor speed and fuselage weight, and to power, weight, fail-safe, and maintainability requirements.

DEVELOPMENT OF SYSTEM TRANSFER FUNCTIONS

In order to present the development of the final system design, the following analyses show: (1) the displacement control capabilities of the selected feedback mechanisms under sustained forces; (2) the inability of wideband active systems to provide both the required transient displacement control and vibration isolation; (3) the characteristics of single-notch systems, both ideal and realizable; and (4) the open- and closed-loop transfer functions of the selected multiple-notch system.

Equivalent Integral Displacement Control

Consider rigid rotor and fuselage masses connected by a hydraulic actuator. Let the flow command signal to the servovalve be the sum of signals proportional to the acceleration of the fuselage $\ddot{y}(t)$ and the relative displacement between the fuselage and the rotor $\delta(t) = y(t) - x(t)$, where $x(t)$ is the rotor displacement. Neglecting for the moment the frequency response of the servovlave and the compressibility of the hydraulic fluid, the flow from the servovalve $q(t)$ in terms of the feedback signals and associated gains is given by

$$q(t) = -\left[C_a \ddot{y}(t) + C_d \delta(t)\right] \tag{1}$$

where the minus sign denotes negative feedback. Symbols are defined in the nomenclature.

The actuator, in response to the flow delivered from the servovalve, displaces the fuselage relative to the rotor with a relative velocity $\dot{\delta}(t)$ which is expressed in terms of the average area A by

$$\dot{\delta}(t) = \frac{q(t)}{A} \tag{2}$$

The rotor-induced force $f(t)$ accelerates both the rotor mass M_R and the fuselage mass M_F ; therefore,

$$f(t) = M_R \ddot{x}(t) + M_F \ddot{y}(t) \tag{3}$$

Using Laplace operator notation, the relative displacement between rotor and fuselage $\Delta(s)$ due to rotor-induced force $F(s)$ can be obtained from Equations (1), (2), and (3), rearranging terms, and letting $M = M_R/(M_R + M_F)$:

$$\Delta(s) = -\left[\frac{\frac{C_a}{A}}{\frac{C_a}{A} M s^2 + s + \frac{C_d}{A}}\right] \frac{F(s)}{M_R + M_F} \tag{4}$$

The final displacement of the system $\delta(\infty)$ due to a constant force F_o applied at the rotor is obtained by applying the final value theorem to Equation (4) (Reference 13, p. 91).

$$\begin{aligned}
\delta(\infty) &= \lim_{t\to\infty} \delta(t) \\
&= \lim_{s\to 0} s\, F(s) \\
&= \lim_{s\to 0} s \left[-\frac{\frac{C_a}{A}}{\frac{C_a}{A} M s^2 + s + \frac{C_d}{A}}\right] \frac{1}{s} \frac{F_o}{M_R + M_F} \qquad (5) \\
&= -\frac{C_a}{C_d} \frac{F_o}{M_R + M_F}
\end{aligned}$$

Examination of Equation (5) indicates that the relative displacement due to a constant force at the rotor can be made to approach zero if either (a) the denominator goes to infinity, or (b) the numerator approaches zero as s approaches zero.

(a) The denominator in Equation (5) can be made to approach infinity if integral relative displacement feedback is added to the control system by means of an active integrating network operating on the displacement signal. Replacing $C_d \delta(t)$ in Equation (1) by $C_d \delta(t) + C_{id} \int \delta(t) dt$, and solving for the relative displacement due to rotor force $F(t)$ expressed in Laplace operator notation, results in

$$\Delta(s) = -\left[\frac{\frac{C_a}{A}}{\frac{C_a}{A} M s^2 + s + \frac{C_d}{A} + \frac{C_{id}}{A s}}\right] \frac{F(s)}{M_R + M_F} \tag{6}$$

Applying the final value theorem to Equation (6), the final displacement $\delta(\infty)$ due to a step in force F_o is given by

$$\delta(\infty) = \lim_{s\to 0} s \left[- \frac{\frac{C_a}{A}}{\frac{C_a}{A} M s^2 + s + \frac{C_d}{A} + \frac{C_{id}}{As}} \right] \frac{1}{s} \frac{F_o}{M_R + M_F}$$

$$= 0 \qquad (7)$$

which indicates that the addition of integral displacement control results in a zero relative displacement for a constant force excitation.

(b) The numerator in Equation (5) can be made to go to zero at low frequencies ($s = j\omega \to 0$) by incorporating a lead network of time constant τ_1 in series with the acceleration feedback signal. A lead network of transfer function $\frac{\tau_1 s}{1+\tau_1 s}$ has unity gain at high frequencies and zero at low frequencies. Replacing C_a in Equation (1) by $C_a \frac{\tau_1 s}{1+\tau_1 s}$, and solving for the relative displacement,

$$\Delta(s) = - \left[\frac{\frac{C_a}{A}\left(\frac{\tau_1 s}{1+\tau_1 s}\right)}{\frac{C_a}{A} M s^2 \left(\frac{\tau_1 s}{1+\tau_1 s}\right) + s + \frac{C_d}{A}} \right] \frac{F(s)}{M_R + M_F} \qquad (8)$$

Applying once again the final value theorem for a step in rotor force F_o,

$$\delta(\infty) = \lim_{s\to 0} s \left[- \frac{\frac{C_a}{A}\left(\frac{\tau_1 s}{1+\tau_1 s}\right)}{\frac{C_a}{A} M s^2 \left(\frac{\tau_1 s}{1+\tau_1 s}\right) + s + \frac{C_d}{A}} \right] \frac{1}{s} \frac{F_o}{M_R + M_F}$$

$$= 0 \qquad (9)$$

Equation (9) indicates that introduction of a simple passive lead network in series with the acceleration feedback signal effectively results in integral displacement control. The static deflection of such a system is the displacement due to a force of magnitude $F_o / M_R + M_F) = 1g$. From Equation (9) the static deflection for this system is zero.

Wideband Active System Applied to Isolation of Rotor-Induced Forces

Consider an electrohydraulic system similar to the one developed in Reference 12 for low-level high-speed aircraft, consisting of an actuator interposed between the rotor and fuselage masses and servovalve, with relative displacement feedback, fuselage acceleration feedback modified by a lead network, and relative velocity feedback. The velocity signal is generated within the servoamplifier by differentiating the displacement signal. Therefore, the flow from the servovalve $Q(s)$ in terms of the servovalve transfer function $G_{sv}(s)$, the transfer function of the compensator required for system stability $G_L(s)$, the various feedback signals, and associated gains is given by

$$Q(s) = -G_{sv}(s)G_L(s)\left[s^2 C_a \left(\frac{\tau_1 s}{1+\tau_1 s}\right) Y(s) + C_{dv}\, s\, \Delta(s) + C_d\, \Delta(s)\right] \qquad (10)$$

The flow delivered to the actuator must equal the flow displaced by the moving piston within the actuator, plus the flow used to compress the hydraulic fluid and the flow that leaks between the piston and the actuator walls.

$$Q(s) = A\, s\, \Delta(s) - \frac{V}{2\beta}\, s\, P_d(s) - C_L\, P_d(s) \qquad (11)$$

The acceleration of the rotor $s^2 X(s)$ is described in terms of the actuator force and the excitation force by

$$M_R\, s^2 X(s) = F(s) + A\, P_d(s) \qquad (12)$$

Similarly, the fuselage acceleration $s^2 Y(s)$ is related to the actuator force by

$$M_F\, s^2\, Y(s) = -A\, P_d(s) \qquad (13)$$

The various transfer functions relating the rotor and fuselage accelerations and the relative displacement between rotor and fuselage to the rotor-induced force are obtained by combining Equations (10) through (13) and are given on the next page.

$$s^2 Y(s) = \left[\frac{s + \left(\frac{C_{dv}}{A} s + \frac{C_d}{A} \right) G_L(s)\, G_{sv}(s)}{M \frac{C_a}{A} s^2 G_L(s)\, G_{sv}(s) \left(\frac{\tau_1 s}{1+\tau_1 s} \right) + s + \left(\frac{C_{dv}}{A} s + \frac{C_d}{A} \right) G_L(s) G_{sv}(s) + \frac{s^3}{\omega_c^2} + \frac{2\zeta_c}{\omega_c} s^2} \right] \frac{F(s)}{M_R + M_F} \qquad (14)$$

$$s^2 X(s) = \left[\frac{\frac{C_a}{A} s^2 G_L(s) G_{sv}(s) \left(\frac{\tau_1 s}{1+\tau_1 s} \right) + s + \left(\frac{C_{dv}}{A} s + \frac{C_d}{A} \right) G_L(s) G_{sv}(s) + \frac{1}{M} \left(\frac{s^3}{\omega_c^2} + \frac{2\zeta_c}{\omega_c} s^2 \right)}{M \frac{C_a}{A} s^2 G_L(s) G_{sv}(s) \left(\frac{\tau_1 s}{1+\tau_1 s} \right) + s + \left(\frac{C_{dv}}{A} s + \frac{C_d}{A} \right) G_L(s)\, G_{sv}(s) + \frac{s^3}{\omega_c^2} + \frac{2\zeta_c}{\omega_c} s^2} \right] \frac{F(s)}{M_R + M_F} \qquad (15)$$

$$\Delta(s) = -\left[\frac{\frac{C_a}{A} s^2 G_L(s) G_{sv}(s) \left(\frac{\tau_1 s}{1+\tau_1 s} \right) + \frac{1}{M} \left(\frac{s}{\omega_c^2} + \frac{2\zeta_c}{\omega_c} \right)}{M \frac{C_a}{A} s^2 G_L(s) G_{sv}(s) \left(\frac{\tau_1 s}{1+\tau_1 s} \right) + s + \left(\frac{C_{dv}}{A} s + \frac{C_d}{A} \right) G_L(s) G_{sv}(s) + \frac{s^3}{\omega_c^2} + \frac{2\zeta_c}{\omega_c} s^2} \right] \frac{F(s)}{M_R + M_F} \qquad (16)$$

Figure 5 shows the fuselage and rotor effectiveness for a 2,000-pound, 4-blade helicopter. The parameters of the isolation system were adjusted to obtain a 10-db gain margin and a peak relative displacement of 0.5 inch during 3 g maneuvers. The system provides a peak fuselage effectiveness of only 7. At the blade passage frequency (26.6 Hz), the fuselage effectiveness is approximately 4.5.

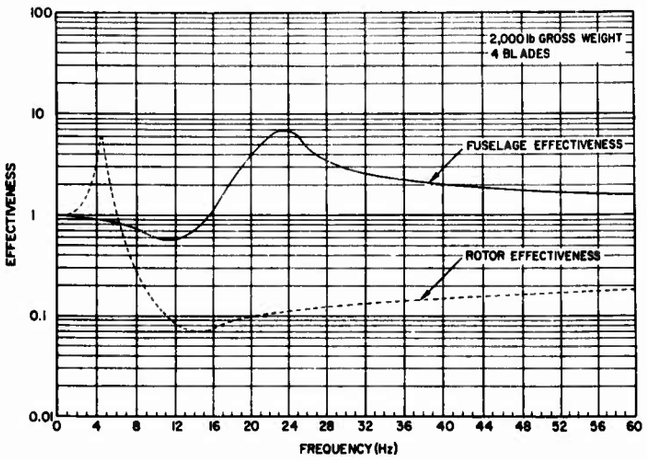

Figure 5. Cruise Effectiveness for Fuselage and Rotor for Wideband Electrohydraulic Isolation System.

Figure 6 shows the displacements during the +3 g, 0.6 sec rise-time maneuver and the 10 ft/sec landing shock. The peak relative displacement during the landing shock condition exceeds the required 0.5-inch value by a factor of six.

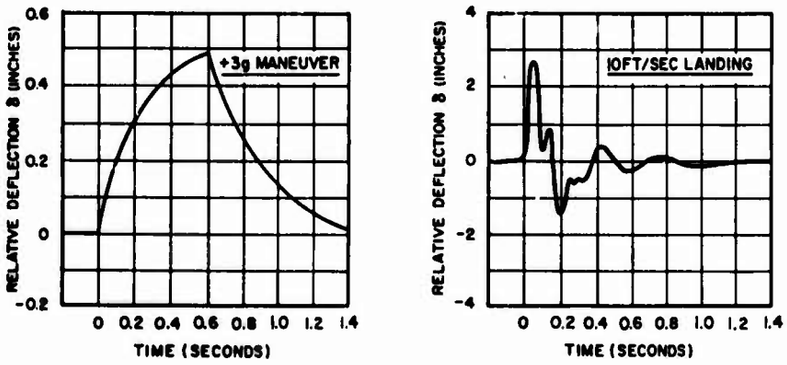

Figure 6. Transient Relative Displacement for 3 g Maneuver and 10 ft/sec Landing Shock for Wideband Electrohydraulic Isolation System.

It is possible, therefore, to utilize a broadband active isolator to provide isolation of the fuselage and adhere to the relative displacement criterion for the 3 g maneuver, at least for the case where the blade passage frequency is very high (26.6 Hz). However, even for this case (which of all those considered gives rise to the smallest displacement), the displacement during the landing velocity shock greatly exceeds the maximum allowable values.

Other wideband active systems were also considered during the feasibility study. Essentially, they consisted of basic electrohydraulic isolators using different compensation methods in order to obtain a larger margin of stability and improve the high frequency isolation performance. Systems using dynamic differential pressure feedback in place of acceleration feedback were evaluated in an attempt to eliminate the effect of the actuator resonance on the system gain margin. An electrohydraulic isolation system having both acceleration and relative displacement feedback and a mechanical spring in series with the actuator was analyzed. Such an arrangement provided both a stable closed-loop system and greatly improved high frequency isolation performance. Combined hydraulic and pneumatic components were also evaluated. For these systems the hydraulic fluid in the actuator was backed up by a compressed gas to give an effective low bulk modulus of the hydraulic fluid. The resulting performance is equivalent to the one discussed above using the spring in series with the actuator. However, none of these wideband vibration isolation systems could be designed using linear gains to provide the required vibration isolation and at the same time limit the peak transient relative displacements during maneuvers and landing shocks to less than 0.5 inch.

Consideration was given to the application of nonlinear feedback methods to result in wideband isolation of the rotor force during vibratory conditions and limit the peak relative displacements during transient excitations to within 0.5 inch. The system nonlinearities would effectively limit the peak transient displacements. However, vibration isolation would be greatly reduced whenever the system operates in its nonlinear region due to maneuver loads. The vibratory forces acting upon the rotor would become more severe during the transient maneuver conditions. Therefore, a loss of isolation under these conditions would be undesirable. Results of the analysis indicated that the design requirements could not be met by wideband linear or nonlinear active isolation systems.

Ideal Single-Notch Isolator

Wideband isolation systems offer vibration reduction at all frequencies above some minimum value. However, the vibratory excitations from the rotor hub occur only at discrete frequencies (Figure 1). Therefore, in order to verify the suitability of providing isolation at these discrete frequencies, a simplified analysis was conducted to define the deflections resulting from a step displacement excitation employing a system which would provide 100 percent vibration isolation at a discrete frequency only. The relative displacements due to a step are greater than the displacements due to any other type of transient excitations. Therefore, the simplified analysis is conservative when used to evaluate the suitability of isolation systems for the dynamic excitation of this study.

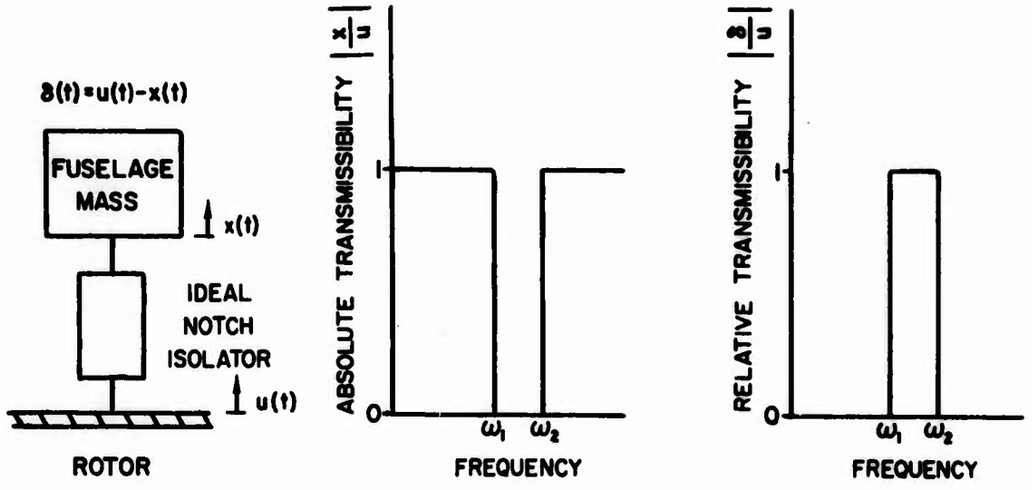

Figure 7. Absolute and Relative Transmissibility of Ideal Notch System.

Consider an ideal notch isolator having the postulated frequency response shown in Figure 7. Complete isolation of the excitation is provided in the frequency range ω_1 to ω_2 with no isolation at all other frequencies. As indicated, relative isolator motion can occur only at frequencies between ω_1 and ω_2. The relative displacement response may be obtained from the use of the Fourier Sine Transformation (Reference 14). In the frequency region between ω_1 and ω_2, the isolator has infinite compliance; thus the resulting relative displacement $\delta(t)$ is equal to the time and frequency summation of the input excitation over the time interval $0 < t < \infty$ and over the frequency bandwidth of the isolation system $\omega_1 < \omega < \omega_2$:

$$\delta(t) = \frac{2}{\pi} \int_{\omega_1}^{\omega_2} \sin \omega t \int_0^{\infty} u(\tau) \sin \omega \tau \, d\tau \, d\omega \tag{17}$$

The solution of Equation (17) has the form of the difference of two Si (integral sine) functions and is given by

$$\delta(t) = \frac{2}{\pi} \left[Si(\omega_2 t) - Si(\omega_1 t) \right] \tag{18}$$

Assume that the maximum relative displacement occurs at the first peak of the response. Solving for the time at which the first peak occurs, $T_1 = \frac{\pi}{\omega_1 + \omega_2}$, and defining the notch bandwidth ratio $\Omega = \frac{\omega_2}{\omega_1}$, the maximum relative displacement $\delta(T_1)$ can be obtained by evaluating Equation (17) at $t = T_1$:

$$\delta(T_1) = \frac{2}{\pi}\left[Si\left(\frac{\pi\Omega}{\Omega+1}\right) - Si\left(\frac{\pi}{\Omega+1}\right)\right] \qquad (19)$$

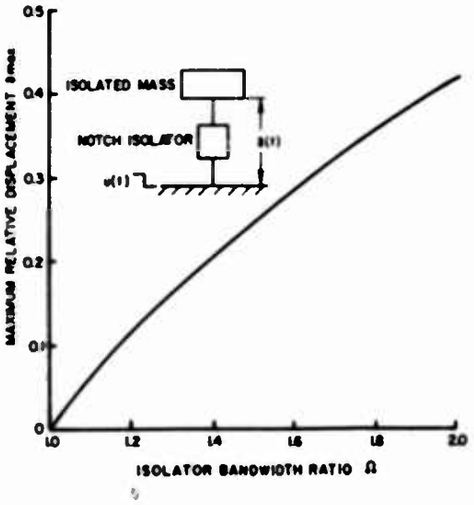

Figure 8. Relationship Between the Maximum Relative Displacement and Bandwidth Ratio for a Unit Step Displacement Excitation of an Ideal Notch Isolation System.

Figure 8 shows the maximum relative displacement excitation as a function of notch bandwidth ratio $\Omega = \frac{\omega_2}{\omega_1}$. A wide-band isolator subjected to the same transient excitation will have a maximum relative displacement of unity. Recalling that the vibratory force excitations induced by the rotor occur only at discrete frequencies, the notch bandwidth required to isolate any one of the rotor-induced forces can be very small. Letting $\Omega = 1.05$, the maximum relative deflection to a unit step displacement excitation will be only 0.03 or 97 percent less than for a wideband isolator. Clearly then, it is seen that if the relative displacement criterion is to be satisfied with a linear system, a narrow-band isolator must be used.

Realizable Single-Notch Isolator

The wideband electrohydraulic vibration isolation system previously discussed can be modified to provide a physically realizable notch isolator. For simplicity, the system configuration is chosen to be a rigid mass connected by an electrohydraulic isolator to a moving foundation similar to that shown in Figure 7. Considering only acceleration feedback, and assuming the fluid to be incompressible, expressions for servovalve flow in terms of the actuator motion, the feedback signal, and the notch compensator $G_c(s)$ can be derived following the analysis shown for the ideal notch isolator. Flow equations are given by

$$Q(s) = A\,s\,\Delta(s) \qquad (20)$$

and

$$Q(s) = -C_a G_c(s)\, s^2\, Y(s) \tag{21}$$

Letting $\delta = y - u$, the transfer functions relating the absolute y and relative δ motions of the isolated mass to the base excitation u can be obtained from Equations (20) and (21), and are given by

$$\frac{Y(s)}{U(s)} = \frac{1}{\frac{C_a}{A} G_c(s)\, s + 1} \tag{22}$$

and

$$\frac{\Delta(s)}{U(s)} = -\frac{\frac{C_a}{A} G_c(s)\, s}{\frac{C_a}{A} G_c(s)\, s + 1} \tag{23}$$

In order to generate the ideal response shown in Figure 7, the electrohydraulic isolation system requires a compensator $G_c(s)$ having infinite gain between ω_1 and ω_2 and zero gain at all other frequencies. Such a system is unrealistic since the construction of a filter having gain only between two discrete frequencies requires an infinite time delay. However, the gain requirement can be approximated by a second-order undamped oscillator network of resonant frequency ω_n having large gain at ω_n and low gain at all other frequencies. The transfer function for such a compensator is given by

$$G_c(s) = \frac{\omega_n^2}{s^2 + \omega_n^2} \tag{24}$$

Substituting Equation (21) in Equations (22) and (23),

$$\frac{Y(s)}{U(s)} = \frac{s^2 + \omega_n^2}{s^2 + \frac{C_a}{A} \omega_n^2 s + \omega_n^2} \tag{25}$$

and

$$\frac{\Delta(s)}{U(s)} = -\frac{\frac{C_a}{A} \omega_n^2 s}{s^2 + \frac{C_a}{A} \omega_n^2 s + \omega_n^2} \tag{26}$$

From Equation (25), the absolute transmissibility $T = \left|\frac{y(j\omega)}{u(j\omega)}\right|$ is given by

$$T = \sqrt{\frac{\left(\omega_n^2 - \omega^2\right)^2}{\left(\omega_n^2 - \omega^2\right)^2 + \left(\frac{C_a}{A}\omega_n^2\,\omega\right)^2}} \qquad (27)$$

The bandwidth for the realizable notch $\Omega_{0.5}$ is defined as the ratio of the two frequencies at which 50 percent isolation is attained. One of the frequencies will be higher than ω_n ; the second one will be lower. Solving Equation (27) for these frequencies with $T = 0.5$, and letting the flow gain term $G = \frac{1}{\sqrt{3}} \frac{C_a}{A} \omega_n$,

$$\Omega_{0.5} = \sqrt{\frac{2 + G^2 + G\sqrt{4 + G^2}}{2 + G^2 - G\sqrt{4 + G^2}}} \qquad (28)$$

Equation (28) is plotted on Figure 9.

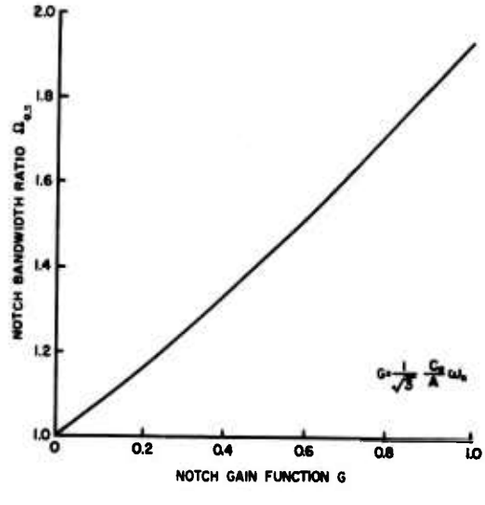

Figure 9. Relationship Between Realizable Notch Bandwidth and Notch Gain Function.

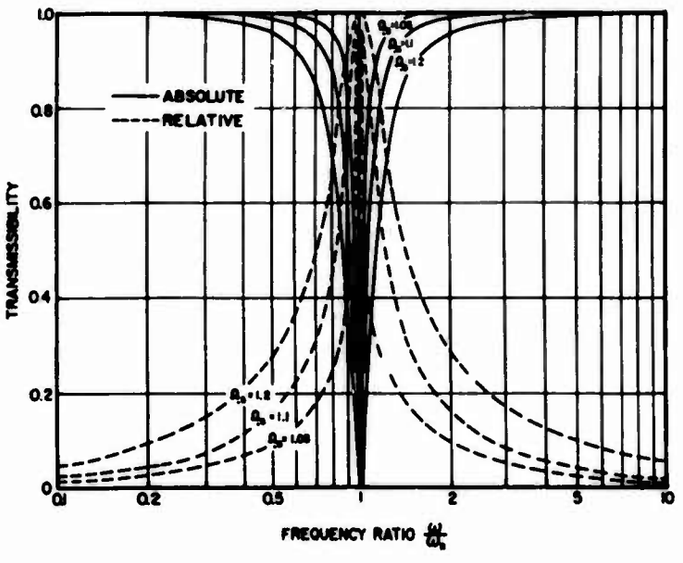

Figure 10 shows the absolute and relative transmissibilities of the isolation system for sinusoidal base motions as a function of frequency for three values of the bandwidth ratio. Values were calculated using Equations (26), (27), and (28). Figure 10 indicates that the electrohydraulic system offers complete isolation of sinusoidal excitations at the notch frequency and little isolation for frequencies outside the bandwidth.

Figure 10. Transmissibility of Realizable Notch.

The relative displacement time function $\delta(t)$ for a unit displacement step at the base can be obtained from Equation (26) and is given by

$$\delta(t) = \frac{\frac{C_a}{A}\omega_n}{\sqrt{1-\frac{1}{4}\left(\frac{C_a}{A}\omega_n\right)^2}}\, e^{-\left(\frac{1}{2}\frac{C_a}{A}\omega_n t\right)} \sin\sqrt{1-\frac{1}{4}\left(\frac{C_a}{A}\omega_n\right)^2}\;\omega_n t \qquad (29)$$

Again, assuming that the maximum relative displacement occurs at the first peak, solving for the time T_1 at which it occurs from Equation (29), and evaluating $\delta(t)$ at $t = T_1$, gives the following expression for the maximum relative displacement:

$$\delta(T_1) = \frac{C_a}{A}\omega_n\, e^{-\frac{1}{2}\frac{C_a}{A}\omega_n\left[\frac{\varphi+\frac{\pi}{2}}{\sqrt{1-\frac{1}{4}\left(\frac{C_a}{A}\omega_n\right)^2}}\right]} \qquad (30)$$

where

$$\varphi = \tan^{-1}\left[\frac{-.5\frac{C_a}{A}\omega_n}{\sqrt{1-\frac{1}{4}\left(\frac{C_a}{A}\omega_n\right)^2}}\right] \tag{31}$$

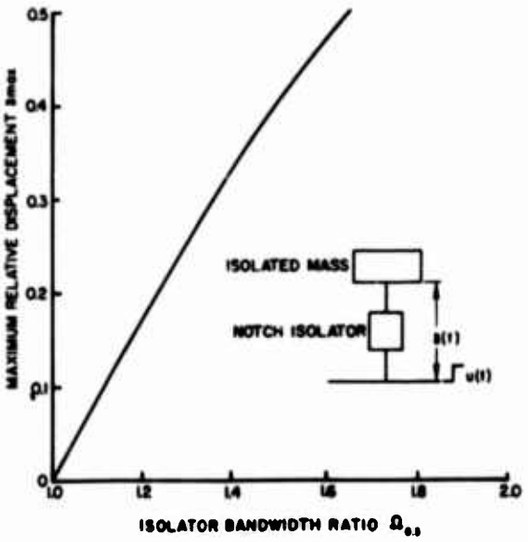

Figure 11. Relationship Between the Maximum Relative Displacement and the Bandwidth Ratio for a Unit Step Displacement Excitation of a Realizable Notch Isolator.

Figure 11 shows the maximum relative displacement resulting from a unit displacement step as a function of the bandwidth ratio $\Omega_{0.5}$. Examination of this figure indicates that for a small bandwidth, the resulting relative displacements are much smaller than would result using a linear wideband isolator. However, the deflections for the realizable notch isolator are about twice as large as those that resulted from the ideal notch isolator of equivalent bandwidths, shown in Figure 8. This is because the realizable filter has finite gain at all frequencies.

The simplified analysis shown above has resulted in the design of an isolation system which yields very small transient relative displacements and at the same time provides a form of vibration isolation suitable for the reduction of helicopter rotor-induced forces.

Multiple-Notch Isolator

Figure 12 shows a schematic representation of the helicopter rotor multiple-notch isolation system including landing gear characteristics. The block diagram shown in Figure 13 indicates that the selected design incorporates notch filters in the fuselage acceleration feedback loop. In order to calculate the response of the system to vibratory and transient excitations, and to define the system stability, it is necessary to derive the closed- and open-loop transfer functions.

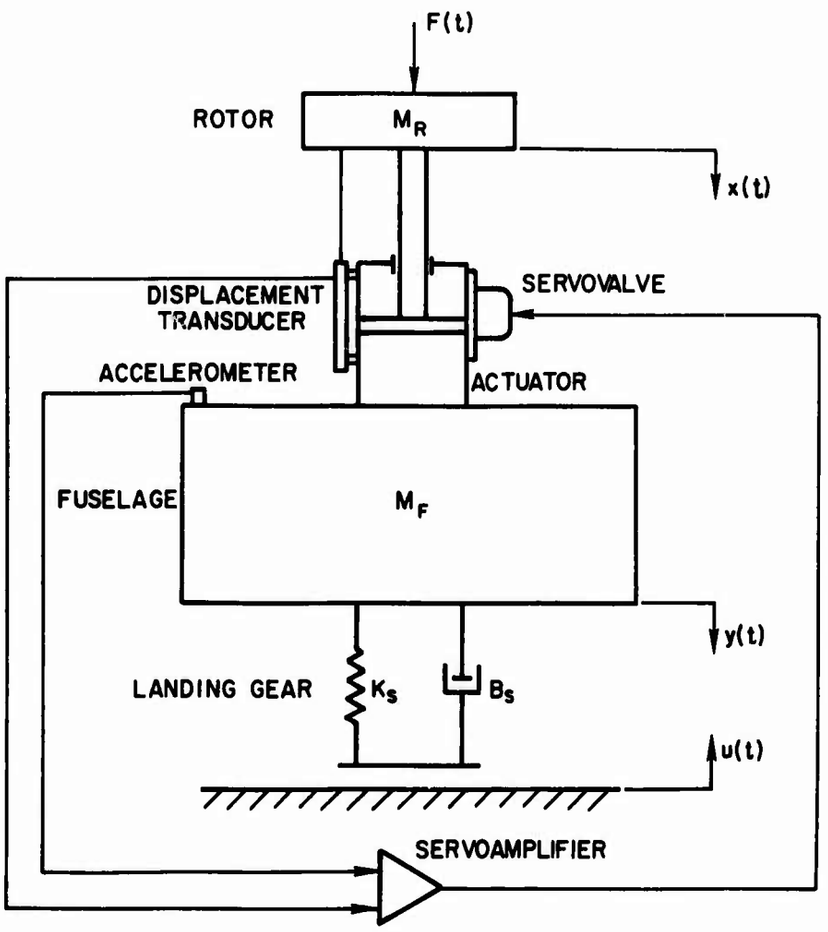

Figure 12. Schematic Representation of Helicopter Rotor Isolation System.

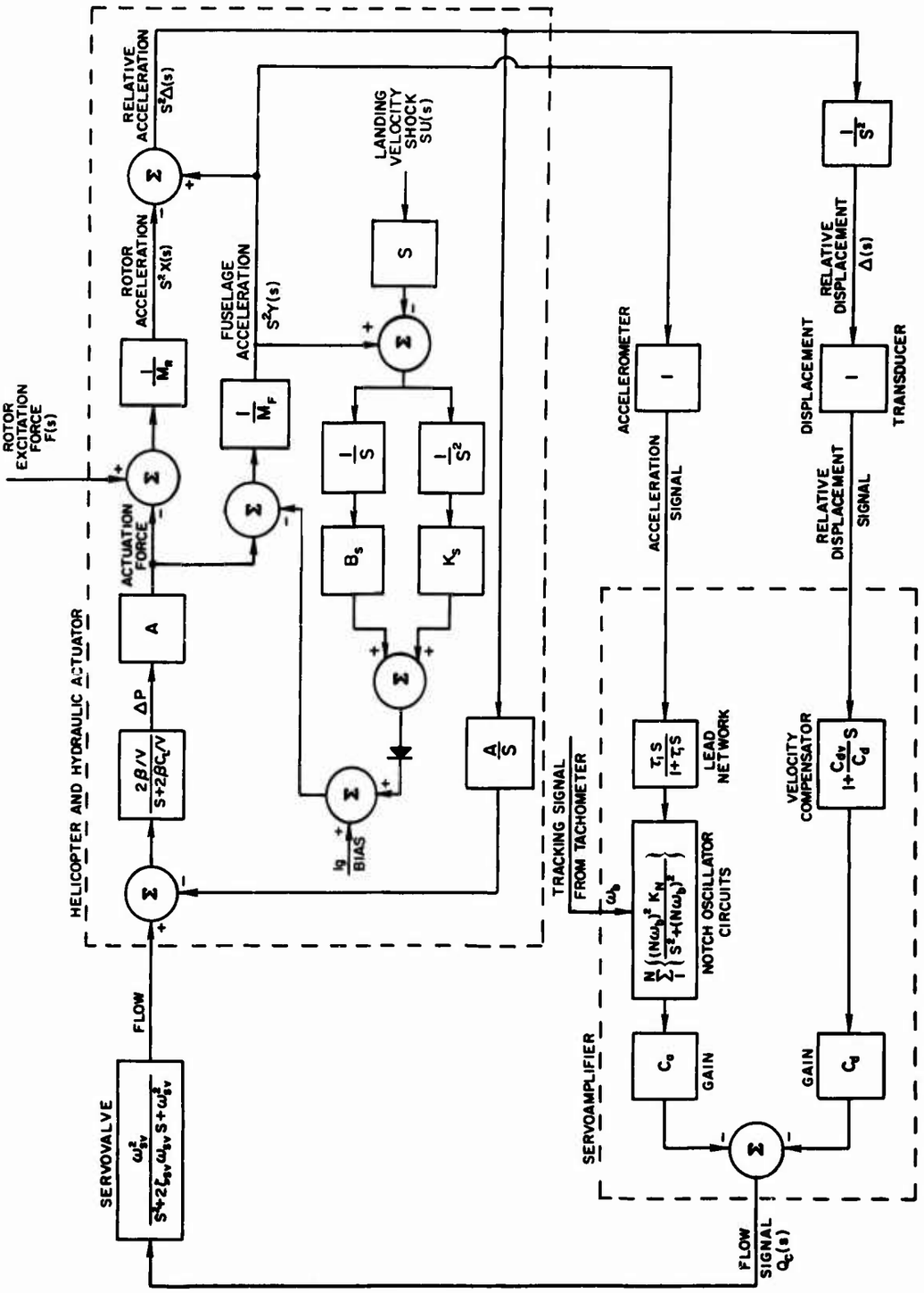

Figure 13. Block Diagram of Helicopter Rotor Isolation System.

System Closed-Loop Transfer Function

The governing equations of motion are derived as follows. Using Laplace notation, the flow from the servovalve expressed in terms of the various feedback signals is given by

$$Q_s(s) = -G_{sv}(s)\left[C_\theta G_c(s)\left(\frac{\tau_1 s}{1+\tau_1 s}\right) s^2 Y(s) + C_{dv} s \Delta(s) + C_d \Delta(s)\right] \qquad (32)$$

The actuator response to the flow from the servovalve and the force summation at the rotor are given by Equations (11) and (12), and are repeated here for continuity:

$$Q_s(s) = A s \Delta(s) - \frac{V}{2\beta} s P_d(s) - C_L P_d(s) \qquad (11)$$

and

$$M_R s^2 X(s) - A P_d(s) = F(s) \qquad (12)$$

The force summation at the fuselage, including the landing gear characteristics, is given by

$$M_F s^2 Y(s) + A P_d(s) + B_s s\left[Y(s) - U(s)\right] + K_s\left[Y(s) - U(s)\right] = 0 \qquad (33)$$

The relationship between feedback flow parameters and the actuator motion is obtained by combining Equations (32) and (11):

$$A s \Delta(s) - \frac{V}{2\beta} s P_d(s) - C_L P_d(s) = -G_{sv}(s)\left[C_\theta G_c(s)\left(\frac{\tau_1 s}{1+\tau_1 s}\right) s^2 Y(s) + C_{dv} s \Delta(s) + C_d \Delta(s)\right] \qquad (34)$$

The relationship between rotor and fuselage motion is obtained by combining Equations (12) and (33):

$$M_R s^2 X(s) + M_F s^2 Y(s) + B_s s\left[Y(s) - U(s)\right] + K_s\left[Y(s) - U(s)\right] = 0 \qquad (35)$$

The transfer functions relating the rotor and fuselage accelerations and the relative displacement between the rotor and fuselage to the rotor-induced force $F(t)$ for in-flight and ground vibrations and maneuver loads are obtained by combining Equations (34) and (35) with $U(s) = 0$:

$$s^2 Y(s) = \frac{s + \left(\frac{C_{dv}}{A} s + \frac{C_d}{A}\right) G_{sv}(s)}{D} \frac{F(s)}{M_R + M_F} \tag{36}$$

$$s^2 X(s) = \frac{\left[\frac{C_m}{A} s^2 G_c(s) G_{sv}(s) \left(\frac{\tau_1 s}{1+\tau_1 s}\right) + s + \left(\frac{C_{dv}}{A} s + \frac{C_d}{A}\right) G_{sv}(s) + \frac{1}{M} \frac{s^3}{\omega_c^2} + \frac{2\zeta_s}{\omega_c} s^2\right]}{D} \frac{F(s)}{M_R + M_F} \tag{37}$$

$$\Delta(s) = \frac{\left[\frac{C_m}{A} s^2 G_c(s) G_{sv}(s) \left(\frac{\tau_1 s}{1+\tau_1 s}\right) + \frac{1}{M}\left(\frac{s}{\omega_c^2} + \frac{2\zeta_s}{\omega_c}\right)\right]}{D} \frac{F(s)}{M_R + M_F} \tag{38}$$

where

$$D = M \frac{C_m}{A} s^2 G_c(s) G_{sv}(s) \left(\frac{\tau_1 s}{1+\tau_1 s}\right) + \left[s + \left(\frac{C_{dv}}{A} s + \frac{C_d}{A}\right) G_{sv}(s)\right]\left[1 + \frac{2\zeta_s \omega_s}{s} + \frac{\omega_s^2}{s^2}\right] + \frac{s^3}{\omega_c^2} + \frac{2\zeta_s}{\omega_c} s^2$$

$\zeta_s = 0$, for cruise vibrations and maneuver loads

$\zeta_s = 0.3$, for ground vibrations and landing shock with nominal gross weight

$\omega_s = 0$, for cruise vibrations and maneuver loads

$\omega_s = 3\pi$ rad/sec, for ground vibrations and landing

The transfer functions relating the rotor and fuselage accelerations and the relative displacement between rotor and fuselage to the simulated upward ground motion $u(t)$ during landing are obtained by combining Equations (34) and (35) with $F(s)=0$:

$$s^2 Y(s) = \frac{M\frac{M_F}{M_R}\left[\frac{G_{sv}}{s^2}\left(\frac{C_{dv}}{A}s+\frac{C_d}{A}\right)+\frac{1}{s}\right]+\frac{s^3}{\omega_c^2}+\frac{2\zeta_c}{\omega_c}s^2\left(2\zeta_s\omega_s s+\omega_s^2\right)}{D} s^2 U(s) \quad (39)$$

$$s^2 X(s) = \frac{M\frac{M_F}{M_R}G_{sv}(s)\left[\frac{C_a}{A}s^2 G_c(s)\left(\frac{\tau_1 s}{1+\tau_1 s}\right)+\frac{C_{dv}}{A}s+\frac{C_d}{A}+s\right]\left(2\zeta_s\omega_s s+\omega_s^2\right)}{D} U(s) \quad (40)$$

$$\Delta(s) = \frac{\left[\frac{s^3}{\omega_c^2}+\frac{2\zeta_c}{\omega_c}s^2-G_{sv}(s)G_c(s)\frac{C_a}{A}s^2\left(\frac{\tau_1 s}{1+\tau_1 s}\right)M\frac{M_F}{M_R}\right]\left(2\zeta_s\omega_s s+\omega_s^2\right)}{D} s^2 U(s) \quad (41)$$

where ζ_s and ω_s have the values shown on page 25, and:

$$D = M\left\{G_{sv}(s)\left[\frac{C_a}{A}s^2 G_c(s)\left(\frac{\tau_1 s}{1+\tau_1 s}\right)\right]+\frac{C_{dv}}{A}s+\frac{C_d}{A}+s\right\}+\left(s^2+2\zeta_s\omega_s s+\omega_s^2\right)\left[M\frac{M_F}{M_R}\frac{G_{sv}(s)}{s^2}\left(\frac{C_{dv}}{A}s+\frac{C_d}{A}\right)+\frac{1}{s}+\frac{s^3}{\omega_c^2}+\frac{2\zeta_c}{\omega_c}s^2\right]$$

For the landing condition, the fuselage can bounce off the ground due to the spring in the landing gear. To simulate the condition, both the values of K_s and B_s are set to zero whenever the summation $sB_s + K_s$ becomes negative. As shown in Figure 13, the summation is passed through a diode. A 1g bias voltage is fed to the summer to simulate the acceleration due to gravity.

System Open-Loop Transfer Function

The design of an active system involves a definition of the system's stability. The approximate degree of stability can be determined from the magnitude and phase diagrams (Reference 13, chapter 10) based on the system's open-loop transfer function $H(s)$. In order to evaluate $H(s)$, the servo loop shown in Figure 13 must be opened between the servoamplifier and the servovalve. A dummy flow command signal $E(s)$ is applied to the servovalve and compared to the flow command signal from the servoamplifier $Q_c(s)$.

$$H(s) = -\frac{Q_c(s)}{E(s)} \tag{42}$$

The equations of motion for the open-loop system, with $F(t) = 0$, are given by

$$Q(s) = G_{sv}(s)\, E(s) \tag{43}$$

$$Q(s) = As\,\Delta(s) + \frac{V}{2\beta}\, s\, P_d(s) + C_L\, P_d(s) \tag{11}$$

$$M_R s^2 X(s) + M_F s^2 Y(s) + B_s s Y(s) + K_s Y(s) = 0 \tag{44}$$

and

$$Q_c(s) = -\left[C_a G_c(s)\left(\frac{\tau_1 s}{1+\tau_1 s}\right) s^2 Y(s) + C_{dv} s\,\Delta(s) + C_d\,\Delta(s)\right] \tag{45}$$

Combining Equations (11) and (42) through (45),

$$H(s) = \frac{G_{sv}(s)\left[M\frac{C_a}{A} G_c(s)\left(\frac{\tau_1 s}{1+\tau_1 s}\right) s^4 + \left(\frac{C_{dv}}{A} s + \frac{C_d}{A}\right)\left(s^2 + 2\zeta_s \omega_s s + \omega_s^2\right)\right]}{s\left[s^2 + 2\zeta_s \omega_s s + \omega_s^2 + \frac{1}{M}\frac{M_R}{M_F}\left(\frac{s^2}{\omega_c^2} + \frac{2\zeta_c}{\omega_c} s\right)\left(M\frac{M_F}{M_R} s^2 + 2\zeta_s \omega_s s + \omega_s^2\right)\right]} \tag{46}$$

The amplitude and phase of $H(s)$ as a function of frequency define the stability margin of the system.

TRACKING OF ROTOR SPEED

Figures 8 and 9 show that the bandwidth of notches $\Omega_{0.5}$ must be narrow in order to provide both a high degree of vibration isolation at the critical frequencies and the desired displacement control during transient conditions. The narrow notches can be effective only if the notch frequencies are equal to the critical excitation frequencies.

TABLE II
VARIATIONS IN ROTOR SPEED

Aircraft	Velocity (knots)	Flight Condition	Rotor Speed (rpm)	Percent Variation
CH-46A (1)	-	Normal operating range	248-270	8
CH-34 (2)	27	Landing approach and flare	201	19
	103	Trim level flight	214	
	7	Partial power descent	234	
	110	Trim level flight out of ground effect	246	
	75	Pull out starting from autorotation	250	
UH-1B(3)	0	Quick stop and turn into wind	289	15
	53	Pull up	310	
	100	Brake and dive	330	
	88	Flare and recovery	343	

(1) Reference 3
(2) Reference 15
(3) Reference 16

Table II indicates that the rotor speed in existing helicopters can vary up to 19 percent depending on the flight conditions. Moreover, during transition from helicopter flight mode to compound flight mode, the rotor speed is expected to be reduced by as much as 20 percent from nominal.

In order to compensate for these expected variations in rotor speed, the filter elements in the notch compensator $G_c(s)$ are designed such that the notch frequencies will follow changes in the blade passage frequency. Details of the notch compensator design are shown in Appendix I.

NOTCH BANDWIDTH

The bandwidth of the notch filters utilized in the multiple-notch isolator can be derived in a manner similar to that used in deriving Equation (28). Consider the notch element at the blade passage frequency. Let

$$G_{SV} = 1$$

$$\beta = \gamma_1 = \infty$$

and $$C_d = C_L = C_{dv} = K_2 = K_3 = K_5 = B_5 = 0$$

Substituting in Equation (36), the fuselage vibration response of a basic rotor isolator having acceleration feedback with only one notch of isolation at the blade passage frequency becomes

$$s^2 Y(s) = \left[\frac{s^2 + \omega_n^2}{s^2 + M\frac{C_a}{A} K_1 \omega_n^2 s + \omega_n^2} \right] \frac{F(s)}{M_R + M_F} \tag{47}$$

Let

$$\alpha = M \frac{C_a}{A} K_1 \tag{48}$$

The transmissibility T is calculated from Equation (47):

$$T = \left| \frac{(j\omega)^2 \, Y(j\omega)}{F(j\omega)/(M_R + M_F)} \right| = \sqrt{\frac{(\omega_n^2 - \omega^2)^2}{(\omega_n^2 - \omega^2)^2 + (\alpha \omega_n^2 \omega)^2}} \tag{49}$$

The two frequencies at which the transmissibility is equal to $0.5\omega_H$ and ω_L can be calculated by solving Equation (49) for $T = 0.5$:

$$\frac{\omega_H}{\omega_n} = \sqrt{\frac{1}{2}\left[2 + \frac{\alpha^2\omega_n^2}{3} + \sqrt{\left(\frac{\alpha^2\omega_n^2}{3}\right)^2 + 4\,\frac{\alpha^2\omega_n^2}{3}}\right]} \tag{50}$$

and

$$\frac{\omega_L}{\omega_n} = \sqrt{\frac{1}{2}\left[2 + \frac{\alpha^2\omega_n^2}{3} - \sqrt{\left(\frac{\alpha^2\omega_n^2}{3}\right)^2 + 4\,\frac{\alpha^2\omega_n^2}{3}}\right]} \tag{51}$$

The percent bandwidth of the notch is defined by $(\omega_H - \omega_L)/\omega_n$.

From Equations (50) and (51),

$$\frac{\omega_H - \omega_L}{\omega_n} = \frac{1}{3}\alpha\omega_n \tag{52}$$

Substituting Equation (48) into (52), the percentage bandwidth is given by

$$\frac{\omega_H - \omega_L}{\omega_n} = \frac{1}{3}\frac{C_a}{A} M K_1 \omega_n \tag{53}$$

The notch compensator transfer function for the multiple-notch isolator is given by

$$G_c(s) = \sum_1^N \frac{(N\omega_n)^2 K_N}{s^2 + (N\omega_n)^2} \quad , \quad N = 1, 2, 3 \tag{54}$$

Therefore, for the case of multiple notches, equal percent bandwidth notches will be obtained if the relationship $(K_N)(N\omega_N)$ is held constant for each value of acceleration feedback gain $\frac{C_a}{A}$.

VIBRATION RESPONSE AT THE NOTCH FREQUENCY

Tracking of the rotor speed insures that the notch frequencies occur at the blade passage frequency and higher harmonics. The fuselage and rotor response at the critical frequencies can be calculated by evaluating Equations (36) through (38) at the critical frequencies. The notch gain at any of the critical frequencies is given by

$$G_c(jN\omega_n) = \sum_1^N \frac{(N\omega_n)^2 K_N}{(jN\omega_n)^2 + (N\omega_n)^2} \quad , \quad N = 1, 2, 3$$

$$= \infty \tag{55}$$

Substituting in Equations (36) through (38), the fuselage and rotor accelerations and the relative displacement between rotor and fuselage at a notch frequency $N\omega_N$, due to rotor-induced force $F_N/(M_R+M_F)$, are given by

$$\ddot{y}(jN\omega_n) = 0 \tag{56}$$

$$\ddot{x}(jN\omega_n) = \frac{1}{M}\,\frac{F_N}{M_R+M_F} \tag{57}$$

$$\delta(jN\omega_n) = \frac{1}{M(N\omega_n)^2}\,\frac{F_N}{M_R+M_F} \tag{58}$$

It is shown that the acceleration transmitted to the isolated fuselage is zero at all the notch frequencies. The acceleration of the isolated rotor is $1/M$ times that of the unisolated rotor.

The total relative displacement between the rotor and fuselage is due to the summation of displacements at each excitation frequency. Consider the rotor-induced excitation to be of the form

$$\frac{f(t)}{M_R+M_F} = a_1 \sin(\omega_b t+\varphi_1) + a_2 \sin(2\omega_b t+\varphi_2) + \cdots + a_N \sin(N\omega_b t+\varphi_N) \tag{59}$$

where ω_b is the blade passage frequency. The maximum possible relative displacement between rotor and fuselage would occur for the case where all forces are in phase. Therefore, if the first notch frequency occurs at $\omega_n = \omega_b$, the total relative deflection is calculated from Equation (58) to be

$$\sum_1^N \delta(jN\omega_b) = \frac{1}{M\,\omega_b^2\,(M_R+M_F)} \sum_1^N \frac{F_N}{N^2} \tag{60}$$

Figure 1 shows the rotor-induced forces at each critical frequency normalized with respect to the force at b/rev. Substituting values into Equation (60), for a three-notch system,

$$\sum_1^{N=3} \delta(jN\omega_b) = \frac{g\,F_1}{M_R+M_F}\,\frac{1}{M\omega_b^2}\left[\frac{1}{(1)^2}+\frac{0.4}{(2)^2}+\frac{0.1}{(3)^2}\right]$$

$$\sum_{1}^{N=3} \delta(jN\omega_b) = 386\left(1+0.1+0.01\right)\frac{F_1}{M(M_R+M_F)\omega_b^2}$$

$$= 430\,\frac{F_1}{M(M_R+M_F)\omega_b^2} \qquad (61)$$

where $\frac{F_1}{M_R+M_F}$ is the unisolated rotor-induced force at the blade passage frequency expressed in g's. For the two-notch system,

$$\sum_{1}^{N=2} \delta(jN\omega_b) = \frac{gF_1}{M_R+M_F}\,\frac{1}{M\omega_b^2}\left[\frac{1}{(1)^2}+\frac{0.4}{(2)^2}\right]$$

$$= 425\,\frac{F_1}{M(M_R+M_F)\omega_b^2} \qquad (62)$$

Equations (61) and (62) were used to calculate the relative displacement between rotor and fuselage during cruise and ground vibrations for the two- and three-notch systems, respectively. It is interesting to note that, at the notch frequencies, the system response to vibratory excitations is independent of the feedback gain parameters [Equations (56), (57), (58), (61) and (62)].

The greater portion of the total relative displacement is caused by the notch at the blade passage frequency, since this is the lowest frequency and the level of excitation is the highest at the blade passage frequency. Equations (61) and (62) do not consider a notch of isolation at the third harmonic of the blade passage frequency (4 b/rev). Since, as shown in Figure 1, there is a vibratory excitation at 4 b/rev, it is necessary to consider the relative displacement at that frequency.

At frequencies higher than the last notch frequency, no isolation is provided by the active elements, and the actuator acts as a passive isolator between the rotor and fuselage. The relative displacement at any frequency above the highest notch frequency can be calculated from Equation (38) by letting $\omega_s = \zeta_s = 0$ and setting all the active element gains equal to zero. Substituting values into Equation (38)

$$(\Delta)_{\omega > 3b/rev} = \frac{1}{Ms^2}\;\frac{gF(s)}{M_R+M_F}\;\frac{\left(\frac{s^2}{\omega_c^2}+\frac{2\zeta_c s}{\omega_c}\right)}{\frac{s^2}{\omega_c^2}+\frac{2\zeta_c s}{\omega_c}+1} \qquad (63)$$

From Figure 1

$$\left|\frac{F(s)}{M_R+M_F}\right|_{s=4j\omega_b} = 0.1\,\frac{F_1}{M_R+M_F} \tag{64}$$

where again $F_1/(M_R+M_F)$ is the unisolated rotor-induced force at the blade passage frequency expressed in g's.

The relative deflection at the third harmonic of the blade passage frequency is obtained by substituting Equation (64) in Equation (63) and letting $s=4j\omega_b$

$$(\Delta)_{\omega=4b/rev} = \frac{g F_1}{M_R+M_F}\,\frac{1}{M\omega_b^2}\left\{0.00625\left|\frac{-16\left(\frac{\omega_b}{\omega_c}\right)^2+8\zeta_c j\frac{\omega_b}{\omega_c}}{-16\left(\frac{\omega_b}{\omega_c}\right)^2+8\zeta_c j\frac{\omega_b}{\omega_c}+1}\right|\right. \tag{65}$$

The worst relative displacement condition occurs for the case where the 4 b/rev frequency is near the actuator resonant frequency. Based on the selected values of blade passage frequency and actuator resonances (shown on Tables III and V), this occurs for $\omega_b = 26.6$ Hz and $\omega_c = 202$ Hz. Substituting in Equation (65)

$$\left|\Delta\right|_{\omega=4b/rev} = 3.2\,\frac{F_1}{M(M_R+M_F)\omega_b^2} \tag{66}$$

Comparing Equation (66) with Equations (61) and (62), it evident that, even for the worst case, the relative displacement contribution due to the vibratory excitation at 4 b/rev is negligible. Therefore, the results of the parametric study are based on the relative displacement due to vibratory excitations at the notch frequencies only.

FINAL RELATIVE DISPLACEMENT DUE TO MANEUVER LOAD

As previously shown, the notch isolator gives rise to zero relative displacement for a step in rotor force [Equation (9)]. Maneuver loads are characterized by a ramp force excitation. Letting t_o be the rise time, and F_o the final value of the rotor-induced force, the final relative displacement due to a maneuver load can be obtained from Equation (36):

$$\delta_{RAMP\,(t=\infty)} = \frac{g}{t_o}\,\frac{C_a}{C_d}\,\tau_1\sum_1^N K_N\,\frac{F_o}{M_R+M_F} \tag{67}$$

Equation (67) was used to evaluate the effect of feedback gain parameters and rise time on the relative displacement due to maneuver loads.

ACTUATOR AREA FOR MINIMUM FLOW

In order to minimize the flow and power requirements for vibratory excitations and also to provide the required forces during maneuver loads, the actuators are considered to have unequal piston areas for the upper and lower chambers. Under a +3 g maneuver, the maximum tensile force exerted by the actuator is given by

$$3W_F = P_1 A_1 - P_2 A_2 \tag{68}$$

where

P_1 is the upper chamber pressure

P_2 is the lower chamber pressure

A_1 is the upper chamber piston area

A_2 is the lower chamber piston area

W_F is the fuselage weight

For the +3 g maneuver, P_1 is set to a maximum value of $P_S - P_V$, where P_S is the supply pressure and P_V is the pressure drop across each land of the servovalve. This pressure drop insures delivery of the required flow for vibration isolation during conditions of combined vibratory and transient excitations. The lower chamber pressure P_2 is set to a minimum value of P_V. Therefore, the limiting actuator force equation based on the +3 g maneuver load is given by

$$3W_F = (P_S - P_V)A_1 - P_V A_2 \tag{69}$$

Under a -0.5 g maneuver, the maximum compressive force exerted by the actuator is given by

$$-\tfrac{1}{2} W_F = P_1 A_1 - P_2 A_2 \tag{70}$$

For this condition, the upper chamber pressure is set equal to P_V and the lower chamber pressure is set equal to $P_S - P_V$. Therefore, the limiting force equation based on the -0.5 g maneuver load is given by

$$-\tfrac{1}{2} W_F = P_V A_1 - (P_S - P_V) A_2 \tag{71}$$

$$A_1 = \frac{W_F (3 P_s - 2.5 P_v)}{P_s^2 - 2 P_s P_v} \tag{72}$$

$$A_2 = \frac{W_F (0.5 P_s - 2.5 P_v)}{P_s^2 - 2 P_s P_v} \tag{73}$$

The average actuation area is then given by

$$A = \frac{A_1 + A_2}{2} = 1.75 \frac{W_F}{P_s - 2 P_v} \tag{74}$$

FLOW AND POWER REQUIREMENTS

The flow required to operate the isolation system is at a maximum during the vibratory cruise flight condition, and results from the relative velocities of the actuator generated to isolate the periodic rotor forces from the fuselage. The peak flow $\hat{Q}$ is given by

$$\hat{Q} = A \hat{\dot{\delta}} \tag{75}$$

where

A is the average actuation area

$\hat{\dot{\delta}}$ is the peak relative velocity between rotor and fuselage

The peak relative velocity occurs at the notch frequencies, when all the rotor-induced forces at each discrete frequency reach their peak magnitude at the same time. From Equation (39), letting $\hat{\dot{\delta}} = s \Delta(s)$ and $s = j\omega_n$, the peak flow for a system with N notches is given by

$$\hat{Q}_N = \frac{A}{M \omega_n} \left[\frac{F_1}{M_R + M_F} + \frac{1}{2} \frac{F_2}{M_R + M_F} + \cdots + \frac{1}{N} \frac{F_N}{M_R + M_F} \right] \tag{76}$$

where $F_1, F_2, F_3, \ldots, F_N$ are the magnitudes of the rotor-induced forces at the blade passage frequency and its higher harmonics. Assuming a representative value of $F_1/(M_R + M_F) = 0.3_g$ for the rotor-induced force at the blade passage frequency, and the relationship between the magnitudes of higher harmonic forces and $F_1/(M_R + M_F)$ to be as shown in Figure 1, the peak flow for a two-notch isolator, in cubic inches per second, is given by

$$\hat{Q}_{N=2} = 139 \frac{A}{M\omega_n} \tag{77}$$

Similarly, for a three-notch isolator,

$$\hat{Q}_{N=3} = 143 \frac{A}{M\omega_n} \tag{78}$$

As in the case of peak flow, the maximum power required to operate the notch isolation system occurs during the vibratory cruise condition, and is equal to the rectified average flow $\bar{Q}$ times the supply pressure P_s. For sinusoidal excitation,

$$\bar{Q} = 0.9\, Q_{RMS} \tag{79}$$

and

$$(Q_{RMS})_N = \sqrt{(\hat{Q}_1)^2 + (\hat{Q}_2)^2 + \cdots + (\hat{Q}_N)^2} \tag{80}$$

Therefore,

$$\bar{Q}_N = 0.9 \frac{A}{M\omega_n} \sqrt{\left(\frac{F_1}{M_R + M_F}\right)^2 + \frac{1}{4}\left(\frac{F_2}{M_R + M_F}\right)^2 + \cdots + \frac{1}{N^2}\left(\frac{F_N}{M_R + M_F}\right)^2} \tag{81}$$

Again assuming representative values of $F_1/(M_R + M_F)$, and the relationship between rotor-induced forces at various frequencies as shown in Figure 1, the maximum power required to operate the hydraulic pump during vibratory conditions for a two-notch system, expressed in horsepower, is given by

$$HP_{N=2} = 0.0160 \frac{A P_s}{M\omega_n} \tag{82}$$

Similarly, for a three-notch system,

$$HP_{N=3} = 0.0161 \frac{A P_s}{M\omega_n} \tag{83}$$

SELECTION OF COMPONENTS AND TYPICAL SYSTEM RESPONSE

Figures 12 and 13 describe the selected multiple-notch isolation system in schematic and block diagram form, respectively. The isolation system operates as follows. Flow from the servovalve enters the actuator and creates a pressure difference P_d between the upper and lower actuation chambers. This pressure difference times the average actuation area A is equal to the force that the actuator applies to the rotor and fuselage masses. The fuselage acceleration is equal to the actuation force divided by the fuselage mass. The rotor acceleration is equal to the excitation force minus the actuation force divided by the rotor mass. The resulting fuselage acceleration is sensed by the accelerometer and fed back to the servoamplifier. The resulting forces, applied to the rotor and fuselage masses, generate a relative displacement between the two masses, which is sensed by the displacement transducer and fed back to the servoamplifier. The relative velocity feedback signal is generated by differentiating the relative displacement signal, thereby avoiding the necessity of a third transducer.

In all cases, notches of isolation are introduced at the blade passage frequency and higher harmonics, and the rotor speed is tracked to insure coincidence between the notch frequencies and the critical excitation frequencies. In the selection of components, the rotor to fuselage mass ratio M_R / M_F was considered to be 1/8 for all gross weights (Reference 5). A review of available literature concerning landing gear configurations indicated that typical undercarriage stiffnesses were found to yield natural frequencies of the total helicopter weight on the undercarriage varying from 1 to 5 Hz, for the range of gross weights under consideration. An average value of 3 Hz was assumed for all gross weights. Similarly, a value of 30 percent of critical damping was selected for the undercarriage in all cases.

Hydraulic components were selected for each case based on force, flow and power requirements. The system response to the various dynamic excitations was calculated using both analog and digital computers, with initial values of feedback parameter gains selected to yield stable systems. The process of selecting final values of gains involved a trial-and-error procedure during which both the open- and closed-loop responses were calculated with different gain settings until all the requirements of the particular design criterion were satisfied.

CASE IDENTIFICATION

Table III shows values of rotor speed, blade passage frequency and higher harmonics, as a function of helicopter weight and number of blades. Originally, seven combinations were to be considered. However, the combination of typical rotor speed and number of blades for the 10,000-, 20,000-, and 40,000-pound helicopters resulted in approximately the same value of blade passage frequency (Reference 5). As shown in the System Analysis and Development Section of this report, the relative displacement and

TABLE III

SUMMARY OF PREDOMINANT EXCITATION FREQUENCIES

Helicopter Gross Weight (lb)	Number of Blades b	Rotor Speed* (rpm)	1/rev	b/rev	2b/rev	3b/rev	4b/rev
			(Hz)				
2,000	2	400	6.65	13.3	26.6	39.9	53.2
2,000	4	400	6.65	26.6	53.2	79.8	106.4
10,000	4	260	4.4	17.5	35.0	52.5	70.0
20,000	5	214	3.6	17.9	35.8	53.7	71.6
40,000	6	177	2.95	17.7	35.4	53.1	70.8
80,000	6	145	2.4	14.5	29.0	43.5	58.0
80,000	7	145	2.4	16.9	33.8	50.7	67.6

* From Reference 5.

response characteristics of the system are a function of the blade passage frequency and its higher harmonics, but independent of gross weight. Therefore, in the parametric study the three cases having approximately equal blade passage frequencies were considered one and the same. However, isolation system weight and power requirements are a function of gross weight, and separate values were calculated for each gross weight classification.

For the purpose of tabulating and discussing the results of this study, each case is identified by a number shown in Table IV. The first digit indicates the total gross weight in thousands of pounds, the second digit indicates the number of blades, and the third digit indicates the number of notches of isolation. For the two- and three-notch systems, the first notch occurs at the blade passage frequency, and the second or third notch occurs at the second or third harmonic of b/rev, respectively. Finally, the letters a, b, c and d refer to nominal gross weight, and 10, 20, and 30 percent increase in fuselage weight, respectively, for a constant rotor weight. In all instances of fuselage weight increase, the rotor weight is held constant and equal to 1/9 the total nominal helicopter gross weight.

SELECTION OF COMPONENTS

For each case identified in Table IV, the actuator area and stroke, servovalve, and feedback gains were defined based on the three criteria shown in Table I, the nominal gross weight, and the blade passage frequency. The dynamic characteristics of each component employed in the calculation of system response are presented below.

Supply Pressure

Sufficient pressure drop P_v across each land of the servovalve is required to insure that the servovalve is capable of supplying the desired peak flow. The supply pressure must be high enough to include this pressure drop, and the pressure drop P_d required to generate forces across the actuator piston area under the maximum expected levels of dynamic excitation. The actuator areas calculated from Equation (74) insure that the required flow and power are a minimum. Combining the expressions for flow [Equations (77) and (78)] and power [Equations (82) and (83)] with Equation (74) indicates that the supply pressure should be as high as possible.

Based on rated maximum pressures of available servovalves and actuator and a 1,000 psi total pressure drop in the servovalve, a supply pressure of 4,000 psi was selected. This high pressure is not normally available on helicopters. However, selection of a lower operating pressure would result in flow demands which exceed those presently available. Therefore, although a supply pressure of 4,000 psi requires an additional hydraulic pump, the higher pressure allows selection of smaller and lighter actuators and valves and a lower overall isolation system weight.

TABLE IV

CASE AND CONFIGURATION IDENTIFICATION

Case Number		Helicopter Gross Weight (lb)	Number of Blades b	Rotor Speed (rpm)	Blade Passage Frequency (Hz)	Number of Notches
2.2.2	a	2,000	2	400	13.3	2
	b	2,177	2	400	13.3	2
	c	2,356	2	400	13.3	2
	d	2,533	2	400	13.3	2
2.4.2	a	2,000	4	400	26.6	2
	b	2,177	4	400	26.6	2
	c	2,356	4	400	26.6	2
	d	2,533	4	400	26.6	2
10.4.2	a	10,000	4	260	17.5	2
	b	10,880	4	260	17.5	2
	c	11,777	4	260	17.5	2
	d	12,660	4	260	17.5	2
20.5.2	a	20,000	5	214	17.9	2
	b	21,780	5	214	17.9	2
	c	23,560	5	214	17.9	2
	d	25,330	5	214	17.9	2
40.6.2	a	40,000	6	177	17.7	2
	b	43,560	6	177	17.7	2
	c	47,120	6	177	17.7	2
	d	50,680	6	177	17.7	2
80.6.2	a	80,000	6	145	14.5	2
	b	87,108	6	145	14.5	2
	c	94,220	6	145	14.5	2
	d	101,331	6	145	14.5	2
80.7.2	a	80,000	7	145	16.9	2
	b	87,108	7	145	16.9	2
	c	94,220	7	145	16.9	2
	d	101,331	7	145	16.9	2

TABLE IV (continued)

Case Number		Helicopter Gross Weight (lb)	Number of Blades b	Rotor Speed (rpm)	Blade Passage Frequency (Hz)	Number of Notches
2.2.3	a	2,000	2	400	13.3	3
	b	2,177	2	400	13.3	3
	c	2,356	2	400	13.3	3
	d	2,533	2	400	13.3	3
2.4.3	a	2,000	4	400	26.6	3
	b	2,177	4	400	26.6	3
	c	2,356	4	400	26.6	3
	d	2,533	4	400	26.6	3
10.4.3	a	10,000	4	260	17.5	3
	b	10,880	4	260	17.5	3
	c	11,777	4	260	17.5	3
	d	12,660	4	260	17.5	3
20.5.3	a	20,000	5	214	17.9	3
	b	21,750	5	214	17.9	3
	c	23,560	5	214	17.9	3
	d	25,330	5	214	17.9	3
40.6.3	a	40,000	6	177	17.7	3
	b	43,560	6	177	17.7	3
	c	47,120	6	177	17.7	3
	d	50,080	6	177	17.7	3
80.6.3	a	80,000	6	145	14.5	3
	b	87,108	6	145	14.5	3
	c	94,220	6	145	14.5	3
	d	101,331	6	145	14.5	3
80.7.3	a	80,000	7	145	16.9	3
	b	87,108	7	145	16.9	3
	c	94,220	7	145	16.9	3
	d	101,331	7	145	16.9	3

Actuator Characteristics

Table V shows the actuator average chamber area A and the resonant frequency ω_c (in hertz), based on nominal helicopter gross weight and supply pressure of 4000 psi, for the three design criteria identified in Table I.

The upper and lower actuator chamber areas given by Equation (74) are designed so that forces are supplied to the fuselage compatible with the + 3 g and -0.5 g maximum required values. Substituting this equation in the expression for the actuator resonant frequency, and letting L be the actuator stroke, results in

$$\omega_c = \sqrt{\frac{2\beta A^2}{V M M_F}}$$

$$= \sqrt{\frac{2\beta A}{L M M_F}}$$

$$= 36.7 \sqrt{\frac{\beta}{LM} \frac{1}{P_s - 2P_v}} \quad \text{rad/sec} \qquad (84)$$

Equation (84) indicates that the actuator resonant frequency is independent of the helicopter weight. Finally, it was assumed that a 10-percent fraction of critical damping would represent the leakage and friction characteristic of the actuators in all cases.

Servovalve Characteristics

Table VI summarizes the dynamic characteristics of the servovalves. Moog Incorporated, Series 30 valves were selected based on their large flow capacities and flat frequency response over the frequency range of interest to this investigation. The required peak flows for the two- and three-notch systems were calculated from Equations (77) and (78), respectively, for 1000 psi supply pressure, and maximum helicopter gross weight (i. e., nominal plus 30 percent fuselage weight increase). The number of valves utilized in each case was defined in terms of the required flows and the maximum rated valve flows as specified by the manufacturer. Similarly, values of servovalve resonant frequency and fraction of critical damping were obtained from the manufacturer's specifications for the expected levels of pressure and flow.

TABLE V

SUMMARY OF ACTUATOR CHARACTERISTICS

Helicopter Gross Weight (lb)	Design Criterion	Chamber Area (in.) Upper	Lower	Average	Stroke ($in.^2$)	Critical Damping* (pct)	Resonant Frequency*, ** (Hz)
2,000	A	1.57	0.47	1.02	±0.5	10	202
	B	1.57	0.47	1.02	±0.2	10	318
	C	1.57	0.47	1.02	±0.2	10	318
10,000	A	7.84	2.37	5.10	±0.5	10	202
	B	7.84	2.37	5.10	±0.2	10	318
	C	7.84	2.37	5.10	±0.2	10	318
20,000	A	15.68	4.74	10.21	±0.5	10	202
	B	15.68	4.74	10.21	±0.2	10	318
	C	15.68	4.74	10.21	±0.2	10	318
40,000	A	31.35	9.48	20.41	±0.5	10	202
	B	31.35	9.48	20.41	±0.2	10	318
	C	31.35	9.48	20.41	±0.2	10	318
80,000	A	62.7	18.96	40.84	±0.5	10	202
	B	62.7	18.96	40.84	±0.2	10	318
	C	62.7	18.96	40.84	±0.2	10	318

* For nominal gross weight
**Based on bulk modulus of fluid = 200,000 $lb/in.^2$

TABLE VI

SUMMARY OF PEAK FLOW REQUIREMENTS AND SERVOVALVE CHARACTERISTICS

Helicopter Gross Weight (lb)	Number of Blades b	Valve Type (Moog Inc.)	Valve Resonant Frequency (Hz)	Critical Damping (pct)	Valve Maximum Rated Flow* ($in.^3/sec$)	Required Peak Valve Flow** ($in.^3/sec$)		Required Number of Valves**
						2-Notch System	3-Notch System	
2,000	2	32	175	70	31	19.9	20.4	1
2,000	4	31	210	70	15	9.9	10.1	1
10,000	4	35	110	70	79	76.6	77.5	1
20,000	5	35	110	70	79	151	155	2
40,000	6	35	110	70	79	302	310	4
80,000	6	35	110	70	79	729	750	10
80,000	7	35	110	70	79	630	650	9

* For no-load valve pressure drop of 1000 psi

** Based on nominal gross weight plus 30 percent fuselage weight increase

Transducer Characteristics

Two feedback transducers are used in the design: a servoaccelerometer and a differential transformer. The dynamic responses of both are assumed to be flat to frequencies well above those of interest.

SELECTION OF FEEDBACK PARAMETERS

Selection of gains for the various feedback parameters was based on: (1) providing as high a degree of vibration isolation as possible at the critical notch frequencies; (2) limiting the relative deflections during 10 ft/sec landing to the values required by each design criteria; and (3) maintaining a safe margin of system stability.

The gain margin can be calculated from the magnitude of the system open-loop transfer function, Equation (46), at the phase crossover frequency. The phase crossover frequency is defined as the frequency where the total phase angle is -180°. All of the feedback loops introduce both gain and phase lag into the system response, but to varying degrees. At frequencies above the highest notch frequency, the acceleration feedback loop has a uniform phase angle of $+90^{\circ}$. The phase contribution from the notch elements is -180°, resulting in a net phase angle of -90°. Since the signal from the displacement transducer is filtered at a low frequency, any remaining gain from the displacement loop at frequencies above the highest notch frequency will also be small. Therefore, at frequencies above the highest notch frequency, the total open-loop phase angle can be approximated by calculating the system response based on the dynamic characteristics of the acceleration loop alone, including the actuator and the servovalve. Since the acceleration loop contributes -90° phase, the phase crossover frequency corresponds to the frequency where the actuator in series with the servovalve provides -90° of phase shift.

Table VII shows the crossover frequency as a function of helicopter gross weight for the acceleration open-loop, including the actuator and servovalve characteristics. In each case, calculations were based on the lowest actuator resonant frequency, namely the longest stroke (Criterion A) and the maximum weight. Comparison of the phase crossover frequency with the frequency of the highest notch (3b/rev) indicates that in all cases the phase crossover frequency is well above the highest notch frequency. As a first approximation, the assumption of selecting gains for the acceleration loop and neglecting the effect of the displacement loop is thus justified.

Knowing the crossover frequency, initial values of the allowable acceleration loop gain were calculated on the basis of a 30-db gain margin. The acceleration loop gain, as a function of frequency, is given by

TABLE VII

SUMMARY OF ACCELERATION OPEN-LOOP CROSSOVER FREQUENCIES

Helicopter Gross Weight (lb)	Number of Blades b	Frequency at which 3rd Notch Occurs 3b/rev (Hz)	Crossover Frequency* (Hz)	
			Based on Gross Weight	Based on 30% Fuselage Weight Increase
2,000	2	39.9	141	133
2,000	4	79.8	158	147
10,000	4	52.5	105	99.8
20,000	5	53.7	105	99.8
40,000	6	53.1	105	99.8
80,000	6	43.5	105	99.8
80,000	7	50.7	105	99.8

* Frequency at which the phase of the acceleration open-loop transfer function, excluding the notch elements, is -90°. The acceleration open-loop transfer function includes the servovalve and actuator dynamics. The actuator resonant frequency is based on Criterion A design.

$$G_{acc.} = M \frac{C_2}{A} \sum_{1}^{N} \left| \frac{K_N}{1 - \frac{\omega^2}{(N\omega_n)^2}} \right| \omega \qquad (85)$$

where K_N is the relative static gain of the Nth notch element. Based on equal percentage notch bandwidths [Equation (54)] and the relationship between the frequencies at which the notches occur (b/rev, 2b/rev and 3b/rev for a three-notch system), Equation (85) can be rewritten as

$$(G_{acc.})_{N=3} = M \frac{C_2}{A} K_1 \omega_b^2 \left[\frac{\omega}{\omega_b^2 - \omega^2} + \frac{2\omega}{4\omega_b^2 - \omega^2} + \frac{3\omega}{9\omega_b^2 - \omega^2} \right] \qquad (86)$$

where

K_1 = gain at the first notch

ω_b = blade passage frequency

$M = \frac{M_R}{M_R + M_F} = \frac{1}{9}$

The maximum value of C_2/A that was selected is unity; lower values would be used to reduce the acceleration gain throughout the frequency range in the event that the displacement criteria are not met. Therefore, as a first approximation, the gain K_1 is set such that Equation (86), evaluated at ω = phase crossover frequency, yields a value of $G_{acc} = 0.032$, which corresponds to approximately a 30-db gain margin. For each case the crossover frequency used in estimating the initial value of K_1 is that shown in Table VII for the nominal gross weight.

Initial selection of the remaining feedback gains was based on a qualitative evaluation of the effect of each parameter on the response of the system. Table VIII summarizes those effects. The relative values of gain shown in parentheses are indicative of very weak effect on the system response.

TABLE VIII

QUALITATIVE SUMMARY OF THE EFFECT OF GAINS ON SYSTEM RESPONSE

	Relative Values of Gain			
Desired Response Characteristics	τ_1	$C_{a/A}$	K_N	$C_{d/A}$
Small Relative Displacement During In-Flight and Landing Transients	Low	Low	Low	High
Fast Speed of Response	Low	Low	Low	High
Large Gain Margin	(High)	Low	Low	(Low)
Low Vibration Peak Amplification	(High)	(Low)	(Low)	(Low)
Wide Notch Bandwidth	High	High	High	Low

The process of final selection of gains involved repetitive solutions of both the open- and closed-loop responses of the system for the various dynamic conditions of the study with different values of gain. In all cases, the gain margin based on the complete system open-loop transfer function, Equation (46), was at least 20 db.

The values of the final gain parameters for each case considered are shown in Tables IX and X for the two- and three-notch systems, respectively.

TABLE IX

SUMMARY OF SERVOAMPLIFIER PARAMETERS FOR TWO-NOTCH SYSTEM

Case Number*	Criterion	C_a/A (sec)	τ_1 (sec)	C_{dv}/A	C_d/A (sec^{-1})	k_1 $x10^{-3}$	k_2 $x10^{-3}$
2.2.2	A	1.0	0.019	0.4	25	14.4	7.2
	B	1.0	0.019	2.5	50	14.4	7.2
	C	0.44	0.0190	0.4	25	14.4	7.2
2.4.2	A	1.0	0.083	0	2.5	3.62	1.81
	B	1.0	0.0444	0	20	3.62	1.81
	C	0.43	0.083	0	2.5	3.62	1.81
10.4.2	A	1.0	0.133	0	20	5.59	2.79
	B	1.0	0.0166	0	27.5	5.59	2.79
	C	0.41	0.133	0	20	5.59	2.79
20.5.2	A	1.0	0.133	0	20	5.59	2.79
	B	1.0	0.0166	0	27.5	5.59	2.79
	C	0.41	0.133	0	20	5.59	2.79
40.6.2	A	1.0	0.133	0	20	5.59	2.79
	B	1.0	0.0166	0	27.5	5.59	2.79
	C	0.41	0.133	0	20	5.59	2.79
80.6.2	A	1.0	0.0265	0	22.5	9.35	4.68
	B	1.0	0.0167	0.75	37.5	9.35	4.68
	C	0.43	0.0265	0	22.5	9.35	4.68
80.7.2	A	1.0	0.0445	0	12.5	6.25	3.13
	B	1.0	0.0167	0	30	6.25	3.13
	C	0.405	0.0445	0	12.5	6.25	3.13

*Values of parameters are the same for all fuselage weight variations considered in each case.

TABLE X

SUMMARY OF SERVOAMPLIFIER PARAMETERS FOR THREE-NOTCH SYSTEM

Case Number*	Criterion	C_a/A (sec)	τ_1 (sec)	C_{dv}/A	C_d/A (sec^{-1})	k_1 $x10^{-3}$	k_2 $x10^{-3}$	k_3 $x10^{-3}$
2.2.3	A	1.0	0.045	0	22.5	7.25	3.63	2.42
	B	1.0	0.022	0.5	35.	7.25	3.63	2.42
	C	0.395	0.045	0	22.5	7.25	3.63	2.42
2.4.3	A**	-	-	-	-	-	-	-
	B	1.0	0.0745	0	5	1.6	0.8	0.52
	C**	-	-	-	-	-	-	-
10.4.3	A	1.0	0.133	0	2.5	2.58	1.26	0.89
	B	1.0	0.0444	0	15	2.58	1.26	0.89
	C	0.415	0.133	0	2.5	2.58	1.26	0.89
20.5.3	A	1.0	0.133	0	2.5	2.58	1.26	0.89
	B	1.0	0.0444	0	15	2.58	1.26	0.89
	C	0.415	0.133	0	2.5	2.58	1.26	0.89
40.6.3	A	1.0	0.133	0	2.5	2.58	1.26	0.89
	B	1.0	0.0444	0	15	2.58	1.26	0.89
	C	0.415	0.133	0	2.5	2.58	1.26	0.89
80.6.3	A	1.0	0.667	0	7.5	4.3	2.15	1.43
	B	1.0	0.222	0	25	4.3	2.15	1.43
	C	0.41	0.667	0	7.5	4.3	2.15	1.43
80.7.3	A	1.0	0.133	0	7.5	4.3	2.15	1.43
	B	1.0	0.0295	0	20	4.3	2.15	1.43
	C	0.43	0.133	0	7.5	4.3	2.15	1.43

*Values of parameters are the same for all fuselage weight variations considered in each case.

** Displacement feedback gain could not be reduced from the value used in Criterion B without resulting in either an unstable system or in a very sluggish system response.

TYPICAL RESPONSE

The parametric study involved calculation of the response of five isolated fuselages to a wide variety of dynamic excitations. Each fuselage is characterized by different gross weights and associated blade passage frequencies. For each nominal gross weight, six different isolation system configurations were evaluated; namely, two- and three-notch systems for the three maximum relative displacement and stability criteria cited in Table I. Finally, the effect of increasing the fuselage weight by 10, 20, and 30 percent on the system response was evaluated for each of the active isolators.

All results are tabulated in the section of this report entitled Discussion of Results. However, in order to clarify some of the comments which will be made therein regarding the effect of parameter variations and design criteria on the system response, and at the same time to limit the number of figures to be presented, typical results for two cases are shown in detail; namely, the 2,000-lb helicopter with a two-blade rotor, and the 2,000-lb helicopter with a four-blade rotor.

The first case is for the lowest blade passage frequency considered in the analysis (13.3 Hz), and represents the worst condition from the point of view of maintaining displacement control under the steady-state vibratory excitation condition described on page 7. For this case, the allowable acceleration loop gain based on stability considerations is large. Very large values of relative displacement gain are therefore required to limit the landing transient displacements to within the desired magnitudes. In-flight transient deflections are very small as a result of the large relative displacement gain.

The second case is for the highest blade passage frequency (26.6 Hz) and represents the worst condition from the point of view of: a) maintaining displacement control under 3 g in-flight maneuver condition, and b) maintaining the required margin of stability. For this case, stability considerations allow only a very small value of acceleration loop gain. Therefore, very little (in fact, zero) relative displacement gain is required to limit the landing transient displacement to within the desired peak magnitude. Due to the low relative displacement gain, the resulting in-flight transient deflections are quite large, but not in excess of the maximum allowable.

In every case, the loop gain margin was maintained at a constant level and the relative displacement gain and lead network time constant were adjusted such that, under the 10 feet per second landing shock, the peak relative displacement was equal to that allowed by the design criterion. Thus, for the system gains selected, the relative displacement during the landing condition is independent of the helicopter configuration.

Open-Loop Response

Figure 14 shows the magnitude and phase diagrams of the complete system open-loop transfer function, Equation (46), for the 2,000-lb, two-blade helicopter designed on the basis of Criterion A. The response of the third notch contributes most to the total open-loop gain at the phase crossover frequency. As indicated by the dotted curve, elimination of the third notch, with all other system parameters remaining constant, results in a larger gain margin. Therefore, when only two notches are used, it is possible to increase the acceleration flow gain and still maintain the desired 20 db gain margin. This increase in flow gain results in a broader bandwidth for the two-notch isolator. In all cases the number of notches is limited to 3. For high blade passage frequencies, stability requirements placed a limitation on the allowable number of notches. For helicopters having low blade passage frequencies, additional notches of isolation could be added. However, the addition of notches would lower the bandwidth of all notches and not materially add to the overall isolation efficiency since high blade passage frequency excitations are quite small.

The allowable increase in acceleration flow gain due to elimination of the third notch is more pronounced for helicopters with high blade passage frequency, as shown in Figure 15. For high values of b/rev, the frequency at which the third notch occurs approaches the resonant frequencies of the actuator and servovalve. Therefore, only a very small acceleration flow gain can be introduced if the desired stability margin is to be maintained. Elimination of the third notch allows a significant increase in flow gain since the contribution of the second notch to the total gain is very small at higher frequencies.

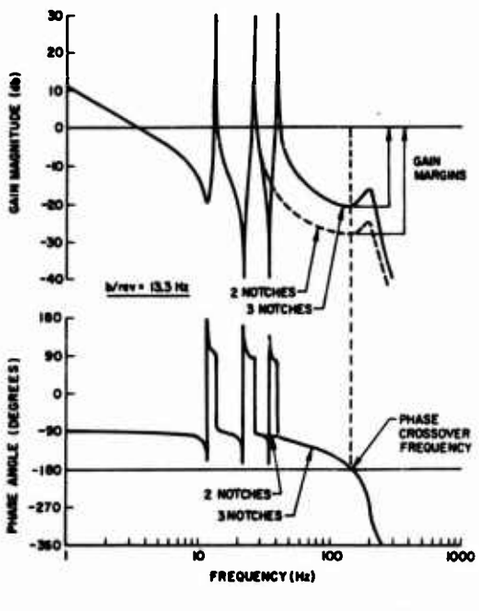

Figure 14. Magnitude and Phase Diagrams of the Open-Loop Transfer Function for 2,000-lb Helicopter, Two-Blade Rotor, Design Criterion A.

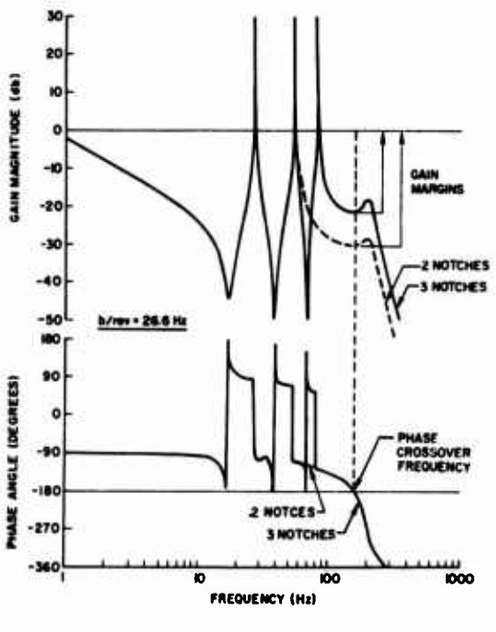

Figure 15. Magnitude and Phase Diagrams of the Open-Loop Transfer Function for 2,000-lb Helicopter, Four-Blade Rotor, Design Criterion A.

The gain margins shown in Figures 14 and 15 for the three-notch systems are typical of the stability margins obtained in all cases. The dotted curves represent the effect of eliminating only the third notch, leaving all feedback gains at the values optimized for the three-notch system. As shown in Tables IX and X, the two-notch system for any given helicopter employs values of feedback gains which differ from those used in the three-notch design. The gain margin for the two-notch system would be closer to the values given by the solid curves in Figures 14 and 15.

Response to Vibratory Excitations

As stated on Page 7, two types of vertical steady-state vibratory excitation conditions were considered, namely cruise and ground vibrations. Effectivenesses were calculated from Equations (36) and (37) for the vertical responses at both the fuselage and rotor centers of gravity, respectively, as a function of frequency. Although the rotor-induced excitations occur only at 1/rev, b/rev, 2b/rev, 3b/rev and 4b/rev, values of effectiveness were calculated at all frequencies from 1 to 1,000 Hz in order to better define the effect of the various feedback parameters, design criteria, and weight variations on the response of each system.

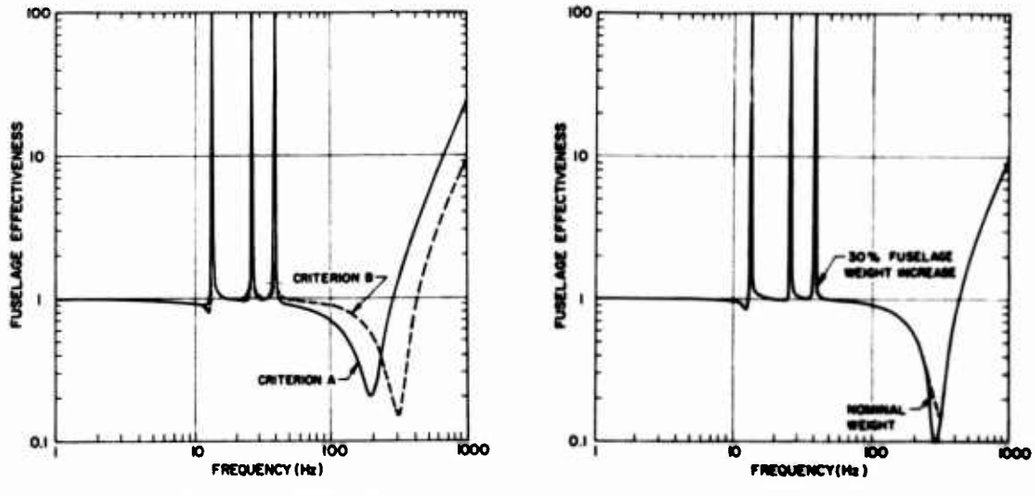

(a) COMPARISON OF DESIGN CRITERIA A AND B (NOMINAL GROSS WEIGHT)

(b) COMPARISON OF NOMINAL GROSS WEIGHT AND 30 % FUSELAGE WEIGHT INCREASE (CRITERION B)

Figure 16. Fuselage Effectiveness for 2,000-lb, Two-Blade Helicopter With Three-Notch Isolator During Cruise Vibrations (b/rev = 13.3 Hz).

Cruise Vibrations

Figure 16 (a) shows the fuselage effectiveness during cruise vibrations for the 2,000-lb, two-blade helicopter isolator with three notches. At the notch frequencies the effectiveness is greater than 100, regardless of isolator design criteria or fuselage weight variation. From Equation (56) the isolated fuselage acceleration is theoretically zero at the notch frequency; therefore, the theoretical fuselage effectiveness should be infinite. At frequencies above the actuator resonance (above $\approx$ 400 Hz), the fuselage effectiveness is greater than one, indicating that passive isolation is provided at high frequencies by the actuator itself.

The isolator designed for Criterion B employs a shorter stroke actuator and different values of gain than Criterion A. For the same supported weight, the actuator resonant frequency for Criterion B is higher than for Criterion A. Therefore, just as for a system with two notches rather than three notches, the use of an actuator of shorter stroke necessitates decreased flow gains resulting in narrower notch bandwidth and a greatly reduced peak transient deflection.

As shown in Figure 16 (b), for any given isolator design, increases in fuselage weight do not affect the fuselage effectiveness except in the region corresponding to actuator resonance frequency and at higher frequencies.

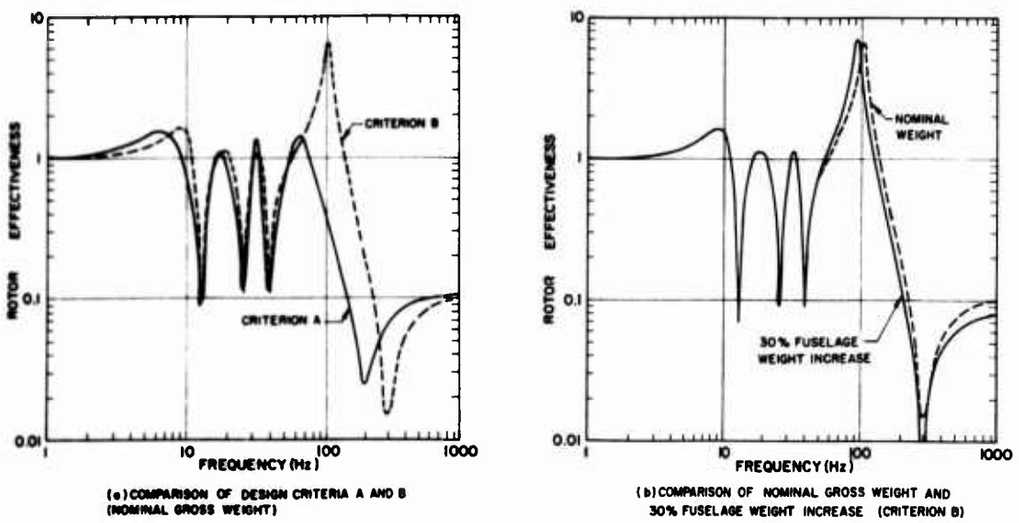

Figure 17. Rotor Effectiveness for 2,000-lb, Two-Blade Helicopter With Three-Notch Isolator During Cruise Vibrations (b/rev = 13.3 Hz).

Figure 17 (a) shows the rotor effectiveness during cruise vibrations for the 2,000-lb, two-blade helicopter isolation system with three notches. At the notch frequencies, the rotor effectiveness is equal to 1/M [Equation (57)]. At high frequencies, the rotor effectiveness also approaches a value of 1/M [Equation (37)]. As in the case of the fuselage effectiveness, the rotor responses for Criteria B and A differ in the neighborhood of the actuator resonance due to the higher actuator resonant frequency and the lower damping coefficient associated with Criterion B. The lower flow gains required for Criterion B again result in narrow bandwidths of isolation at the notches. This effect is more noticeable for the rotor response since any changes in fuselage response are magnified at the rotor by the factor of 1/M. In the low frequency range, the lower gain associated with Criterion B results in a higher resonant frequency and increased damping. Finally, as shown in Figure 17 (b), increases in fuselage weight do not affect the rotor effectiveness except in the region corresponding to the actuator resonant frequency.

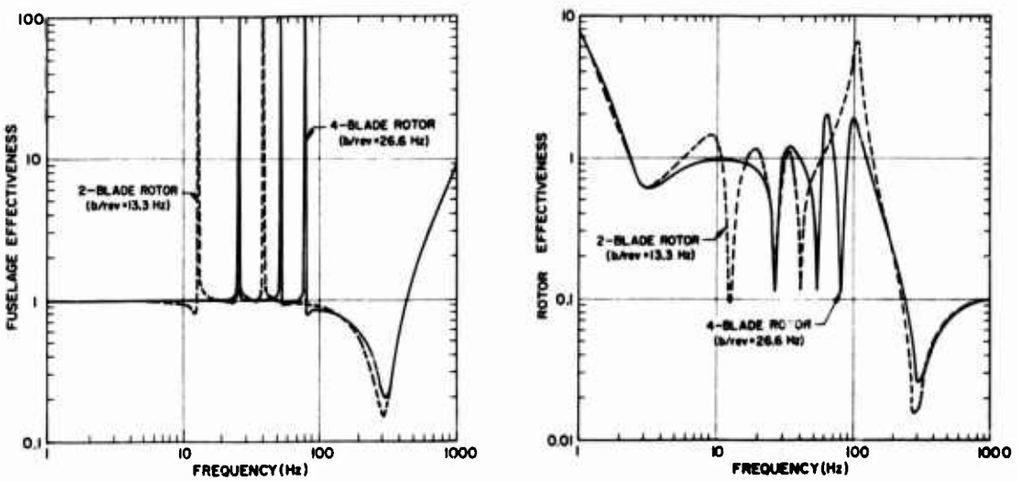

Figure 18. Fuselage and Rotor Effectiveness for 2,000-lb Helicopter With Three-Notch Isolator During Cruise Vibrations (Design Criterion B).

Figure 18 shows the effect of blade passage frequency on the response of both the rotor and fuselage. The effectiveness curves shown are for the 2,000-lb, two-blade and four-blade helicopter isolators with three notches. The excitation frequencies for the four-blade helicopter occur nearer the actuator resonant frequency, resulting in a lower flow gain for the four-blade design than for the two-blade design. The effect of lower gains on the notch bandwidth and effectiveness at low frequencies is similar for both the rotor and fuselage. One difference is evident in the neighborhood of the third notch for the four-blade design, where the phase interaction between the third notch and the actuator resonance results in much lower values of rotor effectiveness.

Comparison of Two- and Three-Notch Systems

Figure 19 shows the fuselage and rotor response to cruise vibrations for the 2,000-lb, two-blade helicopter with two notches of isolation for design Criteria A and B. Elimination of the third notch results in the required displacement control to be attained with lower values of flow gain.

Comparison of Figure 19 with Figures 16 and 17 indicates that the lower values of flow gain result in narrower notch bandwidths and a more stable system. The higher values of effectiveness shown for the 2,000-lb, two-blade, two-notch system in the neighborhood of the actuator resonance for Criterion B are primarily due to the higher value of velocity feedback gain employed in this case (see Tables IX and X). The higher value of velocity gain was required to limit fuselage amplification at low frequencies. The difference in effectiveness between the two- and three-notch designs is not as pronounced in the remaining cases since the gain of the velocity feedback is either much smaller or zero.

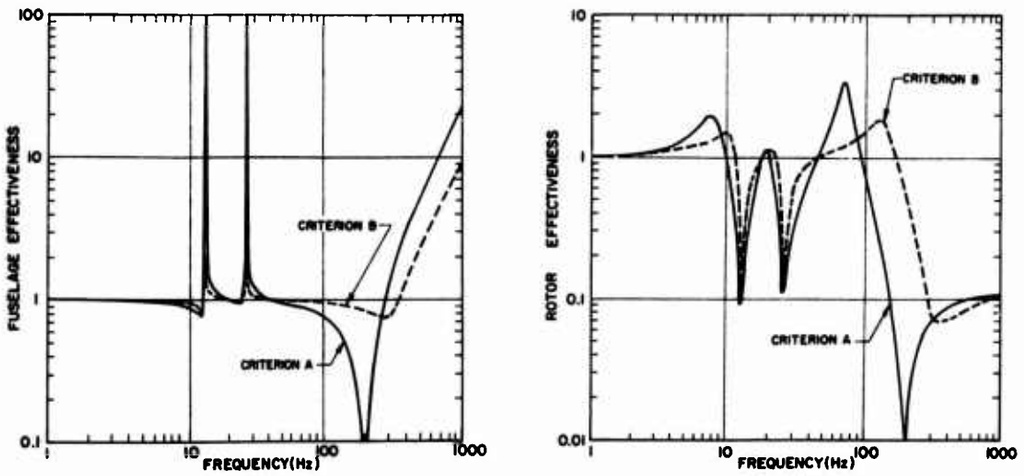

Figure 19. Fuselage and Rotor Effectiveness for 2,000-lb, Two-Blade Helicopter With Two-Notch Isolator During Cruise Vibrations for Nominal Helicopter Gross Weight (b/rev = 13.3 Hz).

Response of System Designed for Criterion C

The feedback parameter gains for Design Criterion C were selected to result in the same displacement control as for Criterion B but with a larger margin of stability. As shown in Tables IX and X, the acceleration flow gain for Criterion C is lower than for Criteria A and B, while the displacement feedback gain is kept the same as for Criterion A. The vibration response of systems designed for Criterion C is similar to the response of Criterion B except for slightly wider notch bandwidths and higher fuselage effectiveness at frequencies other than the notch frequencies.

Ground Vibrations

For ground vibration excitations, the fuselage and rotor effectiveness are given by Equations (36) and (37) with values of 3 Hz and 0.3 for the undercarriage resonant frequency and damping, respectively, based on the nominal total fuselage gross weight. Figures 20 and 21 show the fuselage and rotor effectiveness for ground vibrations for the same cases shown in Figures 16 and 17 for cruise vibrations.

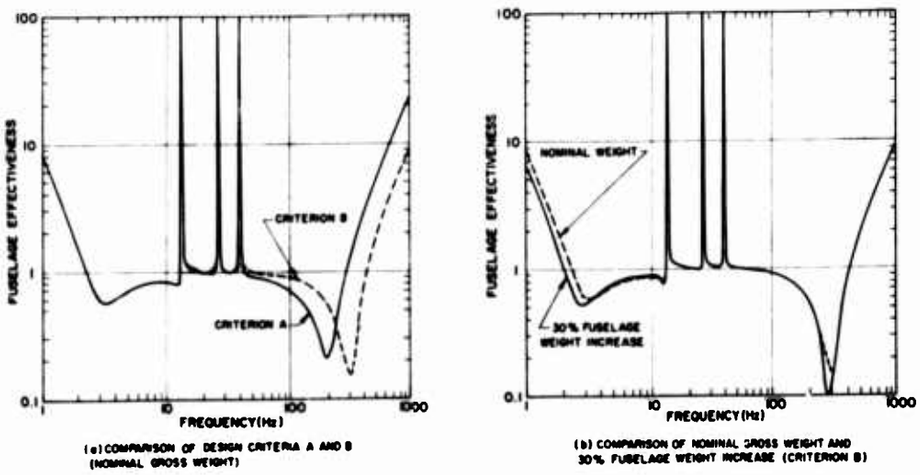

Figure 20. Fuselage Effectiveness for 2,000-lb, Two-Blade Helicopter With Three-Notch Isolator During Ground Vibrations (b/rev = 13.3 Hz).

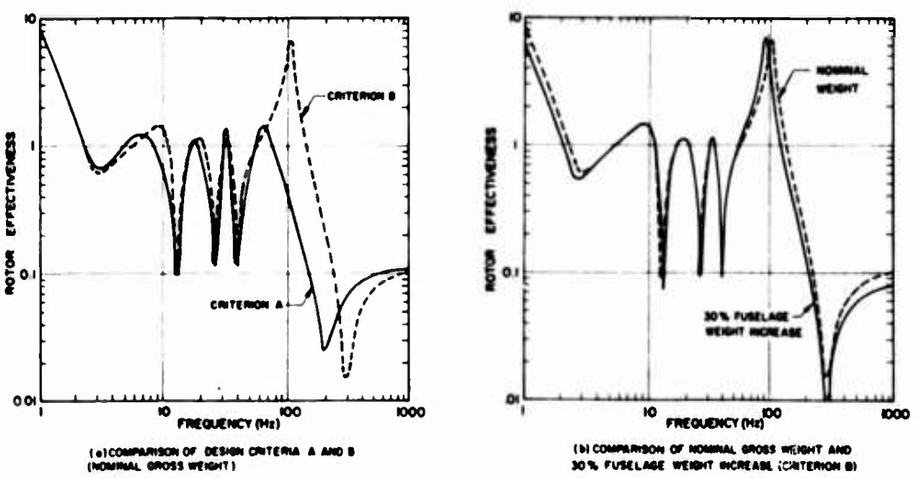

Figure 21. Rotor Effectiveness for 2,000-lb, Two-Blade Helicopter With Three-Notch Isolator During Ground Vibrations (b/rev = 13.3 Hz).

In the frequency range above 10 Hz, the response of the rotor and fuselage to cruise and ground vibrations is identical, since the undercarriage resonant frequency falls well below the first notch of isolation. At low frequencies, the increase in both rotor and fuselage effectiveness is due to the stiffness of the undercarriage and not to the active isolator. As shown in Figures 20 (b) and 21 (b), changes in fuselage weight affect both the rotor and fuselage effectiveness at low frequencies.

Response to Flight Maneuvers

The excitation applied to the rotor during flight maneuvers is a ramp in acceleration. Two values of peak acceleration (+3 g and - 0.5 g) and three values of rise time (0.6, 0.8 and 1.0 sec) were to be considered.

The fuselage and rotor accelerations and relative displacements were calculated from Equations (36) through (38), excluding the actuator and servovalve dynamics, since the response of the system to the long rise-time maneuver loads is controlled primarily by the low-frequency dynamic characteristics of the various components. This simplification allowed generation of the time solutions using a high speed analog computer.

Figure 22 shows the analog diagram of the isolation system, with the associated coefficient and voltage scale factors. The time scale of the solution is 1/100. The magnitude of T in Figure 22 is shown divided by 100 so that the frequencies indicated in the analog diagram are based on real time. The fuselage and rotor acceleration time histories and relative displacement time histories were obtained from oscilloscope traces of the analog computer output.

Typical fuselage acceleration responses to the +3 g, 0.6 sec rise-time maneuver are shown in Figure 23 for the 2,000-lb helicopter with the isolation system designed to Criterion B requirements. The fuselage acceleration follows the excitation very closely except for a very small overshoot. The rotor acceleration responses, for the same cases, are shown in Figure 24. Again the rotor acceleration follows the excitation except for a small overshoot and subsequent oscillations having a frequency content corresponding to the notch frequencies. The oscillations, in both the rotor and fuselage accelerations, result from excitations of the notch-producing elements and are small in magnitude due to the relatively small energy content of the transient excitation at the notch frequencies. The acceleration overshoot of the rotor is greater than that of the fuselage since the control system applies the same force to both the fuselage and rotor masses. Therefore, the lighter mass experiences a larger peak acceleration; however, in neither case does the acceleration overshoot exceed 3 percent.

The fuselage and rotor accelerations for the ramps of longer rise-time (0.8 and 1.0 sec) will show the same characteristics except for lower

values of overshoot, since the system will be able to follow the longer rise-time maneuvers more closely. Equations (36) and (37) indicate that the rotor and fuselage accelerations are directly proportional to the level of peak maneuver acceleration $F_o / (M_R + M_F)$. Therefore, for the case of the -0.5 g maneuvers, the peak accelerations will be - 1/6 the values shown for the +3 g maneuver.

Typical relative displacement time histories for the +3 g, 0.6 rise-time maneuver are shown in Figures 25 (a), (b), and (c). The maximum displacement occurs during the rise-time in the acceleration ramp. Depending on the value of the lead in the acceleration network τ_1 , the relative displacement will either return to zero rapidly and oscillate about zero, or return to zero asymptotically. For high values of b/rev, Figure 25 (c), the selected gain parameters result in a very sluggish response, whereas the response for lower values of b/rev is less damped, Figures 25 (a) and (b). In order to categorize the displacement response to the transient excitations and attempt to define a measure of merit on the speed of response of the system, the characteristics of these two types of displacement time histories are defined as shown in Figure 26. Values of displacement time history characteristics are tabulated in Table XVI for all configurations.

As indicated in Equation (67), the peak displacement due to an acceleration ramp is directly proportional to the level of acceleration input $F_o/(M_R + M_F)$ and inversely proportional to the rise-time. Therefore, for the - 0.5 g maneuvers, the peak displacement will be - 1/6 those for the +3 g maneuver. Longer rise-times than 0.6 second will also result in proportionately lower peak displacements. The typical effect of varying the rise-time of the maneuver load from 0.6 to 1.0 second is shown in Figure 27.

One comment should be made regarding the relative displacements during in-flight transient and steady-state vibratory excitations. For helicopters with high blade passage frequency, the relative displacement under +3 g transient maneuvers is greater than the relative displacement under $\pm$0.3 g vibratory excitations. For low blade passage frequencies the relative displacement under transient excitation is less than under vibratory excitations. As previously stated, in the latter case stability requirements allow introduction of higher values of displacement gain; therefore, better displacement control during transient maneuvers can be achieved. In all cases, of course, the relative displacement under landing transients is kept within the maximum value set forth by the design criterion.

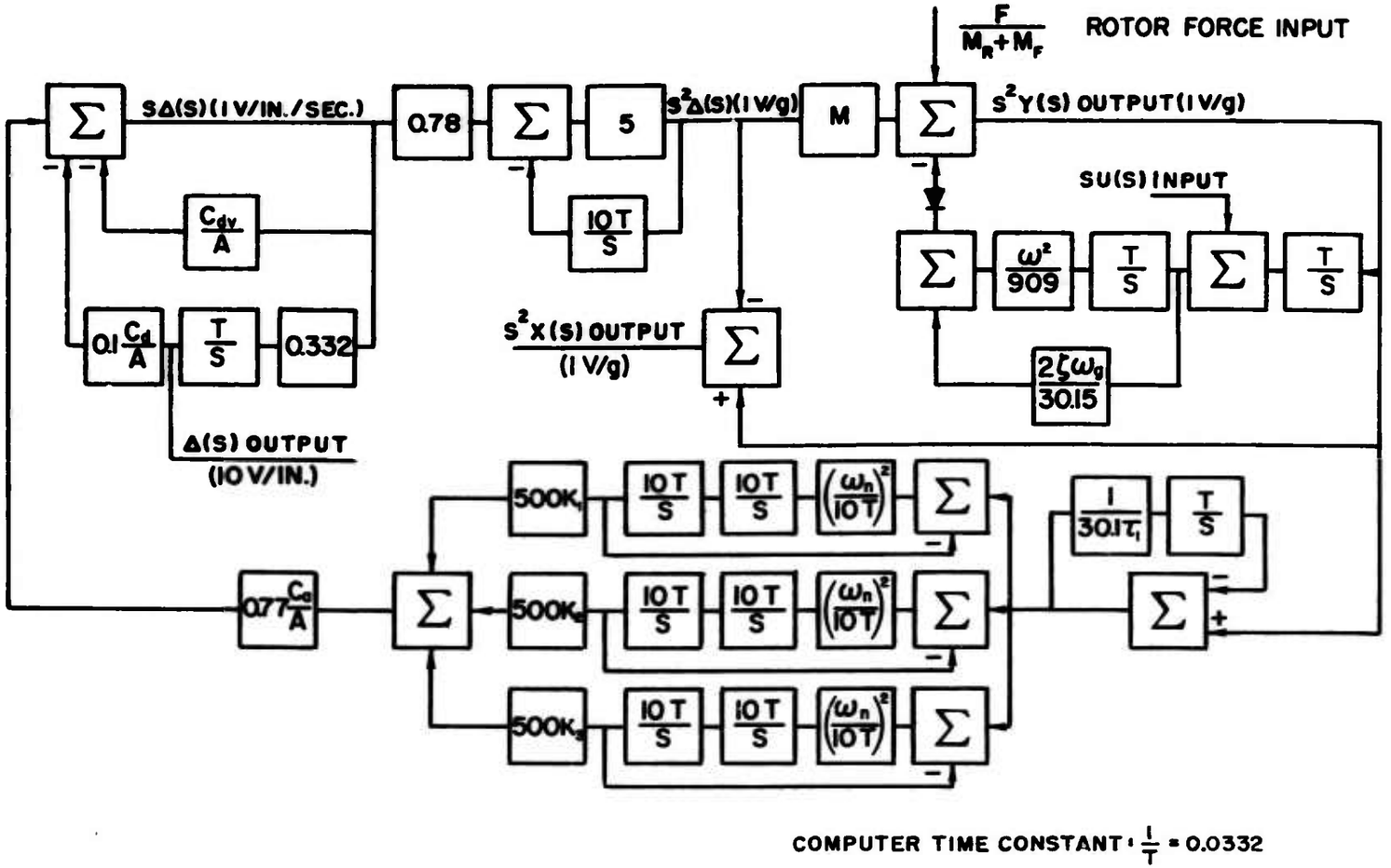

Figure 22. Analog Computer Block Diagram for Electronic System With Three Notches of Isolation.

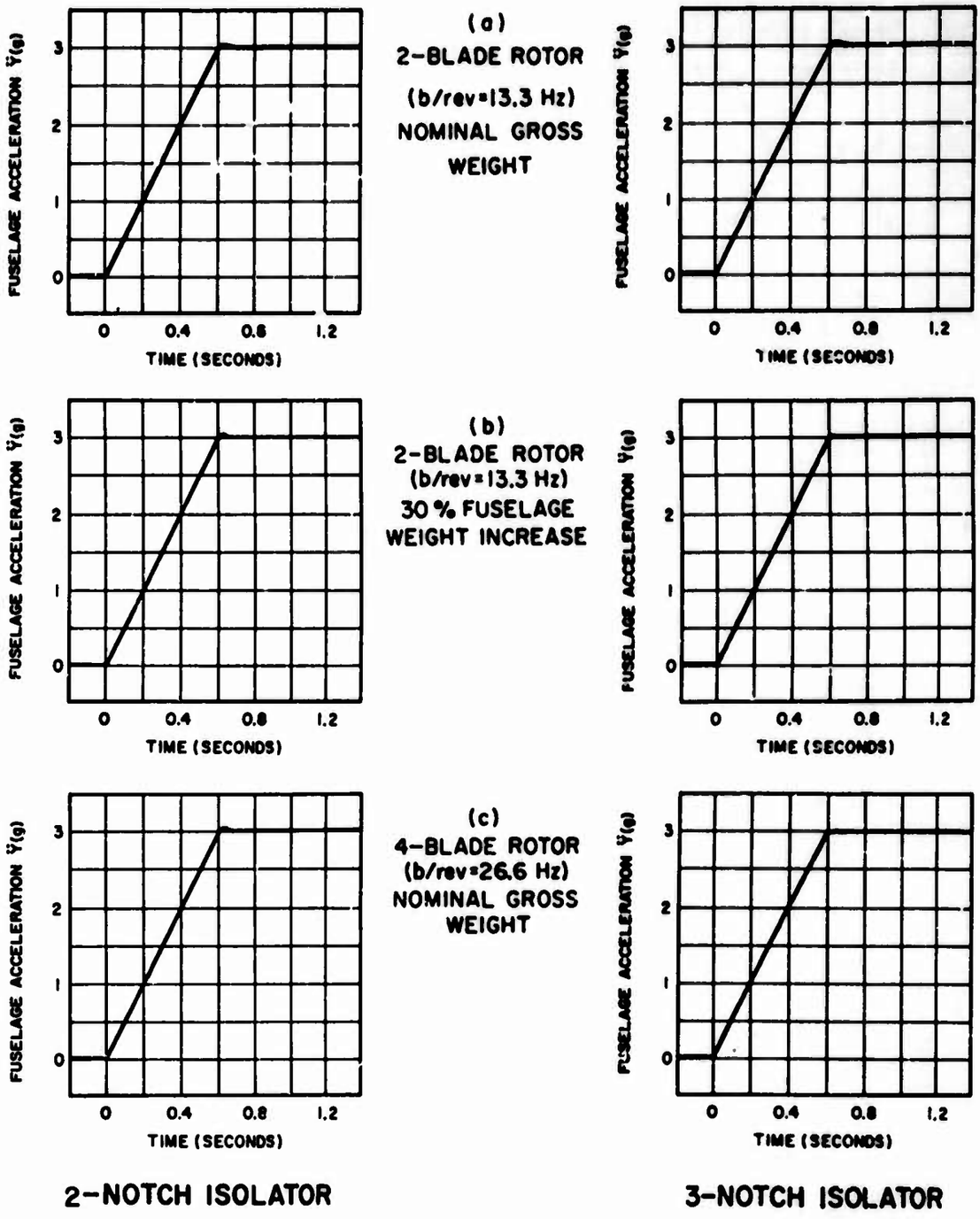

Figure 23. Typical Fuselage Acceleration Response for 2,000-lb Helicopter With Criterion B Isolation System Design Subjected to +3g, 0.6 Second Rise-Time Maneuver.

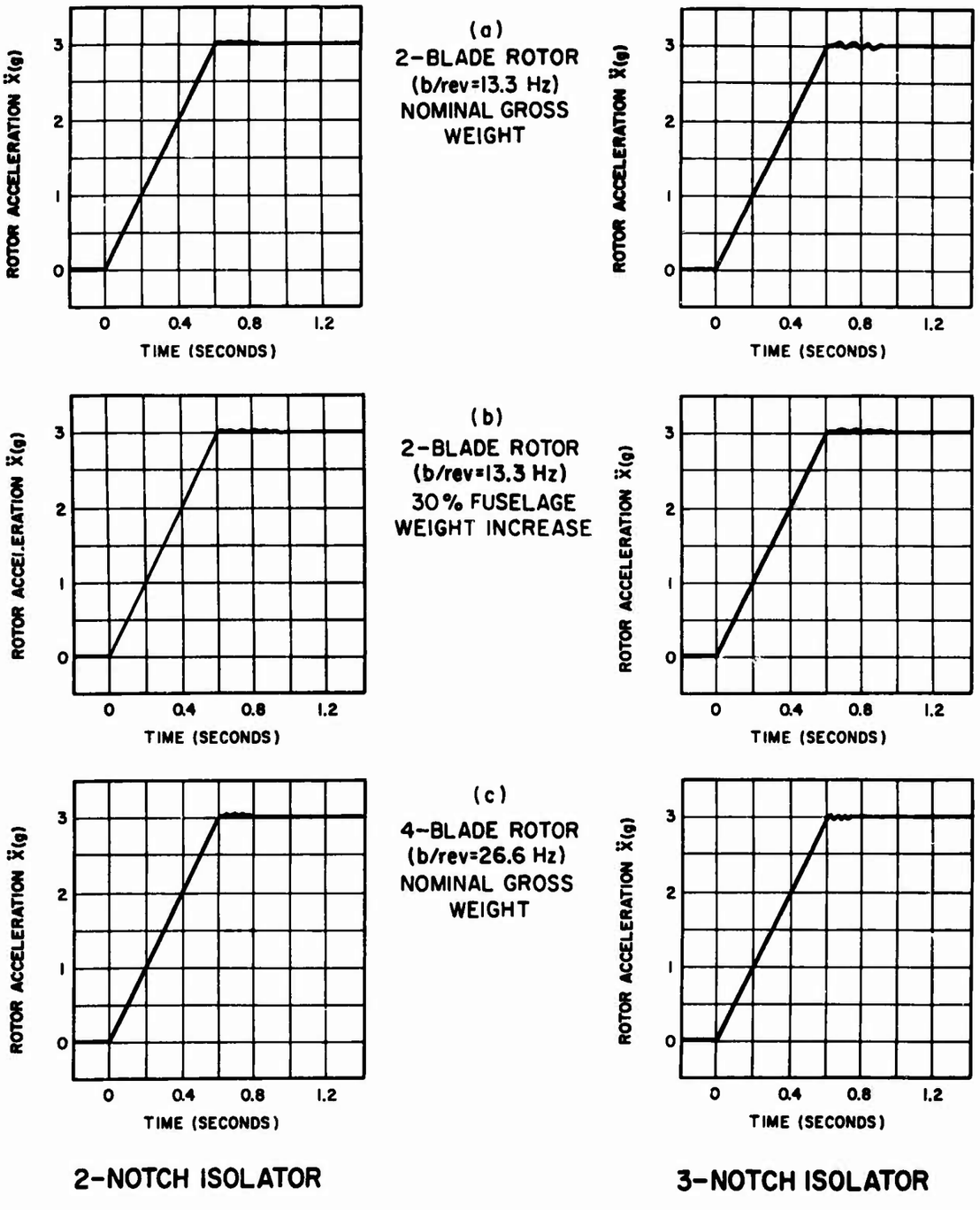

Figure 24. Typical Rotor Acceleration Response for 2,000-lb Helicopter With Criterion B Isolation System Design Subjected to +3 g, 0.6 Second Rise-Time Maneuver.

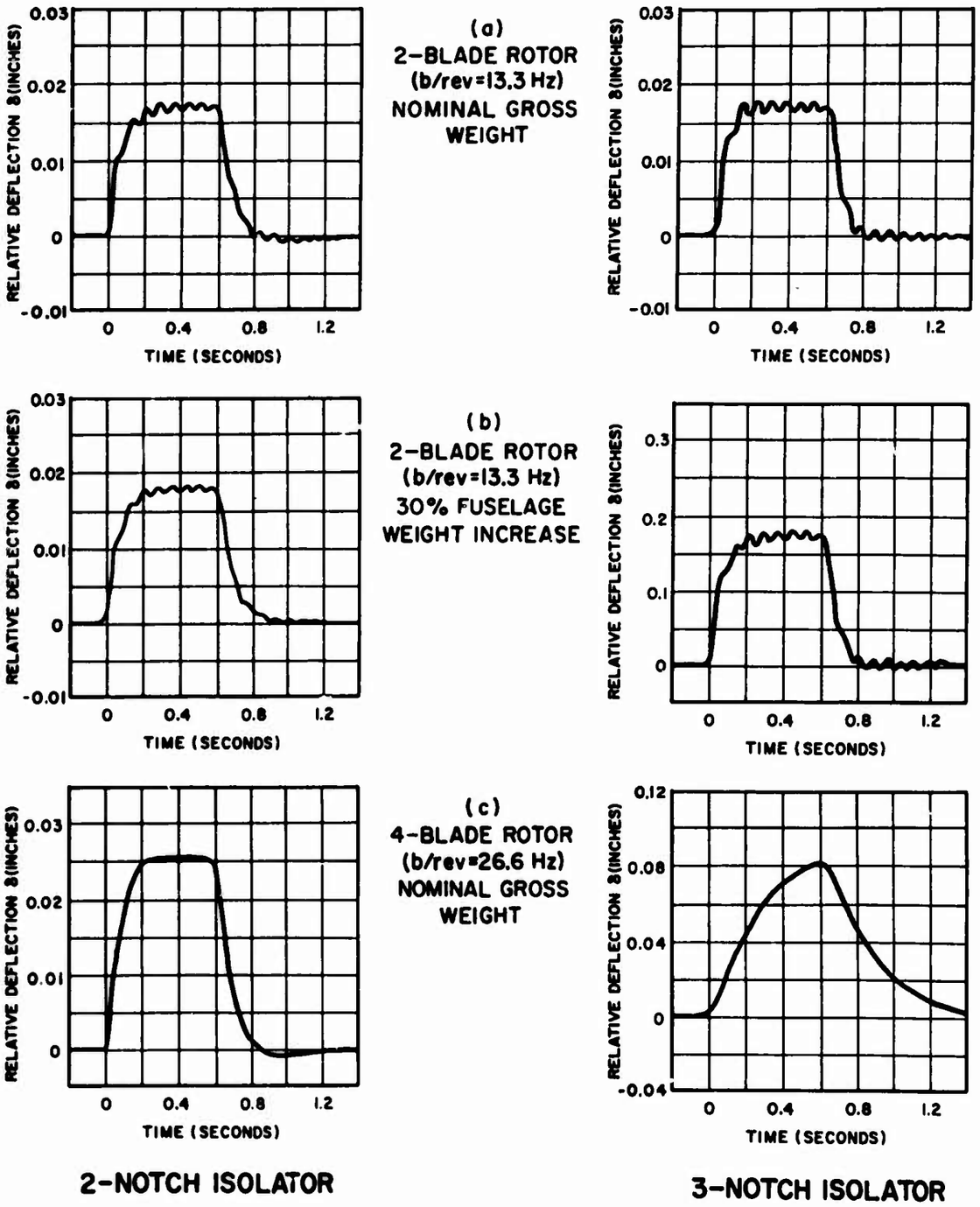

Figure 25. Typical Relative Displacement Response for 2,000-lb Helicopter With Criterion B Isolation System Design Subjected to +3 g, 0.6 Second Rise-Time Maneuver.

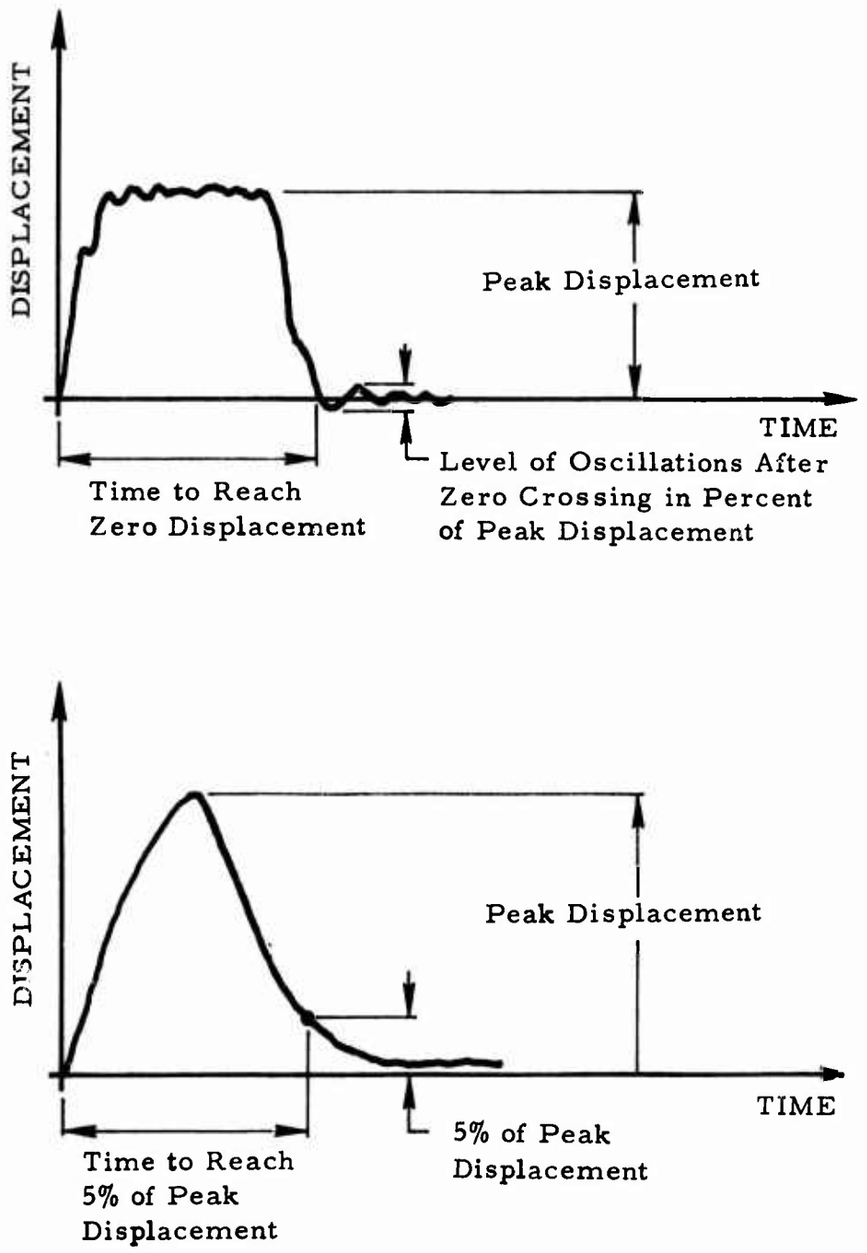

Figure 26. Characteristics of Relative Displacement Between Fuselage and Rotor Due to Transient Maneuver.

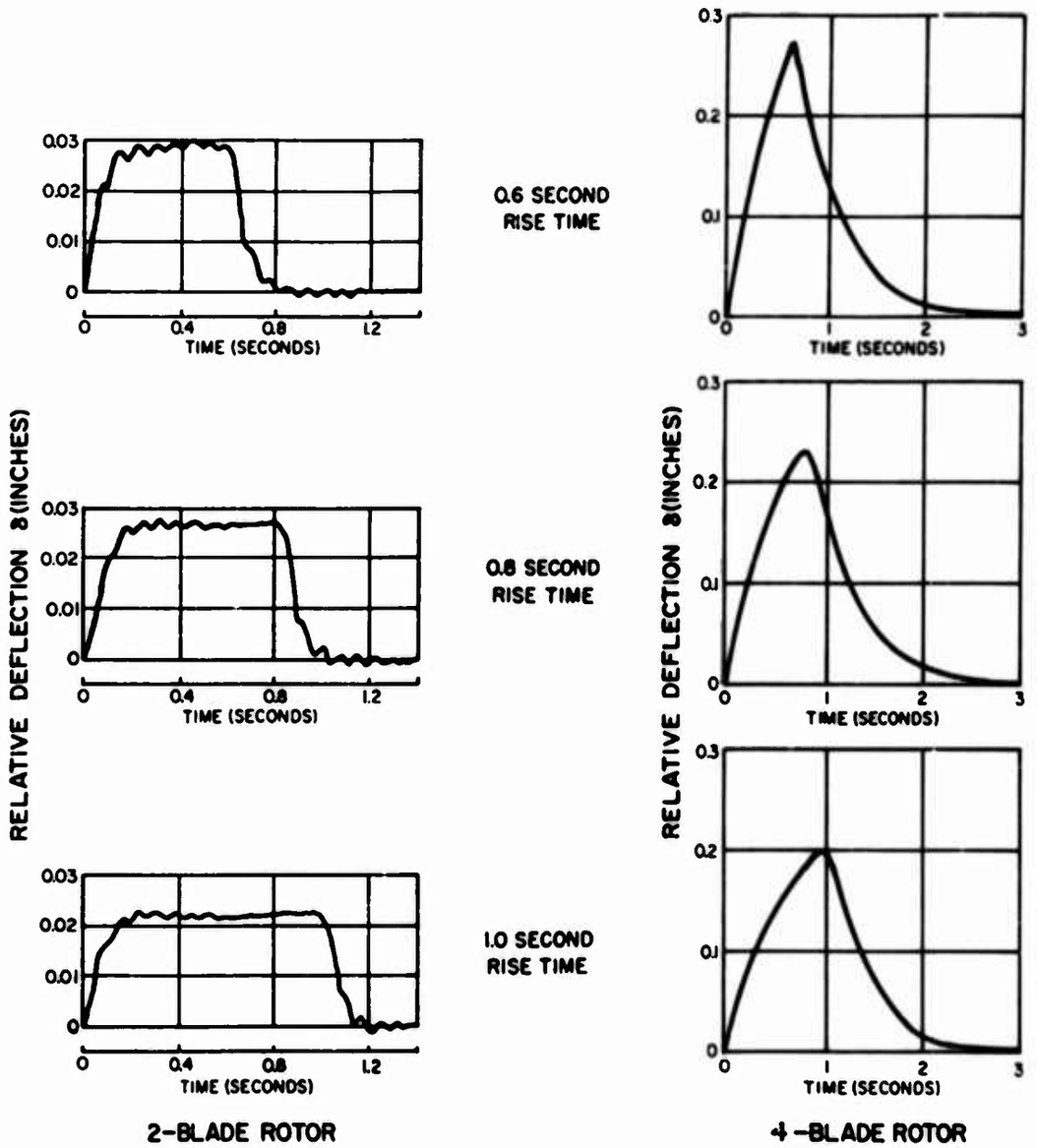

Figure 27. Effect of +3 g Maneuver Load Rise-Time Duration on the Relative Response for 2,000-lb Helicopter With Two-Notch Criterion A Isolation System Design and Nominal Gross Weight.

Response to Landing Shock

The response of the system to the landing velocity shocks was calculated from Equations (39) through (41) using the analog computer simulation shown in Figure 22.

Figures 28 and 29 show typical fuselage and rotor acceleration time histories, respectively, for the 10 ft/sec landing velocity. Examination of the fuselage acceleration indicates that it deviates little from the response that would be obtained without the isolation system, except for the small oscillations at the isolator notch frequencies. The portion of the acceleration time history having zero magnitude indicates that the helicopter bounces off the ground after first impact. It was assumed that the 10 ft/sec landing velocity corresponds to a crash landing, and that no lift is provided by the rotor under this condition. Therefore, the bounce time of the helicopter is kept to a minimum. The rotor response is highly oscillatory, due to the fast rise-time of the fuselage response which excites the notch oscillators in the acceleration loop.

The effect of changing the fuselage mass on the system response is shown by comparing Figure 28 (a) with 28 (b), and Figure 29 (a) with 29 (b). The magnitude of the transmitted accelerations decreases with increasing fuselage mass. This change can be attributed to the lower resonant frequency and damping fraction of the heavier helicopter resting on the landing gear. As the fuselage mass increases, both the resonant frequency and damping fraction of the helicopter decrease, resulting in lower values of the initial fuselage acceleration. The initial fuselage acceleration excites the notch oscillators, and a decrease in its magnitude with increasing fuselage weight causes a reduction in the amplitude of the high-frequency oscillations and the associated reduction in the accelerations transmitted to the rotor during landing.

The effect of blade passage frequency on the system response is indicated by comparing Figures 28 (a) with 28 (c), and 29 (a) with 29 (c).

Typical relative displacement time histories for the 10 ft/sec landing shock are shown in Figure 30. For low values of b/rev [Figures 30 (a) and (b)], the system is relatively undamped, and the displacement response is characterized by a high frequency oscillatory motion superimposed on a lower frequency motion. The lower frequency oscillations are due to the helicopter resting on the landing gear, while the higher frequency motions are due to the response of the notch oscillators. For systems with high b/rev, Figure 30 (c), the response is highly damped and the level of high frequency oscillations is small.

Figure 31 shows the typical system response to a 5 ft/sec landing velocity shock. For this lower level of landing velocity, the helicopter does not bounce off the ground. Comparison of Figure 31 with Figures 28 (a), (b) and (c) shows that the acceleration and relative displacement peak amplitudes are half those for the 10 ft/sec landing shock. However, because the helicopter does not bounce off the ground for the lower level landing velocity shock, the shape of the acceleration and relative displacement time histories after the first peak is slightly different than for the more severe landing condition.

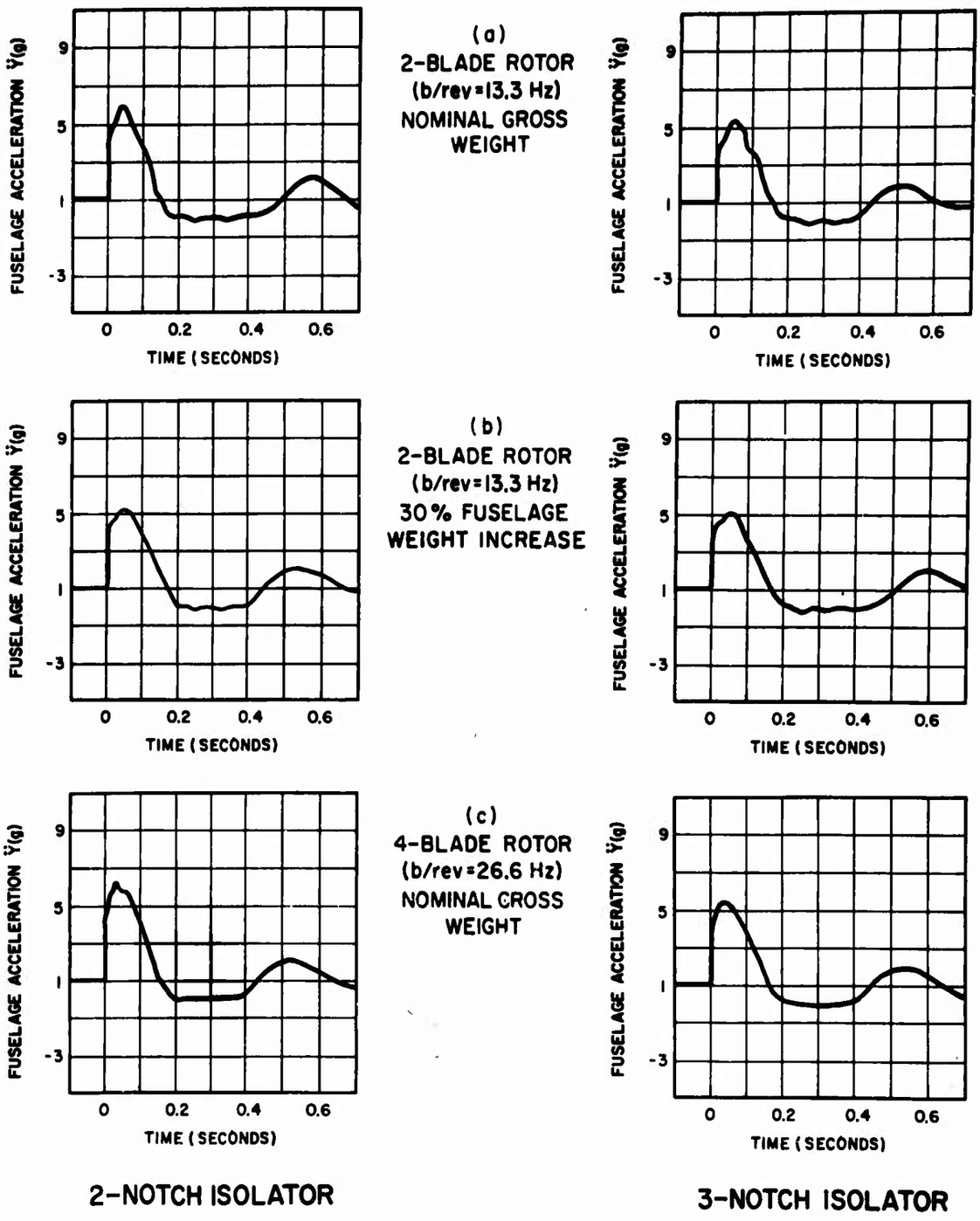

Figure 28. Typical Fuselage Acceleration Response for 2,000-lb Helicopter With Criterion B Isolation System Design Subjected to 10 ft/sec Landing Velocity Shock.

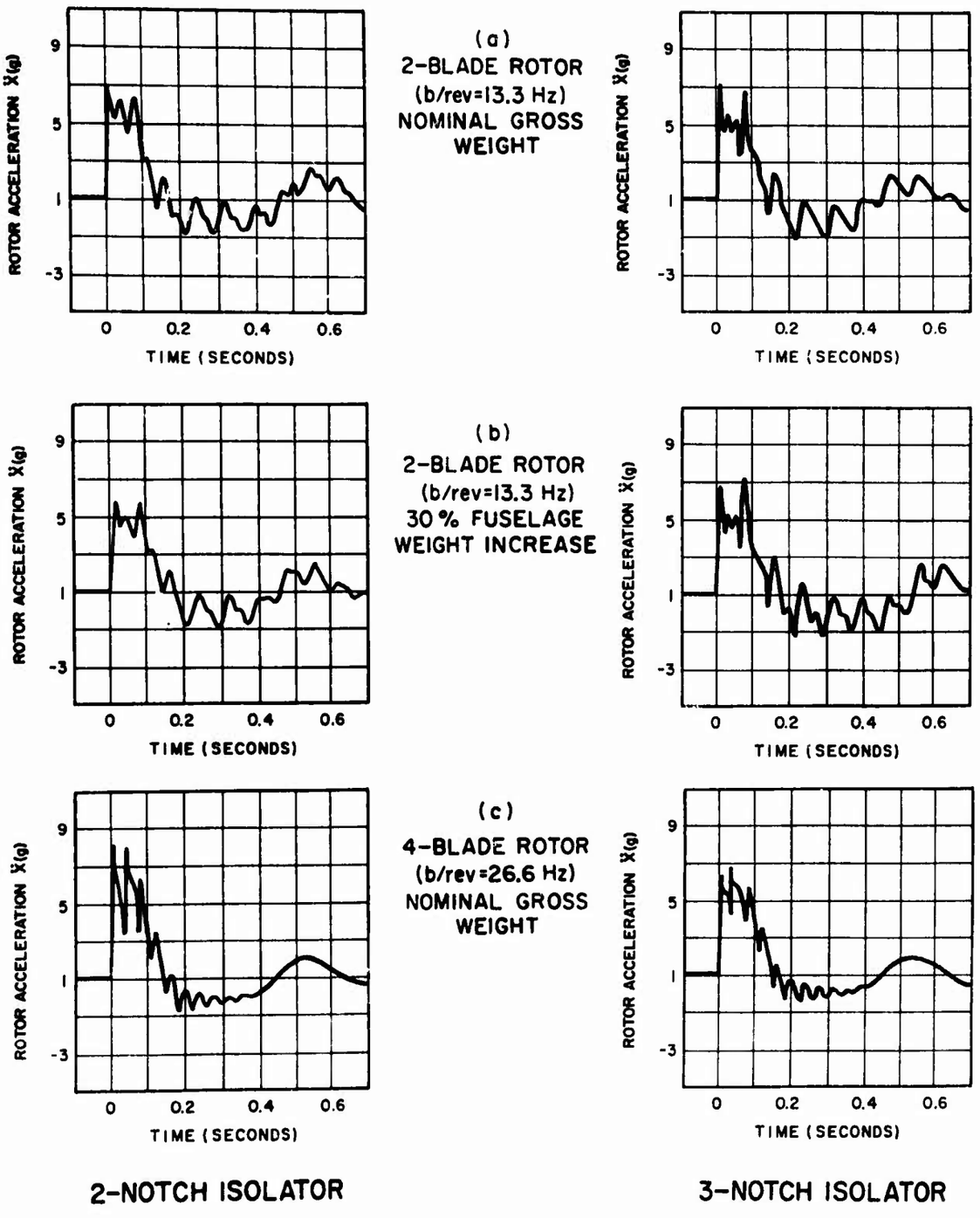

Figure 29. Typical Rotor Acceleration Response for 2,000-lb Helicopter With Criterion B Isolation System Design Subjected to 10 ft/sec Landing Velocity Shock.

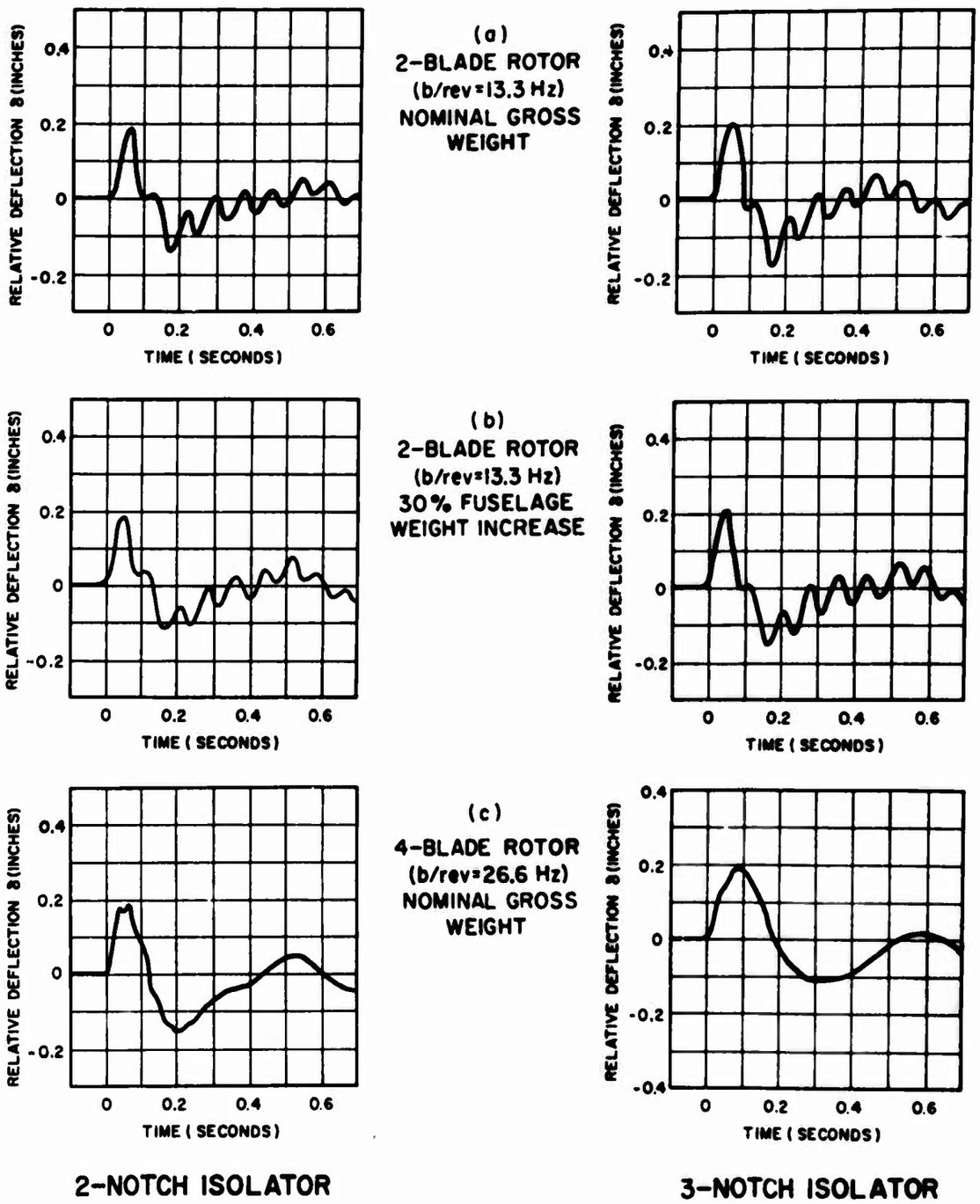

Figure 30. Typical Relative Displacement Response for 2,000-lb Helicopter With Criterion B Isolation System Design Subjected to 10 ft/sec Landing Velocity Shock.

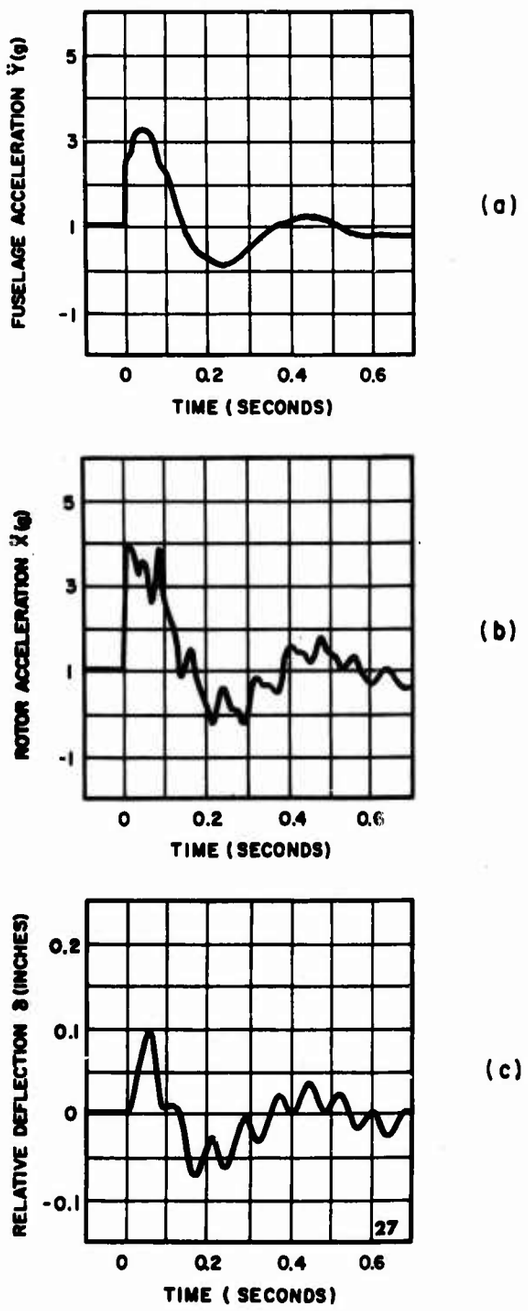

Figure 31. Fuselage Acceleration, Rotor Acceleration and Relative Displacement Response for 2,000-lb, Two-Blade Helicopter With Two-Notch Criterion B Isolation System Design and Nominal Gross Weight Subjected to 5 ft/sec Landing Velocity Shock.

DISCUSSION OF RESULTS

The investigation reported herein is intended tc verify the feasibility of effectively isolating helicopter fuselages from rotor-induced vibratory forces. Existing electrohydraulic systems are modified to result in virtually zero forces being transmitted to the fuselage at the critical excitation frequencies. System parameters are selected to yield maximum relative displacements under transient excitations which are compatible with helicopter control requirements. The evaluation includes helicopter fuselages weighing from 2,000 to 80,000 pounds, with blade passage frequencies ranging from 13.3 Hz to 26.6 Hz. The analysis considers vertical rotor-induced vibratory forces, both cruise and on the ground; vertical rotor-induced transient loads during in-flight maneuvers; and landing velocity shocks. The rotor and fuselage are assumed to be lumped rigid masses, and only single-rotor configurations having the rotor shaft aligned with the center of gravity of the fuselage are considered.

The results of the parametric study show the response of the selected electrohydraulic notch isolation system to the various types of excitations in tabular form, in terms of rotor and fuselage accelerations, relative displacement between the rotor and fuselage, system stability, power requirements, and estimated isolation system weight. System performance and requirements are evaluated as a function of the number of notches of isolation, increases in fuselage weight, and maximum allowable relative displacement during landing.

Identification of each case considered in the study is shown in Table IV. The following paragraphs present a discussion of the results.

STATIC DEFLECTION

The static deflection in all cases is zero [Equation (9)]. In the event the active system becomes inoperative, a pseudo static deflection can be defined in terms of the compressibility of the oil contained within the actuator chambers, the piston area, and the stroke, for the condition of zero leakage. Values of pseudo isolator stiffness and static deflection are shown in Table XI.

TABLE XI

SUMMARY OF SYSTEM PSEUDO STATIC DEFLECTION

Fuselage Weight For All Cases	Design Criterion	Pseudo Isolator Stiffness* (lb/in.)	Pseudo Static Deflection** (in.)
Nominal	A	8.16×10^5	0.00245
+10%	A	8.16×10^5	0.00270
+20%	A	8.16×10^5	0.00294
+30%	A	8.16×10^5	0.00319
Nominal	B and C	2.04×10^6	0.00098
+10%	B and C	2.04×10^6	0.00108
+20%	B and C	2.04×10^6	0.00118
+30%	B and C	2.04×10^6	0.00127

* Defined as $\frac{2\beta A}{L}$ where β = 200,000 lb/in.^{2}
A = average actuator area, in.^{2}
L = actuator stroke, in.

** Defined as the ratio of fuselage weight to pseudo isolator stiffness. The actual static deflection with the active system in operation is zero in all cases.

DYNAMIC RESPONSE

Vibratory Excitations

Figure 32 shows the total normalized relative deflection between the rotor and fuselage due to vibratory excitations at the notch frequencies, calculated for a broad range of blade passage frequencies, using Equations (61) and (62) for the three- and two-notch systems, respectively. As previously noted, at the notch frequencies, the system response to vibratory excitations is independent of the feedback gain parameters. Thus, the relative displacements due to steady-state vibratory excitations are independent of Criteria A, B and C. Based on typical values of unisolated helicopter accelerations $F_{MAX}/(W_R + W_r)$ = 0.3g, the total relative displacement ranges from $\pm$0.165 inch for b/rev of 13.3 Hz to $\pm$0.042 inch for b/rev of 26.6 Hz.

In all cases, the fuselage effectiveness at b/rev, 2b/rev and 3b/rev (the latter frequency applying only to the three-notch isolator) is greater than 100. The isolation system incorporates a tracking network that is able to place the frequency of the isolation notch at the blade passage frequency and its harmonics, even though operational changes in rotor speed may cause the blade passage frequency to vary as much as 20 percent (see Table II). Therefore, since the frequencies of vertical rotor-induced excitation are automatically tracked, the accelerations transmitted to the isolated fuselage will always be at least 1/100 those experienced by the unisolated fuselage subjected to rotor-induced forces of the same magnitude.

The effectiveness curves, however, were calculated as a function of frequency to allow evaluation of the bandwidth of isolation at each of the notches. The notch bandwidth affects the maximum relative deflections under transient conditions. Specifically, broader bandwidths give rise to large transient displacements. The system parameters which define the notch bandwidth also affect system stability. A broad bandwidth would result in less stringent tracking requirements. Therefore, a comparison of bandwidths at each of the notch frequencies between the various cases and criteria considered serves to evaluate the performance of the active isolation systems.

Figure 33 shows the percentage notch bandwidth of all the isolators considered as a function of blade passage frequency. The percentage bandwidth is calculated from Equation (53). The response of the third notch contributes most to the total open-loop gain at the phase crossover frequency. Elimination of the third notch, with all other system parameters remaining constant, results in a larger gain margin (Figures 14 and 15). Therefore, when only two notches are used it is possible to increase the acceleration flow gain and still maintain the desired 20db gain margin. This increase in flow gains results in a broader bandwidth for the two-notch isolator, regardless of isolator design criterion.

The allowable increase in acceleration flow gain due to elimination of the third notch is more significant for helicopters with high blade passage frequency. For high values of b/rev, the frequency at which the third notch

occurs approaches the resonant frequency of the actuator. Therefore, only a very small amount of acceleration flow gain can be introduced if the desired stability margin is to be maintained. Elimination of the third notch allows a significant increase in flow gain since the contribution of the second notch to the total gain is very small at higher frequencies.

In all cases the notch bandwidth decreases with increasing blade passage frequency, due to the inability to introduce a high enough value of flow gain and still maintain the desired system margin of stability. Finally, for the highest value of blade passage frequency considered (b/rev = 26.6 Hz) and three notches, the displacement feedback gain for Criteria A and C could not be reduced from the values used in Criterion B without resulting in a very sluggish system response. The curves shown in Figure 33 for Criteria A and C were extended based on the shape of the curve for Criterion B. Selection of a slightly lower maximum value of b/rev than 26.6 Hz would have allowed definition of the curves at higher values of b/rev.

In all cases, increases in fuselage weight do not significantly change the rotor and fuselage effectiveness. However, the fuselage-to-rotor mass ratio affects the value of the total open-loop gain [Equation (82)]. An increase in the fuselage weight results in a lower acceleration flow gain, an associated increase in system stability, and a decrease in notch bandwidth.

The comments made above apply to both cruise and ground vibratory conditions. The landing gear has no effect upon the response of the system at the notch frequencies, since the resonant frequency of the total helicopter mass on the landing gear is well below the blade passage frequency in all cases.

As previously stated, notches of isolation were introduced at only b/rev, 2b/rev and 3b/rev (the latter only for the three-notch system). Nevertheless, the investigation called for evaluation of effectivenesses at 1/rev and 4b/rev in addition to those at which notches are introduced. Tables XII and XIII show the fuselage and rotor effectivenesses at 1/rev, b/rev, 2b/rev, 3b/rev and 4b/rev for cruise and ground vibrations, respectively.

Tables XIV and XV show the fuselage and rotor accelerations at the five critical frequencies for cruise and ground vibrations, respectively, normalized with respect to the acceleration of the unisolated rotor at b/rev, $F_0/(M_R + M_F)$. The normalized acceleration is calculated as the product of the normalized rotor excitation at each critical frequency (Figure 1) and the inverse of the effectiveness at that frequency.

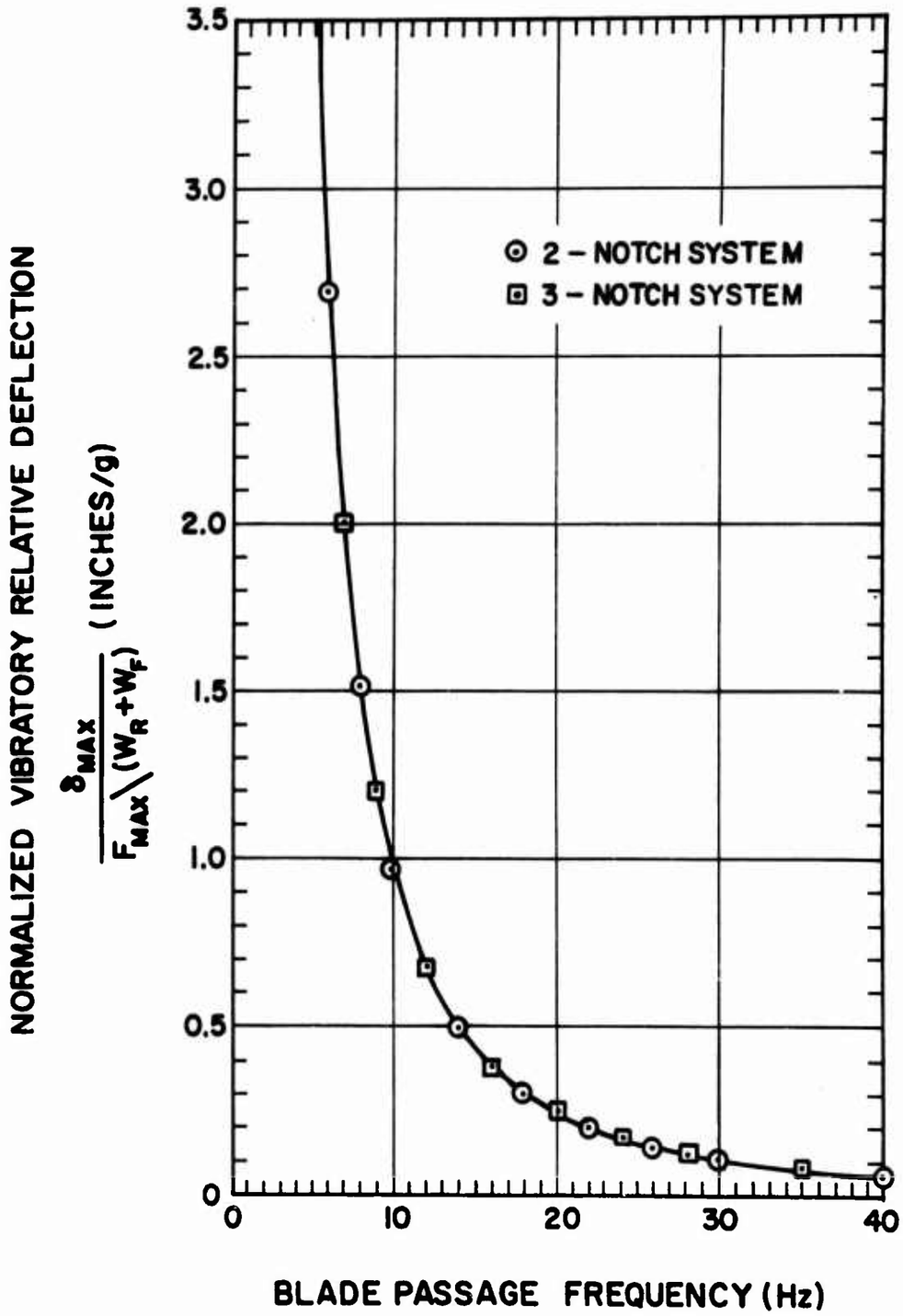

Figure 32. Relationship Between Normalized Peak Relative Deflection and Blade Passage Frequency During Steady-State Vibration

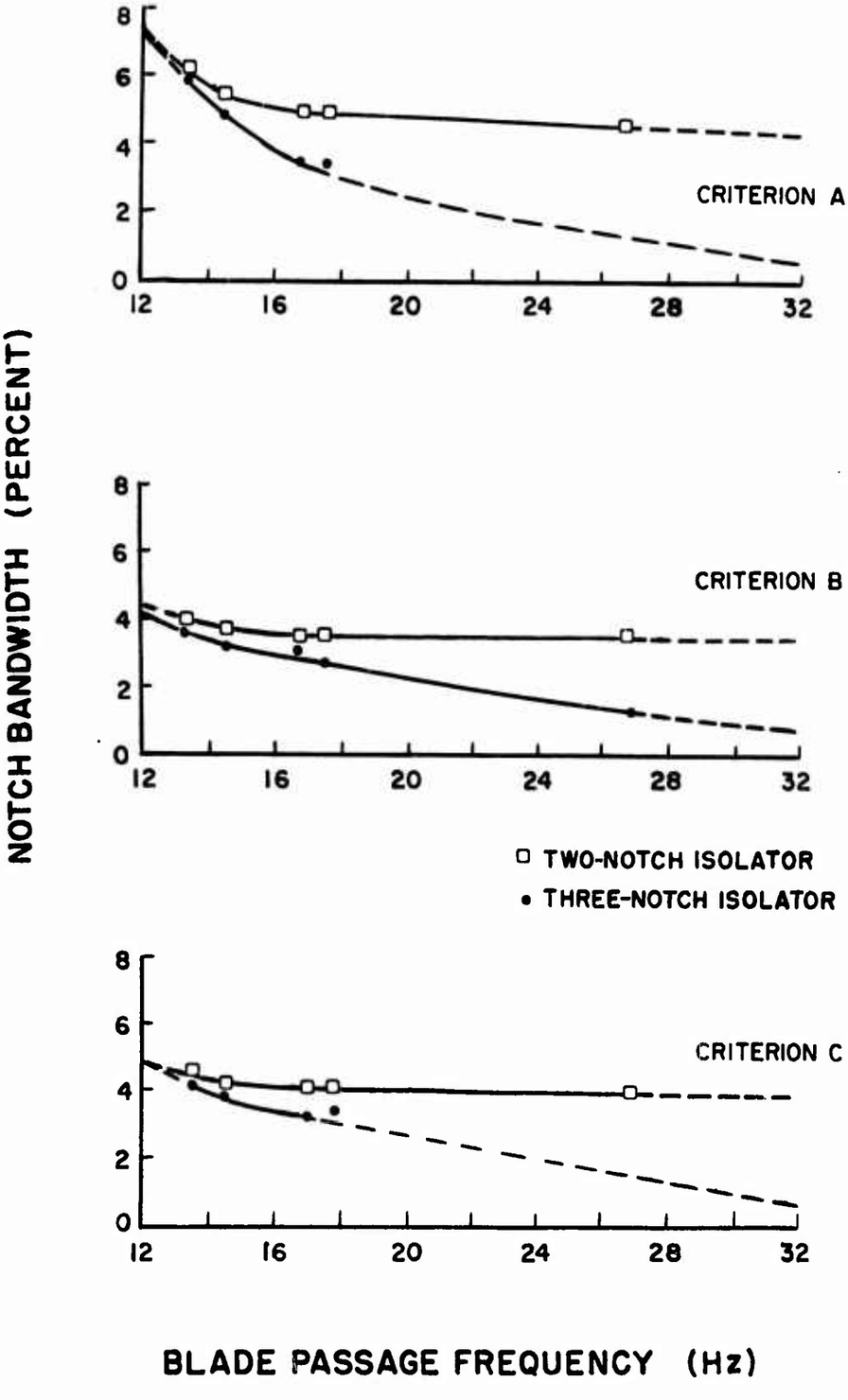

Figure 33. Relationship Between Notch Bandwidth [Equation (53)] and Blade Passage Frequency for Two- and Three-Notch Isolators Having Parameters Based on Criteria A, B, and C.

TABLE XII

SUMMARY OF FUSELAGE AND ROTOR EFFECTIVENESSES FOR CRUISE VIBRATIONS

Case Number	Criterion	Fuselage Effectiveness					Rotor Effectiveness				
		1/rev	b/rev	2b/rev	3b/rev	4b/rev	1/rev	b/rev	2b/rev	3b/rev	4b/rev
2.2.2a	A	0.948	>100	>100	0.982	0.934	1.703	0.111	0.111	0.718	1.418
b	A	0.952	>100	>100	0.979	0.934	1.704	0.102	0.102	0.730	1.492
c	A	0.956	>100	>100	0.978	0.934	1.714	0.094	0.094	0.749	1.626
d	A	0.958	>100	>100	0.976	0.934	1.721	0.088	0.088	0.767	1.768
2.2.2a	B	0.979	>100	>100	1.005	0.992	1.199	0.111	0.111	0.884	1.032
b	B	0.981	>100	>100	1.004	0.991	1.198	0.102	0.102	0.888	1.044
c	B	0.983	>100	>100	1.003	0.991	1.200	0.094	0.094	0.893	1.056
d	B	0.983	>100	>100	1.002	0.992	1.205	0.088	0.088	0.900	1.069
2.2.2a	C	0.976	>100	>100	0.990	0.971	1.176	0.111	0.111	0.988	1.286
b	C	0.979	>100	>100	0.989	0.971	1.231	0.102	0.102	1.003	1.326
c	C	0.980	>100	>100	0.989	0.971	1.235	0.094	0.094	1.021	1.375
d	C	0.981	>100	>100	0.988	0.971	1.238	0.088	0.088	1.040	1.426
2.4.2a	A	0.992	>100	>100	0.790	0.682	1.032	0.111	0.111	0.878	0.348
b	A	0.992	>100	>100	0.792	0.683	1.032	0.102	0.102	0.763	0.305
c	A	0.993	>100	>100	0.795	0.684	1.032	0.094	0.094	0.671	0.272
d	A	0.993	>100	>100	0.796	0.683	1.032	0.088	0.088	0.601	0.246
2.4.2a	B	0.981	>100	>100	0.886	0.843	1.163	0.111	0.111	2.120	2.065
b	B	0.983	>100	>100	0.889	0.846	1.167	0.102	0.102	2.320	1.510
c	B	0.984	>100	>100	0.892	0.848	1.170	0.094	0.094	2.469	1.247
d	B	0.985	>100	>100	0.893	0.848	1.172	0.088	0.088	2.510	1.101
2.4.2a	C	0.973	>100	>100	0.786	0.721	0.806	0.111	0.111	0.2262	0.364
b	C	0.975	>100	>100	0.789	0.731	0.805	0.102	0.102	0.228	0.360
c	C	0.977	>100	>100	0.794	0.742	0.805	0.094	0.094	0.230	0.355
d	C	0.978	>100	>100	0.797	0.748	0.804	0.088	0.088	0.232	0.348

TABLE XII (continued)
SUMMARY OF FUSELAGE AND ROTOR EFFECTIVENESSES FOR CRUISE VIBRATIONS

Case Number	Criterion	Fuselage Effectiveness					Rotor Effectiveness				
		1/rev	b/rev	2b/rev	3b/rev	4b/rev	1/rev	b/rev	2b/rev	3b/rev	4b/rev
10.4.2a	A	0.981	>100	>100	0.862	0.824	1.163	0.111	0.111	2.083	1.255
b	A	0.983	>100	>100	0.868	0.827	1.167	0.102	0.102	2.037	1.048
c	A	0.984	>100	>100	0.870	0.830	1.171	0.094	0.094	1.930	0.898
d	A	0.985	>100	>100	0.873	0.831	1.174	0.088	0.088	1.794	0.793
10.4.2a	B	0.991	>100	>100	0.922	0.903	1.082	0.111	0.111	1.432	7.329
b	B	0.991	>100	>100	0.925	0.906	1.084	0.102	0.102	1.528	9.626
c	B	0.992	>100	>100	0.928	0.909	1.086	0.094	0.094	1.639	8.824
d	B	0.992	>100	>100	0.930	0.910	1.089	0.088	0.088	1.759	6.481
10.4.2a	C	0.992	>100	>100	0.943	0.929	1.068	0.111	0.111	1.933	2.100
b	C	0.992	>100	>100	0.945	0.930	1.070	0.102	0.102	2.055	2.146
c	C	0.993	>100	>100	0.947	0.931	1.072	0.094	0.094	2.180	2.145
d	C	0.993	>100	>100	0.948	0.931	1.074	0.088	0.088	2.308	2.109
20.5.2a	A	0.985	>100	>100	0.855	0.817	1.138	0.111	0.111	1.860	1.119
b	A	0.986	>100	>100	0.859	0.819	1.141	0.102	0.102	1.788	0.945
c	A	0.987	>100	>100	0.863	0.822	1.145	0.094	0.094	1.678	0.816
d	A	0.987	>100	>100	0.866	0.824	1.146	0.088	0.088	1.556	0.724
20.5.2a	B	0.994	>100	>100	0.917	0.898	1.047	0.111	0.111	1.441	10.650
b	B	0.995	>100	>100	0.920	0.901	1.048	0.102	0.102	1.539	11.728
c	B	0.995	>100	>100	0.923	0.904	1.050	0.094	0.094	1.652	7.843
d	B	0.995	>100	>100	0.925	0.906	1.051	0.088	0.088	1.773	5.356
20.5.2a	C	0.993	>100	>100	0.940	0.926	1.057	0.111	0.111	2.039	2.169
b	C	0.994	>100	>100	0.942	0.927	1.058	0.102	0.102	2.181	2.202
c	C	0.994	>100	>100	0.944	0.928	1.060	0.094	0.094	2.328	2.179
d	C	0.994	>100	>100	0.945	0.928	1.062	0.088	0.088	2.480	2.118

TABLE XII (continued)
SUMMARY OF FUSELAGE AND ROTOR EFFECTIVENESSES FOR CRUISE VIBRATIONS

Case Number	Criterion	Fuselage Effectiveness					Rotor Effectiveness				
		1/rev	b/rev	2b/rev	3b/rev	4b/rev	1/rev	b/rev	2b/rev	3b/rev	4b/rev
40.6.2a	A	0.988	>100	>100	0.859	0.821	1.107	0.111	0.111	2.039	1.190
b	A	0.989	>100	>100	0.864	0.824	1.110	0.102	0.102	1.971	0.998
c	A	0.989	>100	>100	0.868	0.826	1.113	0.094	0.094	1.851	0.760
d	A	0.990	>100	>100	0.870	0.828	1.115	0.088	0.088	1.710	0.760
40.6.2a	B	0.997	>100	>100	0.920	0.901	1.027	0.111	0.111	1.459	8.284
b	B	0.997	>100	>100	0.923	0.904	1.028	0.102	0.102	1.560	10.178
c	B	0.997	>100	>100	0.926	0.907	1.029	0.094	0.094	1.677	8.180
d	B	0.997	>100	>100	0.928	0.908	1.030	0.088	0.088	1.803	5.825
40.6.2a	C	0.995	>100	>100	0.942	0.927	1.044	0.111	0.111	1.971	2.122
b	C	0.995	>100	>100	0.944	0.928	1.046	0.102	0.102	2.099	2.163
c	C	0.995	>100	>100	0.946	0.930	1.047	0.094	0.094	2.230	2.152
d	C	0.996	>100	>100	0.947	0.930	1.048	0.088	0.088	2.365	2.105
80.6.2a	A	0.995	>100	>100	0.898	0.858	1.045	0.111	0.111	0.990	1.342
b	A	0.995	>100	>100	0.901	0.861	1.046	0.102	0.102	1.036	2.303
c	A	0.995	>100	>100	0.904	0.864	1.048	0.094	0.094	1.085	1.925
d	A	0.995	>100	>100	0.905	0.865	1.049	0.088	0.088	1.106	1.875
80.6.2a	B	0.998	>100	>100	0.983	0.959	1.015	0.111	0.111	0.919	1.342
b	B	0.998	>100	>100	0.983	0.959	1.016	0.102	0.102	0.935	1.399
c	B	0.998	>100	>100	0.982	0.960	1.017	0.094	0.094	0.951	1.462
d	B	0.998	>100	>100	0.982	0.954	1.017	0.088	0.088	0.968	1.632
80.6.2a	C	0.997	>100	>100	0.955	0.942	1.021	0.111	0.111	1.437	2.113
b	C	0.998	>100	>100	0.957	0.942	1.022	0.102	0.102	1.503	2.142
c	C	0.998	>100	>100	0.958	0.943	1.022	0.094	0.094	1.576	2.265
d	C	0.998	>100	>100	0.959	0.944	1.023	0.088	0.088	1.653	2.378

TABLE XII (continued)
SUMMARY OF FUSELAGE AND ROTOR EFFECTIVENESSES FOR CRUISE VIBRATIONS

Case Number	Criterion	Fuselage Effectiveness					Rotor Effectiveness				
		1/rev	b/rev	2b/rev	3b/rev	4b/rev	1/rev	b/rev	2b/rev	3b/rev	4b/rev
80.7.2a	A	0.992	>100	>100	0.871	0.833	1.071	0.111	0.111	1.905	1.526
b	A	0.992	>100	>100	0.875	0.837	1.073	0.102	0.102	1.975	1.249
c	A	0.993	>100	>100	0.879	0.839	1.075	0.094	0.094	1.976	1.059
d	A	0.993	>100	>100	0.881	0.841	1.077	0.088	0.088	1.928	0.925
80.7.2a	B	0.998	>100	>100	0.925	0.904	1.015	0.111	0.111	1.244	6.351
b	B	0.998	>100	>100	0.928	0.907	1.015	0.102	0.102	1.313	10.263
c	B	0.998	>100	>100	0.931	0.910	1.016	0.094	0.094	1.390	17.896
d	B	0.998	>100	>100	0.932	0.912	1.017	0.088	0.088	1.470	13.961
80.7.2a	C	0.996	>100	>100	0.947	0.933	1.030	0.111	0.111	1.799	2.048
b	C	0.997	>100	>100	0.949	0.934	1.031	0.102	0.102	1.902	2.116
c	C	0.997	>100	>100	0.950	0.935	1.032	0.094	0.094	2.008	2.146
d	C	0.997	>100	>100	0.951	0.936	1.033	0.088	0.088	2.1192	2.163
2.2.3a	A	0.947	>100	>100	>100	0.878	1.499	0.111	0.111	0.111	0.849
b	A	0.953	>100	>100	>100	0.880	1.487	0.102	0.102	0.102	0.875
c	A	0.956	>100	>100	>100	0.882	1.037	0.094	0.094	0.094	0.899
d	A	0.959	>100	>100	>100	0.883	1.498	0.088	0.088	0.088	0.917
2.2.3a	B	0.969	>100	>100	>100	0.970	1.326	0.111	0.111	0.111	0.840
b	B	0.972	>100	>100	>100	0.970	1.330	0.102	0.102	0.102	0.881
c	B	0.974	>100	>100	>100	0.970	1.335	0.094	0.094	0.094	0.902
d	B	0.976	>100	>100	>100	0.970	1.340	0.088	0.088	0.088	0.975
2.2.3a	C	0.979	>100	>100	>100	0.947	1.190	0.111	0.111	0.111	1.665
b	C	0.981	>100	>100	>100	0.949	1.194	0.102	0.102	0.102	1.700
c	C	0.982	>100	>100	>100	0.950	1.197	0.094	0.094	0.094	1.826
d	C	0.983	>100	>100	>100	0.951	1.201	0.088	0.088	0.088	1.969

TABLE XII (continued)
SUMMARY OF FUSELAGE AND ROTOR EFFECTIVENESSES FOR CRUISE VIBRATIONS

Case Number	Criterion	Fuselage Effectiveness					Rotor Effectiveness				
		1/rev	b/rev	2b/rev	3b/rev	4b/rev	1/rev	b/rev	2b/rev	3b/rev	4b/rev
2.4.3a*	A	-	-	-	-	-	-	-	-	-	-
b*	A	-	-	-	-	-	-	-	-	-	-
c*	A	-	-	-	-	-	-	-	-	-	-
d*	A	-	-	-	-	-	-	-	-	-	-
2.4.3a	B	0.994	>100	>100	>100	0.834	1.039	0.111	0.111	0.111	1.374
b	B	0.994	>100	>100	>100	0.838	1.040	0.102	0.102	0.102	1.579
c	B	0.995	>100	>100	>100	0.842	1.040	0.094	0.094	0.094	1.332
d	B	0.995	>100	>100	>100	0.841	1.040	0.088	0.088	0.088	1.117
2.4.3a*	C	-	-	-	-	-	-	-	-	-	-
b*	C	-	-	-	-	-	-	-	-	-	-
c*	C	-	-	-	-	-	-	-	-	-	-
d*	C	-	-	-	-	-	-	-	-	-	-
10.4.3a	A	0.995	>100	>100	>100	0.815	1.029	0.111	0.111	0.111	1.328
b	A	0.995	>100	>100	>100	0.819	1.030	0.102	0.102	0.102	1.133
c	A	0.995	>100	>100	>100	0.823	1.030	0.094	0.094	0.094	0.986
d	A	0.996	>100	>100	>100	0.825	1.030	0.088	0.088	0.088	0.470
10.4.3a	B	0.989	>100	>100	>100	0.886	1.096	0.111	0.111	0.111	19.59
b	B	0.990	>100	>100	>100	0.890	1.099	0.102	0.102	0.102	12.97
c	B	0.990	>100	>100	>100	0.895	1.101	0.094	0.094	0.094	7.56
d	B	0.991	>100	>100	>100	0.897	1.103	0.088	0.088	0.088	5.191
10.4.3a	C	0.998	>100	>100	>100	0.925	1.016	0.111	0.111	0.111	2.470
b	C	0.998	>100	>100	>100	0.926	1.016	0.102	0.102	0.102	2.530
c	C	0.998	>100	>100	>100	0.928	1.016	0.094	0.094	0.094	2.523
d	C	0.998	>100	>100	>100	0.929	1.017	0.088	0.088	0.088	2.468

TABLE XII (continued)
SUMMARY OF FUSELAGE AND ROTOR EFFECTIVENESSES FOR CRUISE VIBRATIONS

Case Number	Criterion	Fuselage Effectiveness					Rotor Effectiveness				
		1/rev	b/rev	2b/rev	3b/rev	4b/rev	1/rev	b/rev	2b/rev	3b/rev	4b/rev
20.5.3a	A	0.995	>100	>100	>100	0.806	1.034	0.111	0.111	0.111	1.187
b	A	0.995	>100	>100	>100	0.810	1.034	0.102	0.102	0.102	1.023
c	A	0.995	>100	>100	>100	0.814	1.035	0.094	0.094	0.094	0.898
d	A	0.996	>100	>100	>100	0.816	1.035	0.088	0.088	0.088	0.805
20.5.3a	B	0.992	>100	>100	>100	0.880	1.073	0.111	0.111	0.111	11.27
b	B	0.992	>100	>100	>100	0.885	1.074	0.102	0.102	0.102	7.42
c	B	0.993	>100	>100	>100	0.890	1.076	0.094	0.094	0.094	5.192
d	B	0.993	>100	>100	>100	0.892	1.078	0.088	0.088	0.088	3.93
20.5.3a	C	0.998	>100	>100	>100	0.921	1.016	0.111	0.111	0.111	2.415
b	C	0.998	>100	>100	>100	0.923	1.017	0.102	0.102	0.102	2.634
c	C	0.998	>100	>100	>100	0.925	1.017	0.094	0.094	0.094	2.591
d	C	0.998	>100	>100	>100	0.926	1.017	0.088	0.088	0.088	2.497
40.6.3a	A	0.995	>100	>100	>100	0.822	1.036	0.111	0.111	0.111	1.239
b	A	0.995	>100	>100	>100	0.825	1.036	0.102	0.102	0.102	1.065
c	A	0.995	>100	>100	>100	0.828	1.037	0.094	0.094	0.094	0.932
d	A	0.996	>100	>100	>100	0.830	1.037	0.088	0.088	0.088	0.835
40.6.3a	B	0.994	>100	>100	>100	0.894	1.052	0.111	0.111	0.111	12.419
b	B	0.994	>100	>100	>100	0.898	1.053	0.102	0.102	0.102	8.577
c	B	0.994	>100	>100	>100	0.901	1.054	0.094	0.094	0.094	5.864
d	B	0.995	>100	>100	>100	0.904	1.055	0.088	0.088	0.088	4.341
40.6.3a	C	0.998	>100	>100	>100	0.928	1.016	0.111	0.111	0.111	2.567
b	C	0.998	>100	>100	>100	0.929	1.017	0.102	0.102	0.102	2.618
c	C	0.998	>100	>100	>100	0.930	1.017	0.094	0.094	0.094	2.591
d	C	0.998	>100	>100	>100	0.931	1.017	0.088	0.088	0.088	2.514

TABLE XII (continued)
SUMMARY OF FUSELAGE AND ROTOR EFFECTIVENESSES FOR CRUISE VIBRATIONS

Case Number	Criterion	Fuselage Effectiveness					Rotor Effectiveness				
		1/rev	b/rev	2b/rev	3b/rev	4b/rev	1/rev	b/rev	2b/rev	3b/rev	4b/rev
80.6.3a	A	0.993	>100	>100	>100	0.836	1.056	0.111	0.111	0.111	1.852
b	A	0.993	>100	>100	>100	0.841	1.058	0.102	0.102	0.102	1.608
c	A	0.994	>100	>100	>100	0.846	1.059	0.094	0.094	0.094	1.454
d	A	0.994	>100	>100	>100	0.850	1.060	0.088	0.088	0.088	1.322
80.6.3a	B	0.998	>100	>100	>100	0.897	1.020	0.111	0.111	0.111	1.799
b	B	0.998	>100	>100	>100	0.901	1.021	0.102	0.102	0.102	1.941
c	B	0.998	>100	>100	>100	0.906	1.022	0.094	0.094	0.094	2.097
d	B	0.998	>100	>100	>100	0.908	1.023	0.088	0.088	0.088	2.256
80.6.3a	C	0.997	>100	>100	>100	0.933	1.026	0.111	0.111	0.111	2.428
b	C	0.997	>100	>100	>100	0.935	1.026	0.102	0.102	0.102	2.610
c	C	0.997	>100	>100	>100	0.937	1.027	0.094	0.094	0.094	2.783
d	C	0.997	>100	>100	>100	0.939	1.028	0.088	0.088	0.088	2.944
80.7.3a	A	0.990	>100	>100	>100	0.784	1.081	0.111	0.111	0.111	0.942
b	A	0.991	>100	>100	>100	0.791	1.083	0.102	0.102	0.102	0.859
c	A	0.992	>100	>100	>100	0.797	1.085	0.094	0.094	0.094	0.787
d	A	0.992	>100	>100	>100	0.802	1.086	0.088	0.088	0.088	0.728
80.7.3a	B	0.996	>100	>100	>100	0.894	1.031	0.111	0.111	0.111	1.778
b	B	0.996	>100	>100	>100	0.895	1.032	0.102	0.102	0.102	1.794
c	B	0.997	>100	>100	>100	0.901	1.033	0.094	0.094	0.094	1.788
d	B	0.997	>100	>100	>100	0.904	1.034	0.088	0.088	0.088	1.752
80.7.3a	C	0.996	>100	>100	>100	0.928	1.036	0.111	0.111	0.111	4.678
b	C	0.996	>100	>100	>100	0.929	1.037	0.102	0.102	0.102	5.083
c	C	0.996	>100	>100	>100	0.931	1.038	0.094	0.094	0.094	5.053
d	C	0.996	>100	>100	>100	0.932	1.038	0.088	0.088	0.088	4.662

*Displacement feedback gain could not be reduced from the value used in Criterion B without resulting in either an unstable system or in a very sluggish system response.

TABLE XIII

SUMMARY OF FUSELAGE AND ROTOR EFFECTIVENESSES FOR GROUND VIBRATIONS

Case Number	Criterion	Fuselage Effectiveness					Rotor Effectiveness				
		1/rev	b/rev	2b/rev	3b/rev	.4b/rev	1/rev	b/rev	2b/rev	3b/rev	4b/rev
2.2.2a	A	0.786	>100	>100	0.982	0.934	1.419	0.111	0.111	0.718	1.418
b	A	0.799	>100	>100	0.979	0.934	1.431	0.102	0.102	0.731	1.492
c	A	0.812	>100	>100	0.978	0.934	1.457	0.094	0.094	0.749	1.626
d	A	0.821	>100	>100	0.976	0.934	1.475	0.088	0.088	0.767	1.768
2.2.2a	B	0.781	>100	>100	1.005	0.992	0.957	0.111	0.111	0.885	1.032
b	B	0.830	>100	>100	1.004	0.991	1.014	0.102	0.102	0.888	1.044
c	B	0.841	>100	>100	1.003	0.991	1.027	0.094	0.094	0.893	1.056
d	B	0.848	>100	>100	1.002	0.992	1.040	0.088	0.088	0.900	1.070
2.2.2a	C	0.817	>100	>100	0.990	0.971	1.031	0.111	0.111	0.988	1.286
b	C	0.828	>100	>100	0.989	0.971	1.041	0.102	0.102	1.003	1.326
c	C	0.838	>100	>100	0.989	0.971	1.056	0.094	0.094	1.021	1.375
d	C	0.846	>100	>100	0.988	0.971	1.067	0.088	0.088	1.040	1.426
2.4.2a	A	0.823	>100	>100	0.790	0.682	0.857	0.111	0.111	0.879	0.348
b	A	0.835	>100	>100	0.792	0.683	0.868	0.102	0.102	0.764	0.306
c	A	0.845	>100	>100	0.795	0.684	0.879	0.094	0.094	0.671	0.272
d	A	0.852	>100	>100	0.796	0.683	0.886	0.088	0.088	0.601	0.247
2.4.2a	B	0.816	>100	>100	0.886	0.843	0.971	0.111	0.111	2.120	2.065
b	B	0.829	>100	>100	0.889	0.846	0.985	0.102	0.102	2.320	1.510
c	B	0.840	>100	>100	0.892	0.848	0.999	0.094	0.094	2.469	1.247
d	B	0.848	>100	>100	0.893	0.848	1.010	0.088	0.088	2.510	1.101
2.4.2a	C	0.781	>100	>100	0.786	0.721	0.647	0.111	0.111	0.227	0.365
b	C	0.797	>100	>100	0.789	0.731	0.659	0.102	0.102	0.228	0.361
c	C	0.812	>100	>100	0.794	0.742	0.670	0.094	0.094	0.230	0.356
d	C	0.823	>100	>100	0.797	0.748	0.677	0.088	0.088	0.232	0.348

TABLE XIII (continued)
SUMMARY OF FUSELAGE AND ROTOR EFFECTIVENESSES FOR GROUND VIBRATIONS

Case Number	Criterion	Fuselage Effectiveness					Rotor Effectiveness				
		1/rev	b/rev	2b/rev	3b/rev	4b/rev	1/rev	b/rev	2b/rev	3b/rev	4b/rev
10.4.2a	A	0.649	>100	>100	0.862	0.824	0.76	0.111	0.111	2.083	1.255
b	A	0.663	>100	>100	0.868	0.827	0.787	0.102	0.102	2.037	1.048
c	A	0.678	>100	>100	0.870	0.830	0.807	0.094	0.094	1.930	0.899
d	A	0.689	>100	>100	0.873	0.831	0.822	0.088	0.088	1.794	0.793
10.4.2a	B	0.667	>100	>100	0.922	0.903	0.729	0.111	0.111	1.432	7.329
b	B	0.679	>100	>100	0.925	0.906	0.743	0.102	0.102	1.930	0.899
c	B	0.693	>100	>100	0.928	0.909	0.759	0.094	0.094	1.639	8.824
d	B	0.703	>100	>100	0.930	0.910	0.771	0.088	0.088	1.759	6.481
10.4.2a	C	0.675	>100	>100	0.943	0.929	0.714	0.111	0.111	1.933	2.100
b	C	0.676	>100	>100	0.945	0.930	0.729	0.102	0.102	2.055	2.146
c	C	0.690	>100	>100	0.947	0.931	0.745	0.094	0.094	2.180	2.145
d	C	0.700	>100	>100	0.948	0.931	0.757	0.088	0.088	2.308	2.109
20.5.2a	A	0.569	>100	>100	0.855	0.817	0.658	0.111	0.111	1.860	1.119
b	A	0.569	>100	>100	0.859	0.819	0.659	0.102	0.102	1.788	0.945
c	A	0.576	>100	>100	0.863	0.822	0.669	0.094	0.094	1.678	0.817
d	A	0.582	>100	>100	0.866	0.824	0.677	0.088	0.088	1.556	0.725
20.5.2a	B	0.585	>100	>100	0.917	0.898	0.615	0.111	0.111	1.441	10.650
b	B	0.584	>100	>100	0.920	0.901	0.615	0.102	0.102	1.539	11.728
c	B	0.603	>100	>100	0.923	0.904	0.636	0.094	0.094	1.652	7.843
d	B	0.595	>100	>100	0.925	0.906	0.628	0.088	0.088	1.773	5.356
20.5.2a	C	0.579	>100	>100	0.940	0.926	0.616	0.111	0.111	2.039	2.169
b	C	0.579	>100	>100	0.942	0.927	0.616	0.102	0.102	2.181	2.202
c	C	0.585	>100	>100	0.944	0.928	0.624	0.094	0.094	2.328	2.179
d	C	0.591	>100	>100	0.945	0.928	0.630	0.088	0.088	2.480	2.118

TABLE XIII (continued)
SUMMARY OF FUSELAGE AND ROTOR EFFECTIVENESSES FOR GROUND VIBRATIONS

Case Number	Criterion	Fuselage Effectiveness					Rotor Effectiveness				
		1/rev	b/rev	2b/rev	3b/rev	4b/rev	1/rev	b/rev	2b/rev	3b/rev	4b/rev
40.6.2a	A	0.606	>100	>100	0.859	0.821	0.679	0.111	0.111	2.039	1.190
b	A	0.557	>100	>100	0.864	0.824	0.625	0.102	0.102	1.971	0.999
c	A	0.524	>100	>100	0.868	0.826	0.589	0.094	0.094	1.851	0.859
d	A	0.503	>100	>100	0.870	0.828	0.567	0.088	0.088	1.710	0.760
40.6.2a	B	0.612	>100	>100	0.920	0.901	0.631	0.111	0.111	1.459	8.284
b	B	0.564	>100	>100	0.923	0.904	0.582	0.102	0.102	1.560	10.178
c	B	0.531	>100	>100	0.926	0.907	0.548	0.094	0.094	1.677	8.180
d	B	0.511	>100	>100	0.928	0.908	0.528	0.088	0.088	1.803	5.825
40.6.2a	C	0.609	>100	>100	0.942	0.927	0.639	0.111	0.111	1.971	2.122
b	C	0.560	>100	>100	0.944	0.928	0.589	0.102	0.102	2.099	2.163
c	C	0.528	>100	>100	0.946	0.930	0.555	0.094	0.094	2.230	2.152
d	C	0.508	>100	>100	0.947	0.930	0.534	0.088	0.088	2.365	2.105
80.6.2a	A	0.941	>100	>100	0.898	0.858	0.989	0.111	0.111	0.990	2.749
b	A	0.818	>100	>100	0.901	0.861	0.861	0.102	0.102	1.036	2.303
c	A	0.711	>100	>100	0.904	0.864	0.749	0.094	0.094	1.085	1.925
d	A	0.741	>100	>100	0.905	0.865	0.746	0.088	0.088	1.106	1.875
80.6.2a	B	0.938	>100	>100	0.983	0.959	0.955	0.111	0.111	0.919	1.342
b	B	0.816	>100	>100	0.983	0.959	0.830	0.102	0.102	0.935	1.399
c	B	0.709	>100	>100	0.982	0.960	0.722	0.094	0.094	0.952	1.462
d	B	0.633	>100	>100	0.982	0.954	0.644	0.088	0.088	0.968	1.632
80.6.2a	C	0.938	>100	>100	0.955	0.942	0.960	0.111	0.111	1.437	2.113
b	C	0.816	>100	>100	0.957	0.942	0.835	0.102	0.102	1.503	2.142
c	C	0.709	>100	>100	0.958	0.943	0.727	0.094	0.094	1.576	2.265
d	C	0.633	>100	>100	0.959	0.944	0.649	0.088	0.088	1.653	2.378

TABLE XIII (continued)
SUMMARY OF FUSELAGE AND ROTOR EFFECTIVENESSES FOR GROUND VIBRATIONS

Case Number	Criterion	Fuselage Effectiveness					Rotor Effectiveness				
		1/rev	b/rev	2b/rev	3b/rev	4b/rev	1/rev	b/rev	2b/rev	3b/rev	4b/rev
80.7.2a	A	0.941	>100	>100	0.871	0.833	1.016	0.111	0.111	1.905	1.526
b	A	0.817	>100	>100	0.875	0.837	0.884	0.102	0.102	1.975	1.249
c	A	0.710	>100	>100	0.879	0.839	0.769	0.094	0.094	1.976	1.059
d	A	0.633	>100	>100	0.881	0.841	0.686	0.088	0.088	1.928	0.925
80.7.2a	B	0.938	>100	>100	0.925	0.904	0.954	0.111	0.111	1.244	6.351
b	B	0.816	>100	>100	0.928	0.907	0.830	0.102	0.102	1.313	10.263
c	B	0.720	>100	>100	0.931	0.910	0.732	0.094	0.094	1.390	17.896
d	B	0.633	>100	>100	0.932	0.912	0.644	0.088	0.088	1.470	13.961
80.7.2a	C	0.939	>100	>100	0.947	0.933	0.969	0.111	0.111	1.799	2.048
b	C	0.815	>100	>100	0.949	0.934	0.843	0.102	0.102	1.902	2.116
c	C	0.709	>100	>100	0.950	0.935	0.733	0.094	0.094	2.008	2.146
d	C	0.631	>100	>100	0.951	0.936	0.654	0.088	0.088	2.119	2.163
2.2.3a	A	0.780	>100	>100	>100	0.878	1.209	0.111	0.111	0.111	0.849
b	A	0.783	>100	>100	>100	0.880	1.243	0.102	0.102	0.102	0.875
c	A	0.808	>100	>100	>100	0.882	1.264	0.094	0.094	0.094	0.899
d	A	0.817	>100	>100	>100	0.883	1.280	0.088	0.088	0.088	0.917
2.2.3a	B	0.784	>100	>100	>100	0.970	1.114	0.111	0.111	0.111	0.841
b	B	0.821	>100	>100	>100	0.970	1.124	0.102	0.102	0.102	0.881
c	B	0.832	>100	>100	>100	0.970	1.141	0.094	0.094	0.094	0.903
d	B	0.839	>100	>100	>100	0.970	1.150	0.088	0.088	0.088	0.917
2.2.3a	C	0.816	>100	>100	>100	0.947	0.994	0.111	0.111	0.111	1.665
b	C	0.824	>100	>100	>100	0.949	1.008	0.102	0.102	0.102	1.700
c	C	0.836	>100	>100	>100	0.950	1.024	0.094	0.094	0.094	1.826
d	C	0.845	>100	>100	>100	0.951	1.034	0.088	0.088	0.088	1.969

TABLE XIII (continued)
SUMMARY OF FUSELAGE AND ROTOR EFFECTIVENESSES FOR GROUND VIBRATIONS

Case Number	Criterion	Fuselage Effectiveness					Rotor Effectiveness				
		1/rev	b/rev	2b/rev	3b/rev	4b/rev	1/rev	b/rev	2b/rev	3b/rev	4b/rev
2.4.3a*	A	-	-	-	-	-	-	-	-	-	-
b*	A	-	-	-	-	-	-	-	-	-	-
c*	A	-	-	-	-	-	-	-	-	-	-
d*	A	-	-	-	-	-	-	-	-	-	-
2.4.3a	B	0.828	>100	>100	>100	0.834	0.870	0.111	0.111	0.111	1.374
b	B	0.841	>100	>100	>100	0.838	0.880	0.102	0.102	0.102	1.579
c	B	0.851	>100	>100	>100	0.842	0.891	0.094	0.094	0.094	1.332
d	B	0.858	>100	>100	>100	0.841	0.887	0.088	0.088	0.088	1.117
2.4.3a*	C	-	-	-	-	-	-	-	-	-	-
b*	C	-	-	-	-	-	-	-	-	-	-
c*	C	-	-	-	-	-	-	-	-	-	-
d*	C	-	-	-	-	-	-	-	-	-	-
10.4.3a	A	0.659	>100	>100	>100	0.815	0.684	0.111	0.111	0.111	1.328
b	A	0.672	>100	>100	>100	0.819	0.699	0.102	0.102	0.102	1.133
c	A	0.688	>100	>100	>100	0.823	0.714	0.094	0.094	0.094	0.986
d	A	0.698	>100	>100	>100	0.925	0.735	0.088	0.088	0.088	0.470
10.4.3a	B	0.661	>100	>100	>100	0.886	0.600	0.111	0.111	0.111	19.59
b	B	0.674	>100	>100	>100	0.890	0.750	0.102	0.102	0.102	12.97
c	B	0.688	>100	>100	>100	0.895	0.767	0.094	0.094	0.094	7.56
d	B	0.698	>100	>100	>100	0.897	0.770	0.088	0.088	0.088	5.191
10.4.3a	C	0.667	>100	>100	>100	0.925	0.680	0.111	0.111	0.111	2.470
b	C	0.680	>100	>100	>100	0.926	0.694	0.102	0.102	0.102	2.530
c	C	0.689	>100	>100	>100	0.928	0.708	0.094	0.094	0.094	2.523
d	C	0.704	>100	>100	>100	0.929	0.718	0.088	0.088	0.088	2.468

TABLE XIII (continued)
SUMMARY OF FUSELAGE AND ROTOR EFFECTIVENESSES FOR GROUND VIBRATIONS

Case Number	Criterion	Fuselage Effectiveness					Rotor Effectiveness				
		1/rev	b/rev	2b/rev	3b/rev	4b/rev	1/rev	b/rev	2b/rev	3b/rev	4b/rev
20.5.3a	A	0.571	>100	>100	>100	0.806	0.596	0.111	0.111	0.111	1.187
b	A	0.572	>100	>100	>100	0.810	0.597	0.102	0.102	0.102	1.023
c	A	0.580	>100	>100	>100	0.814	0.605	0.094	0.094	0.094	0.898
d	A	0.586	>100	>100	>100	0.816	0.612	0.088	0.088	0.088	0.805
20.5.3a	B	0.579	>100	>100	>100	0.880	0.628	0.111	0.111	0.111	11.27
b	B	0.578	>100	>100	>100	0.885	0.628	0.102	0.102	0.102	7.42
c	B	0.585	>100	>100	>100	0.889	0.635	0.094	0.094	0.094	5.192
d	B	0.590	>100	>100	>100	0.892	0.642	0.088	0.088	0.088	3.93
20.5.3a	C	0.579	>100	>100	>100	0.921	0.591	0.111	0.111	0.111	2.415
b	C	0.579	>100	>100	>100	0.922	0.592	0.102	0.102	0.102	2.634
c	C	0.586	>100	>100	>100	0.925	0.599	0.094	0.094	0.094	2.591
d	C	0.592	>100	>100	>100	0.925	0.605	0.088	0.088	0.088	2.497
40.6.3a	A	0.600	>100	>100	>100	0.822	0.627	0.111	0.111	0.111	1.239
b	A	0.552	>100	>100	>100	0.825	0.578	0.102	0.102	0.102	1.065
c	A	0.520	>100	>100	>100	0.828	0.544	0.094	0.094	0.094	0.932
d	A	0.501	>100	>100	>100	0.830	0.524	0.088	0.088	0.088	0.835
40.6.3a	B	0.610	>100	>100	>100	0.894	0.645	0.111	0.111	0.111	12.419
b	B	0.561	>100	>100	>100	0.898	0.595	0.102	0.102	0.102	8.577
c	B	0.528	>100	>100	>100	0.901	0.561	0.094	0.094	0.094	5.864
d	B	0.508	>100	>100	>100	0.904	0.540	0.088	0.088	0.088	4.341
40.6.3a	C	0.606	>100	>100	>100	0.928	0.618	0.111	0.111	0.111	2.567
b	C	0.558	>100	>100	>100	0.929	0.570	0.102	0.102	0.102	2.618
c	C	0.526	>100	>100	>100	0.930	0.537	0.094	0.094	0.094	2.591
d	C	0.506	>100	>100	>100	0.931	0.517	0.088	0.088	0.088	2.514

TABLE XIII (continued)
SUMMARY OF FUSELAGE AND ROTOR EFFECTIVENESSES FOR GROUND VIBRATIONS

Case Number	Criterion	Fuselage Effectiveness					Rotor Effectiveness				
		1/rev	b/rev	2b/rev	3b/rev	4b/rev	1/rev	b/rev	2b/rev	3b/rev	4b/rev
80.6.3a	A	0.930	>100	>100	>100	0.836	0.990	0.111	0.111	0.111	1.852
b	A	0.807	>100	>100	>100	0.841	0.860	0.102	0.102	0.102	1.608
c	A	0.701	>100	>100	>100	0.846	0.747	0.094	0.094	0.094	1.454
d	A	0.624	>100	>100	>100	0.849	0.666	0.088	0.088	0.088	1.322
80.6.3a	B	0.938	>100	>100	>100	0.897	0.959	0.111	0.111	0.111	1.799
b	B	0.815	>100	>100	>100	0.903	0.834	0.102	0.102	0.102	1.941
c	B	0.709	>100	>100	>100	0.906	0.726	0.094	0.094	0.094	2.097
d	B	0.632	>100	>100	>100	0.908	0.650	0.088	0.088	0.088	2.256
80.6.3a	C	0.934	>100	>100	>100	0.934	0.961	0.111	0.111	0.111	2.428
b	C	0.811	>100	>100	>100	0.935	0.835	0.102	0.102	0.102	2.610
c	C	0.705	>100	>100	>100	0.937	0.726	0.094	0.094	0.094	2.783
d	C	0.630	>100	>100	>100	0.938	0.648	0.088	0.088	0.088	2.944
80.7.3a	A	0.935	>100	>100	>100	0.784	1.021	0.111	0.111	0.111	0.942
b	A	0.812	>100	>100	>100	0.791	0.887	0.102	0.102	0.102	0.860
c	A	0.705	>100	>100	>100	0.797	0.771	0.094	0.094	0.094	0.787
d	A	0.627	>100	>100	>100	0.801	0.740	0.088	0.088	0.088	0.728
80.7.3a	B	0.939	>100	>100	>100	0.894	0.655	0.111	0.111	0.111	1.778
b	B	0.816	>100	>100	>100	0.895	0.845	0.102	0.102	0.102	1.794
c	B	0.710	>100	>100	>100	0.902	0.736	0.094	0.094	0.094	1.788
d	B	0.633	>100	>100	>100	0.904	0.657	0.088	0.088	0.088	1.752
80.7.3a	C	0.935	>100	>100	>100	0.928	0.973	0.111	0.111	0.111	4.678
b	C	0.813	>100	>100	>100	0.929	0.846	0.102	0.102	0.102	5.083
c	C	0.706	>100	>100	>100	0.931	0.736	0.094	0.094	0.094	5.053
d	C	0.629	>100	>100	>100	0.931	0.656	0.088	0.088	0.088	4.662

*Displacement feedback gain could not be reduced from the value used in Criterion B without resulting in either an unstable system or in a very sluggish system response.

TABLE XIV
SUMMARY OF FUSELAGE AND ROTOR NORMALIZED ACCELERATIONS FOR CRUISE VIBRATIONS*

Case Number	Criterion	Fuselage Normalized Acceleration					Rotor Normalized Acceleration				
		1/rev	b/rev	2b/rev	3b/rev	4b/rev	1/rev	b/rev	2b/rev	3b/rev	4b/rev
2.2.2a	A	0.1055	<0.01	<0.004	0.1018	0.1070	0.0589	9.01	3.60	0.1392	0.0722
b	A	0.1050	<0.01	<0.004	0.1021	0.1070	0.0587	9.80	3.92	0 1368	0.0670
c	A	0.1046	<0.01	<0.004	0.1023	0.1070	0.0583	10.64	4.25	0.1335	0.0566
d	A	0.1043	<0.01	<0.004	0.1024	0.1071	0.0581	11.36	4.54	0.1304	0.0566
2.2.2a	B	0.1021	<0.01	<0.004	0.0995	0.1008	0.0834	9.01	3.60	0.1130	0.0969
b	B	0.1019	<0.01	<0.004	0.0996	0.1009	0.0835	9.80	3.92	0.1126	0.0969
c	B	0.1017	<0.01	<0.004	0.0997	0.1009	0.0833	10.64	4.25	0.1120	0.0947
d	B	0.1017	<0.01	<0.004	0.0998	0.1009	0.0830	11.36	4.54	0.1111	0.0935
2.2.2a	C	0.1023	<0.01	<0.004	0.1010	0.1030	0.0812	9.01	3.60	0.1012	0.0789
b	C	0.1022	<0.01	<0.004	0.1011	0.1030	0.0812	9.80	3.92	0.0997	0.0754
c	C	0.1020	<0.01	<0.004	0.1011	0.1030	0.0810	10.64	4.25	0.0979	0.0727
d	C	0.1019	<0.01	<0.004	0.1012	0.1030	0.0808	11.36	4.54	0.0962	0.0702
2.4.2a	A	0.1009	<0.01	<0.004	0.1266	0.1465	0.0969	9.01	3.60	0.1130	0.2873
b	A	0.1008	<0.01	<0.004	0.1262	0.1465	0.0969	9.80	3.92	0.1310	0.3272
c	A	0.1008	<0.01	<0.004	0.1258	0.1463	0.0969	10.64	4.25	0.1489	0.3672
d	A	0.1007	<0.01	<0.004	0.1257	0.1464	0.0969	11.36	4.54	0.1664	0.4054
2.4.2a	B	0.1019	<0.01	<0.004	0.1129	0.1185	0.0859	9.01	3.60	0.0472	0.0535
b	B	0.1018	<0.01	<0.004	0.1125	0.1182	0.0857	9.80	3.92	0.0431	0.0662
c	B	0.1017	<0.01	<0.004	0.1121	0.1179	0.0855	10.64	4.25	0.0405	0.0802
d	B	0.1015	<0.01	<0.004	0.1120	0.1179	0.0853	11.36	4.54	0.0398	0.0958
2.4.2a	C	0.1027	<0.01	<0.004	0.1272	0.1386	0.1240	9.01	3.60	0.4414	0.2741
b	C	0.1026	<0.01	<0.004	0.1267	0.1367	0.1241	9.80	3.92	0.4383	0.2774
c	C	0.1024	<0.01	<0.004	0.1260	0.1349	0.1242	10.64	4.25	0.4344	0.2811
d	C	0.1023	<0.01	<0.004	0.1255	0.1337	0.1243	11.36	4.54	0.4315	0.2871

TABLE XIV (continued)
SUMMARY OF FUSELAGE AND ROTOR NORMALIZED ACCELERATIONS FOR CRUISE VIBRATIONS*

Case Number	Criterion	Fuselage Normalized Acceleration					Rotor Normalized Acceleration				
		1/rev	b/rev	2b/rev	3b/rev	4b/rev	1/rev	b/rev	2b/rev	3b/rev	4b/rev
10.4.2a	A	0.1019	<0.01	<0.004	0.1160	0.1213	0.0860	9.01	3.60	0.0480	0.0797
b	A	0.1018	<0.01	<0.004	0.1155	0.1209	0.0857	9.80	3.92	0.0491	0.0954
c	A	0.1017	<0.01	<0.004	0.1149	0.1205	0.0854	10.64	4.25	0.0518	0.1113
d	A	0.1016	<0.01	<0.004	0.1146	0.1203	0.0852	11.36	4.54	0.0558	0.1261
10.4.2a	B	0.1009	<0.01	<0.004	0.1085	0.1108	0.0924	9.01	3.60	0.0699	0.0136
b	B	0.1009	<0.01	<0.004	0.1081	0.1104	0.0922	9.80	3.92	0.0654	0.0104
c	B	0.1008	<0.01	<0.004	0.1078	0.1101	0.0920	10.64	4.25	0.0610	0.0113
d	B	0.1008	<0.01	<0.004	0.1075	0.1099	0.0919	11.36	4.54	0.0568	0.0154
10.4.2a	C	0.1008	<0.01	<0.004	0.1060	0.1077	0.0936	9.01	3.60	0.0517	0.0476
b	C	0.1008	<0.01	<0.004	0.1058	0.1076	0.0934	9.80	3.92	0.0487	0.0466
c	C	0.1007	<0.01	<0.004	0.1056	0.1074	0.0932	10.64	4.25	0.0459	0.0466
d	C	0.1007	<0.01	<0.004	0.1055	0.1074	0.0931	11.36	4.54	0 0433	0.0474
20.5.2a	A	0.1016	<0.01	<0.004	0.1170	0.1225	0.0879	9.01	3.60	0.0538	0.0894
b	A	0.1015	<0.01	<0.004	0.1164	0.1221	0.0876	9.80	3.92	0.0559	0.1058
c	A	0.1014	<0.01	<0.004	0.1158	0.1216	0.0874	10.64	4.25	0.0596	0.1224
d	A	0.1013	<0.01	<0.004	0.1154	0.1214	0.0871	11.36	4.54	0.0643	0.1380
20.5.2a	B	0.1006	<0.01	<0.004	0.1091	0.1114	0.0955	9.01	3.60	0.0694	0.0094
b	B	0.1005	<0.01	<0.004	0.1087	0.1110	0.0954	9.80	3.92	0.0650	0.0085
c	B	0.1005	<0.01	<0.004	0.1083	0.1106	0.0952	10.64	4.25	0.0605	0.0128
d	B	0.1005	<0.01	<0.004	0.1081	0.1104	0.0951	11.36	4.54	0.0564	0.0187
20.5.2a	C	0.1007	<0.01	<0.004	0.1064	0.1081	0.0946	9.01	3.60	0.0490	0.0461
b	C	0.1006	<0.01	<0.004	0.1062	0.1079	0.0945	9.80	3.92	0.0458	0.0454
c	C	0.1006	<0.01	<0.004	0.1059	0.1078	0.0943	10.64	4.25	0.0429	0.0459
d	C	0.1006	<0.01	<0.004	0.1058	0.1077	0.0942	11.36	4.54	0.0403	0.0472

TABLE XIV (continued)
SUMMARY OF FUSELAGE AND ROTOR NORMALIZED ACCELERATIONS FOR CRUISE VIBRATIONS*

Case Number	Criterion	Fuselage Normalized Acceleration					Rotor Normalized Acceleration				
		1/rev	b/rev	2b/rev	3b/rev	4b/rev	1/rev	b/rev	2b/rev	3b/rev	4b/rev
40.6.2a	A	0.1012	<0.01	<0.004	0.1164	0.1218	0.0903	9.01	3.60	0.0490	0.0841
b	A	0.1011	<0.01	<0.004	0.1158	0.1214	0.0901	9.80	3.92	0.0507	0.1001
c	A	0.1011	<0.01	<0.004	0.1153	0.1210	0.0899	10.64	4.25	0.0540	0.1164
d	A	0.1010	<0.01	<0.004	0.1149	0.1208	0.0897	11.36	4.54	0.0585	0.1316
40.6.2a	B	0.1003	<0.01	<0.004	0.1087	0.1110	0.0974	9.01	3.60	0.0686	0.0121
b	B	0.1003	<0.01	<0.004	0.1083	0.1107	0.0973	9.80	3.92	0.0641	0.0098
c	B	0.1003	<0.01	<0.004	0.1080	0.1103	0.0972	10.64	4.25	0.0596	0.0122
d	B	0.1003	<0.01	<0.004	0.1078	0.1101	0.0971	11.36	4.54	0.0555	0.0172
40.6.2a	C	0.1005	<0.01	<0.004	0.1061	0.1078	0.0957	9.01	3.60	0.0507	0.0471
b	C	0.1005	<0.01	<0.004	0.1060	0.1077	0.0956	9.80	3.92	0.0476	0.0462
c	C	0.1005	<0.01	<0.004	0.1057	0.1076	0.0955	10.64	4.25	0.0448	0.0465
d	C	0.1005	<0.01	<0.004	0.1056	0.1075	0.0954	11.36	4.54	0.0423	0.0475
80.6.2a	A	0.1005	<0.01	<0.004	0.1113	0.1166	0.0957	9.01	3.60	0.1010	0.0364
b	A	0.1005	<0.01	<0.004	0.1110	0.1161	0.0956	9.80	3.92	0.0965	0.0434
c	A	0.1005	<0.01	<0.004	0.1107	0.1158	0.0954	10.64	4.25	0.0922	0.0520
d	A	0.1005	<0.01	<0.004	0.1105	0.1155	0.0953	11.36	4.54	0.0904	0.0534
80.6.2a	B	0.1002	<0.01	<0.004	0.1017	0.1043	0.0985	9.01	3.60	0.1088	0.0745
b	B	0.1002	<0.01	<0.004	0.1018	0.1042	0.0984	9.80	3.92	0.1070	0.0715
c	B	0.1002	<0.01	<0.004	0.1018	0.1042	0.0984	10.64	4.25	0.1051	0.0684
d	B	0.1002	<0.01	<0.004	0.1018	0.1048	0.0983	11.36	4.54	0.1033	0.0613
80.6.2a	C	0.1003	<0.01	<0.004	0.1047	0.1061	0.0980	9.01	3.60	0.0696	0.0474
b	C	0.1002	<0.01	<0.004	0.1045	0.1062	0.0979	9.80	3.92	0.0665	0.0467
c	C	0.1002	<0.01	<0.004	0.1044	0.1060	0.0978	10.64	4.25	0.0634	0.0441
d	C	0.1002	<0.01	<0.004	0.1043	0.1059	0.0977	11.36	4.54	0.0605	0.0420

TABLE XIV (continued)
SUMMARY OF FUSELAGE AND ROTOR NORMALIZED ACCELERATIONS FOR CRUISE VIBRATIONS*

Case Number	Criterion	Fuselage Normalized Acceleration					Rotor Normalized Acceleration				
		1/rev	b/rev	2b/rev	3b/rev	4b/rev	1/rev	b/rev	2b/rev	3b/rev	4b/rev
80.7.2a	A	0.1008	<0.01	<0.004	0.1148	0.1120	0.0934	9.01	3.60	0.0525	0.0655
b	A	0.1008	<0.01	<0.004	0.1143	0.1195	0.0932	9.80	3.92	0.0506	0.0801
c	A	0.1007	<0.01	<0.004	0.1138	0.1191	0.0930	10.64	4.25	0.0506	0.0944
d	A	0.1007	<0.01	<0.004	0.1135	0.1189	0.0929	11.36	4.54	0.0519	0.1081
80.7.2a	B	0.1002	<0.01	<0.004	0.1081	0.1107	0.0986	9.01	3.60	0.0804	0.0157
b	B	0.1002	<0.01	<0.004	0.1078	0.1103	0.0985	9.80	3.92	0.0762	0.0097
c	B	0.1002	<0.01	<0.004	0.1075	0.1099	0.0984	10.64	4.25	0.0720	0.0056
d	B	0.1002	<0.01	<0.004	0.1073	0.1097	0.0984	11.36	4.54	0.0680	0.0072
80.7.2a	C	0.1004	<0.01	<0.004	0.1056	0.1072	0.0971	9.01	3.60	0.0556	0.0488
b	C	0.1003	<0.01	<0.004	0.1054	0.1071	0.0970	9.80	3.92	0.0526	0.0473
c	C	0.1003	<0.01	<0.004	0.1052	0.1069	0.0969	10.64	4.25	0.0498	0.0466
d	C	0.1003	<0.01	<0.004	0.1051	0.1070	0.0968	11.36	4.54	0.0472	0.0463
2.2.3a	A	0.1055	<0.01	<0.004	<0.001	0.1138	0.0666	9.01	3.60	0.90	0.1216
b	A	0.1049	<0.01	<0.004	<0.001	0.1136	0.0672	9.80	3.92	0.98	0.1143
c	A	0.1046	<0.01	<0.004	<0.001	0.1134	0.0964	10.64	4.25	1.06	0.1112
d	A	0.1042	<0.01	<0.004	<0.001	0.1132	0.0667	11.36	4.54	1.14	0.1090
2.2.3a	B	0.1032	<0.01	<0.004	<0.001	0.1030	0.0757	9.01	3.60	0.90	0.1189
b	B	0.1029	<0.01	<0.004	<0.001	0.1030	0.0752	9.80	3.92	0.98	0.1133
c	B	0.1027	<0.01	<0.004	<0.001	0.1030	0.0746	10.64	4.25	1.06	0.1107
d	B	0.1024	<0.01	<0.004	<0.001	0.1030	0.0746	11.36	4.54	1.14	0.1090
2.2.3a	C	0.1021	<0.01	<0.004	<0.001	0.1056	0.0833	9.01	3.60	0.90	0.0651
b	C	0.1019	<0.01	<0.004	<0.001	0.1054	0.0838	9.80	3.92	0.98	0.0588
c	C	0.1018	<0.01	<0.004	<0.001	0.1053	0.0835	10.64	4.25	1.06	0.0547
d	C	0.1017	<0.01	<0.004	<0.001	0.1051	0.0833	11.36	4.54	1.14	0.0508

TABLE XIV (continued)
SUMMARY OF FUSELAGE AND ROTOR NORMALIZED ACCELERATIONS FOR CRUISE VIBRATIONS*

Case Number	Criterion	Fuselage Normalized Acceleration					Rotor Normalized Acceleration				
		1/rev	b/rev	2b/rev	3b/rev	4b/rev	1/rev	b/rev	2b/rev	3b/rev	4b/rev
2.4.3a**	A	-	-	-	-	-	-	-	-	-	-
b**	A	-	-	-	-	-	-	-	-	-	-
c**	A	-	-	-	-	-	-	-	-	-	-
d**	A	-	-	-	-	-	-	-	-	-	-
2.4.3a	B	0.1006	<0.01	<0.004	<0.001	0.1199	0.0963	9.01	3.60	0.90	0.0683
b	B	0.1006	<0.01	<0.004	<0.001	0.1193	0.0962	9.80	3.92	0.98	0.0633
c	B	0.1005	<0.01	<0.004	<0.001	0.1187	0.0961	10.64	4.25	1.06	0.0751
d	B	0.1005	<0.01	<0.004	<0.001	0.1189	0.0961	11.36	4.54	1.14	0.0835
2.4.3a**	C	-	-	-	-	-	-	-	-	-	-
b**	C	-	-	-	-	-	-	-	-	-	-
c**	C	-	-	-	-	-	-	-	-	-	-
d**	C	-	-	-	-	-	-	-	-	-	-
10.4.3a	A	0.1005	<0.01	<0.004	<0.001	0.1227	0.0971	9.01	3.60	0.90	0.0753
b	A	0.1005	<0.01	<0.004	<0.001	0.1221	0.0971	9.80	3.92	0.98	0.0883
c	A	0.1005	<0.01	<0.004	<0.001	0.1215	0.0971	10.64	4.25	1.06	0.1014
d	A	0.1004	<0.01	<0.004	<0.001	0.1212	0.0971	11.36	4.54	1.14	0.2112
10.4.3a	B	0.1011	<0.01	<0.004	<0.001	0.1128	0.0912	9.01	3.60	0.90	0.0051
b	B	0.1010	<0.01	<0.004	<0.001	0.1123	0.0910	9.80	3.92	0.98	0.0077
c	B	0.1009	<0.01	<0.004	<0.001	0.1117	0.0909	10.64	4.25	1.06	0.0132
d	B	0.1009	<0.01	<0.004	<0.001	0.1114	0.0907	11.36	4.54	1.14	0.0192
10.4.3a	C	0.1002	<0.01	<0.004	<0.001	0.1081	0.0985	9.01	3.60	0.90	0.0404
b	C	0.1002	<0.01	<0.004	<0.001	0.1079	0.0984	9.80	3.92	0.98	0.0395
c	C	0.1002	<0.01	<0.004	<0.001	0.1077	0.0984	10.64	4.25	1.06	0.0396
d	C	0.1002	<0.01	<0.004	<0.001	0.1076	0.0984	11.36	4.54	1.14	0.0405

TABLE XIV (continued)
SUMMARY OF FUSELAGE AND ROTOR NORMALIZED ACCELERATIONS FOR CRUISE VIBRATIONS*

Case Number	Criterion	Fuselage Normalized Acceleration					Rotor Normalized Acceleration				
		1/rev	b/rev	2b/rev	3b/rev	4b/rev	1/rev	b/rev	2b/rev	3b/rev	4b/rev
20.5.3a	A	0.1005	<0.01	<0.004	<0.001	0.1240	0.0967	9.01	3.60	0.90	0.0842
b	A	0.1004	<0.01	<0.004	<0.001	0.1234	0.0967	9.80	3.92	0.98	0.0977
c	A	0.1004	<0.01	<0.004	<0.001	0.1228	0.0966	10.64	4.25	1.06	0.1114
d	A	0.1004	<0.01	<0.004	<0.001	0.1224	0.0966	11.36	4.54	1.14	0.1241
20.5.3a	B	0.1008	<0.01	<0.004	<0.001	0.1135	0.0932	9.01	3.60	0.90	0.0089
b	B	0.1007	<0.01	<0.004	<0.001	0.1129	0.0930	9.80	3.92	0.98	0.0135
c	B	0.1007	<0.01	<0.004	<0.001	0.1124	0.0929	10.64	4.25	1.06	0.0193
d	B	0.1007	<0.01	<0.004	<0.001	0.1120	0.0927	11.36	4.54	1.14	0.0254
20.5.3a	C	0.1002	<0.01	<0.004	<0.001	0.1085	0.0940	9.01	3.60	0.90	0.0414
b	C	0.1002	<0.01	<0.004	<0.001	0.1083	0.0984	9.80	3.92	0.98	0.0380
c	C	0.1002	<0.01	<0.004	<0.001	0.1081	0.0983	10.64	4.25	1.06	0.0386
d	C	0.1002	<0.01	<0.004	<0.001	0.1080	0.0983	11.36	4.54	1.06	0.0400
40.6.3a	A	0.1005	<0.01	<0.004	<0.001	0.1216	0.0965	9.01	3.60	0.90	0.0807
b	A	0.1004	<0.01	<0.004	<0.001	0.1212	0.0965	9.80	3.92	0.98	0.0939
c	A	0.1004	<0.01	<0.004	<0.001	0.1207	0.0964	10.64	4.25	1.06	0.1072
d	A	0.1004	<0.01	<0.004	<0.001	0.1205	0.0964	11.36	4.54	1.14	0.1198
40.6.3a	B	0.1006	<0.01	<0.004	<0.001	0.1118	0.0951	9.01	3.60	0.90	0.0081
b	B	0.1006	<0.01	<0.004	<0.001	0.1114	0.0950	9.80	3.92	0.98	0.0116
c	B	0.1005	<0.01	<0.004	<0.001	0.1109	0.0948	10.64	4.25	1.06	0.0170
d	B	0.1005	<0.01	<0.004	<0.001	0.1106	0.0947	11.36	4.54	1.14	0.0230
40.6.3a	C	0.1002	<0.01	<0.004	<0.001	0.1078	0.0984	9.01	3.60	0.90	0.0390
b	C	0.1002	<0.01	<0.004	<0.001	0.1076	0.0984	9.80	3.92	0.98	0.0382
c	C	0.1002	<0.01	<0.004	<0.001	0.1075	0.0983	10.64	4.25	1.06	0.0386
d	C	0.1002	<0.01	<0.004	<0.001	0.1074	0.0983	11.36	4.54	1.14	0.0398

TABLE XIV (continued)
SUMMARY OF FUSELAGE AND ROTOR NORMALIZED ACCELERATIONS FOR CRUISE VIBRATIONS*

Case Number	Criterion	Fuselage Normalized Acceleration					Rotor Normalized Acceleration				
		1/rev	b/rev	2b/rev	3b/rev	4b/rev	1/rev	b/rev	2b/rev	3b/rev	4b/rev
80.6.3a	A	0.1007	<0.01	<0.004	<0.001	0.1196	0.0947	9.01	3.60	0.90	0.0540
b	A	0.1006	<0.01	<0.004	<0.001	0.1188	0.0945	9.80	3.92	0.98	0.0622
c	A	0.1006	<0.01	<0.004	<0.001	0.1181	0.0944	10.64	4.25	1.06	0.0688
d	A	0.1006	<0.01	<0.004	<0.001	0.1177	0.0943	11.36	4.54	1.14	0.0757
80.6.3a	B	0.1002	<0.01	<0.004	<0.001	0.1115	0.0980	9.01	3.60	0.90	0.0556
b	B	0.1002	<0.01	<0.004	<0.001	0.1108	0.0980	9.80	3.92	0.98	0.0515
c	B	0.1002	<0.01	<0.004	<0.001	0.1104	0.0978	10.64	4.25	1.06	0.0477
d	B	0.1002	<0.01	<0.004	<0.001	0.1100	0.0978	11.36	4.54	1.14	0.0443
80.6.3a	C	0.1003	<0.01	<0.004	<0.001	0.1072	0.0975	9.01	3.60	0.90	0.0412
b	C	0.1003	<0.01	<0.004	<0.001	0.1069	0.0974	9.80	3.92	0.98	0.0383
c	C	0.1003	<0.01	<0.004	<0.001	0.1066	0.0973	10.64	4.25	1.06	0.0359
d	C	0.1002	<0.01	<0.004	<0.001	0.1065	0.0973	11.36	4.54	1.14	0.0340
80.7.3a	A	0.1009	<0.01	<0.004	<0.001	0.1274	0.0925	9.01	3.60	0.90	0.1061
b	A	0.1009	<0.01	<0.004	<0.001	0.1264	0.0923	9.80	3.92	0.98	0.1163
c	A	0.1008	<0.01	<0.004	<0.001	0.1254	0.0922	10.64	4.25	1.06	0.1270
d	A	0.1008	<0.01	<0.004	<0.001	0.1247	0.0921	11.36	4.54	1.14	0.1373
80.7.3a	B	0.1004	<0.01	<0.004	<0.001	0.1118	0.0970	9.01	3.60	0.90	0.0562
b	B	0.1003	<0.01	<0.004	<0.001	0.1117	0.0969	9.80	3.92	0.98	0.0558
c	B	0.1003	<0.01	<0.004	<0.001	0.1109	0.0968	10.64	4.25	1.06	0.0559
d	B	0.1003	<0.01	<0.004	<0.001	0.1106	0.0967	11.36	4.54	1.14	0.0571
80.7.3a	C	0.1004	<0.01	<0.004	<0.001	0.1078	0.0965	9.01	3.60	0.90	0.0214
b	C	0.1004	<0.01	<0.004	<0.001	0.1076	0.0964	9.80	3.92	0.98	0.0197
c	C	0.1004	<0.01	<0.004	<0.001	0.1074	0.0964	10.64	4.25	1.06	0.0198
d	C	0.1003	<0.01	<0.004	<0.001	0.1073	0.0963	11.36	4.54	1.14	0.0214

TABLE XIV (continued)

* Normalized acceleration values relate the levels of acceleration experienced by the isolated fuselage and rotor to the unisolated rotor excitation at the blade passage frequency. The normalized acceleration at each critical frequency is equal to the normalized rotor excitation at that frequency (Figure 1) divided by the effectiveness at that frequency (Table XI).

** Displacement feedback gain could not be reduced from the value used in Criterion B without resulting in either an unstable system or a very sluggish system response.

TABLE XV

SUMMARY OF FUSELAGE AND ROTOR NORMALIZED ACCELERATIONS FOR GROUND VIBRATIONS*

Case Number	Criterion	Fuselage Normalized Acceleration					Rotor Normalized Acceleration				
		1/rev	b/rev	2b/rev	3b/rev	4b/rev	1/rev	b/rev	2b/rev	3b/rev	4b/rev
2.2.2a	A	0.1273	<0.01	<0.004	0.1018	0.1070	0.0711	9.01	3.60	0.1392	0.0722
b	A	0.1251	<0.01	<0.004	0.1021	0.1070	0.0699	9.80	3.92	0.1368	0.0670
c	A	0.1231	<0.01	<0.004	0.1023	0.1070	0.0686	10.64	4.25	0.1335	0.0615
d	A	0.1218	<0.01	<0.004	0.1024	0.1071	0.0678	11.36	4.54	0.1304	0.0566
2.2.2a	B	0.1282	<0.01	<0.004	0.0995	0.1008	0.1047	9.01	3.60	0.1130	0.0969
b	B	0.1205	<0.01	<0.004	0.0996	0.1009	0.0986	9.80	3.92	0.1126	0.0958
c	B	0.1190	<0.01	<0.004	0.0997	0.1009	0.0974	10.64	4.25	0.1120	0.0947
d	B	0.1179	<0.01	<0.004	0.0998	0.1009	0.0962	11.36	4.54	0.1111	0.0935
2.2.2a	C	0.1224	<0.01	<0.004	0.1010	0.1030	0.0972	9.01	3.60	0.1012	0.0789
b	C	0.1208	<0.01	<0.004	0.1011	0.1030	0.0960	9.80	3.92	0.0997	0.0754
c	C	0.1193	<0.01	<0.004	0.1011	0.1030	0.0947	10.64	4.25	0.0979	0.0727
d	C	0.1183	<0.01	<0.004	0.1012	0.1030	0.0938	11.36	4.54	0.0962	0.0702
2.4.2a	A	0.1214	<0.01	<0.004	0.1266	0.1465	0.1167	9.01	3.60	0.1138	0.2873
b	A	0.1198	<0.01	<0.004	0.1262	0.1465	0.1152	9.80	3.92	0.1310	0.3272
c	A	0.1183	<0.01	<0.004	0.1258	0.1463	0.1138	10.64	4.25	0.1489	0.3672
d	A	0.1173	<0.01	<0.004	0.1257	0.1464	0.1129	11.36	4.54	0.1664	0.4054
2.4.2a	B	0.1221	<0.01	<0.004	0.1129	0.1185	0.1031	9.01	3.60	0.0472	0.0535
b	B	0.1206	<0.01	<0.004	0.1125	0.1182	0.1015	9.80	3.92	0.0431	0.0662
c	B	0.1191	<0.01	<0.004	0.1121	0.1179	0.1001	10.64	4.25	0.0405	0.0802
d	B	0.1180	<0.01	<0.004	0.1120	0.1179	0.0981	11.36	4.54	0.0398	0.0958
2.4.2a	C	0.1280	<0.01	<0.004	0.1272	0.1386	0.1546	9.01	3.60	0.4414	0.2741
b	C	0.1254	<0.01	<0.004	0.1267	0.1367	0.1518	9.80	3.92	0.4383	0.2774
c	C	0.1231	<0.01	<0.004	0.1260	0.1349	0.1493	10.64	4.25	0.4344	0.2811
d	C	0.1215	<0.01	<0.004	0.1255	0.1337	0.1478	11.36	4.54	0.4315	0.2871

TABLE XV (continued)
SUMMARY OF FUSELAGE AND ROTOR NORMALIZED ACCELERATIONS FOR GROUND VIBRATIONS*

Case Number	Criterion	Fuselage Normalized Acceleration					Rotor Normalized Acceleration				
		1/rev	b/rev	2b/rev	3b/rev	4b/rev	1/rev	b/rev	2b/rev	3b/rev	4b/rev
10.4.2a	A	0.1541	<0.01	<0.004	0.1160	0.1213	0.1301	9.01	3.60	0.0480	0.0797
b	A	0.1509	<0.01	<0.004	0.1155	0.1209	0.1271	9.80	3.92	0.0491	0.0954
c	A	0.1475	<0.01	<0.004	0.1149	0.1205	0.1239	10.64	4.25	0.0518	0.1113
d	A	0.1452	<0.01	<0.004	0.1146	0.1203	0.1217	11.36	4.54	0.0558	0.1261
10.4.2a	B	0.1499	<0.01	<0.004	0.1085	0.1108	0.1373	9.01	3.60	0.0699	0.0136
b	B	0.1472	<0.01	<0.004	0.1081	0.1104	0.1346	9.80	3.92	0.0654	0.0104
c	B	0.1443	<0.01	<0.004	0.1078	0.1101	0.1317	10.64	4.25	0.0610	0.0113
d	B	0.1423	<0.01	<0.004	0.1075	0.1099	0.1297	11.36	4.54	0.0568	0.0154
10.4.2a	C	0.1482	<0.01	<0.004	0.1060	0.1077	0.1401	9.01	3.60	0.0517	0.0476
b	C	0.1480	<0.01	<0.004	0.1058	0.1076	0.1372	9.80	3.92	0.0487	0.0466
c	C	0.1449	<0.01	<0.004	0.1056	0.1074	0.1342	10.64	4.25	0.0459	0.0466
d	C	0.1428	<0.01	<0.004	0.1055	0.1074	0.1321	11.36	4.54	0.0433	0.0474
20.5.2a	A	0.1756	<0.01	<0.004	0.1170	0.1225	0.1520	9.01	3.60	0.0538	0.0894
b	A	0.1756	<0.01	<0.004	0.1164	0.1221	0.1517	9.80	3.92	0.0559	0.1058
c	A	0.1735	<0.01	<0.004	0.1158	0.1216	0.1496	10.64	4.25	0.0596	0.1224
d	A	0.1718	<0.01	<0.004	0.1154	0.1214	0.1478	11.36	4.54	0.0643	0.1380
20.5.2a	B	0.1711	<0.01	<0.004	0.1091	0.1114	0.1625	9.01	3.60	0.0694	0.0094
b	B	0.1713	<0.01	<0.004	0.1087	0.1110	0.1626	9.80	3.92	0.0650	0.0085
c	B	0.1659	<0.01	<0.004	0.1083	0.1106	0.1573	10.64	4.25	0.0605	0.0128
d	B	0.1682	<0.01	<0.004	0.1081	0.1104	0.1592	11.36	4.54	0.0564	0.0187
20.5.2a	C	0.1728	<0.01	<0.004	0.1064	0.1081	0.1624	9.01	3.60	0.0490	0.0461
b	C	0.1729	<0.01	<0.004	0.1062	0.1079	0.1623	9.80	3.92	0.0458	0.0454
c	C	0.1710	<0.01	<0.004	0.1059	0.1078	0.1603	10.64	4.25	0.0429	0.0459
d	C	0.1693	<0.01	<0.004	0.1058	0.1077	0.1586	11.36	4.54	0.0403	0.0472

TABLE XV (continued)
SUMMARY OF FUSELAGE AND ROTOR NORMALIZED ACCELERATIONS FOR GROUND VIBRATIONS*

Case Number	Criterion	Fuselage Normalized Acceleration					Rotor Normalized Acceleration				
		1/rev	b/rev	2b/rev	3b/rev	4b/rev	1/rev	b/rev	2b/rev	3b/rev	4b/rev
40.5.2a	A	0.1650	<0.01	<0.004	0.1164	0.1218	0.1472	9.01	3.60	0.0490	0.0841
b	A	0.1795	<0.01	<0.004	0.1158	0.1214	0.1599	9.80	3.92	0.0507	0.1001
c	A	0.1909	<0.01	<0.004	0.1153	0.1210	0.1697	10.64	4.25	0.0540	0.1164
d	A	0.1987	<0.01	<0.004	0.1149	0.1208	0.1764	11.36	4.54	0.0585	0.1316
40.5.2a	B	0.1633	<0.01	<0.004	0.1087	0.1110	0.1586	9.01	3.60	0.0686	0.0121
b	B	0.1773	<0.01	<0.004	0.1083	0.1107	0.1720	9.80	3.92	0.0641	0.0098
c	B	0.1882	<0.01	<0.004	0.1080	0.1103	0.1824	10.64	4.25	0.0596	0.0122
d	B	0.1957	<0.01	<0.004	0.1078	0.1101	0.1895	11.36	4.54	0.0555	0.0172
40.5.2a	C	0.1643	<0.01	<0.004	0.1061	0.1078	0.1565	9.01	3.60	0.0507	0.0471
b	C	0.1784	<0.01	<0.004	0.1060	0.1077	0.1698	9.80	3.92	0.0476	0.0462
c	C	0.1895	<0.01	<0.004	0.1057	0.1076	0.1801	10.64	4.25	0.0448	0.0465
d	C	0.1970	<0.01	<0.004	0.1056	0.1075	0.1871	11.36	4.54	0.0423	0.0475
80.6.2a	A	0.1063	<0.01	<0.004	0.1113	0.1166	0.1012	9.01	3.60	0.1010	0.0364
b	A	0.1222	<0.01	<0.004	0.1110	0.1161	0.1162	9.80	3.92	0.0965	0.0434
c	A	0.1406	<0.01	<0.004	0.1107	0.1158	0.1335	10.64	4.25	0.0922	0.0520
d	A	0.1351	<0.01	<0.004	0.1105	0.1155	0.1341	11.36	4.54	0.0904	0.0534
80.6.2a	B	0.1066	<0.01	<0.004	0.1017	0.1043	0.1048	9.01	3.60	0.1088	0.0745
b	B	0.1266	<0.01	<0.004	0.1018	0.1042	0.1204	9.80	3.92	0.1070	0.0715
c	B	0.1410	<0.01	<0.004	0.1018	0.1042	0.1385	10.64	4.25	0.1051	0.0684
d	B	0.1581	<0.01	<0.004	0.1018	0.1048	0.1552	11.36	4.54	0.1033	0.0613
80.6.2a	C	0.1066	<0.01	<0.004	0.1047	0.1061	0.1041	9.01	3.60	0.0696	0.0474
b	C	0.1226	<0.01	<0.004	0.1045	0.1062	0.1197	9.80	3.92	0.0665	0.0467
c	C	0.1410	<0.01	<0.004	0.1044	0.1060	0.1376	10.64	4.25	0.0634	0.0441
d	C	0.1581	<0.01	<0.004	0.1043	0.1059	0.1542	11.36	4.54	0.0605	0.0420

TABLE XV (continued)
SUMMARY OF FUSELAGE AND ROTOR NORMALIZED ACCELERATIONS FOR GROUND VIBRATIONS*

Case Number	Criterion	Fuselage Normalized Acceleration					Rotor Normalized Acceleration				
		1/rev	b/rev	2b/rev	3b/rev	4b/rev	1/rev	b/rev	2b/rev	3b/rev	4b/rev
80.7.2a	A	0.1063	<0.01	<0.004	0.1148	0.1120	0.0985	9.01	3.60	0.0525	0.0655
b	A	0.1223	<0.01	<0.004	0.1143	0.1195	0.1131	9.80	3.92	0.0506	0.0801
c	A	0.1408	<0.01	<0.004	0.1138	0.1191	0.1301	10.64	4.25	0.0506	0.0944
d	A	0.1580	<0.01	<0.004	0.1135	0.1189	0.1457	11.36	4.54	0.0519	0.1081
80.7.2a	B	0.1066	<0.01	<0.004	0.1081	0.1107	0.1049	9.01	3.60	0.0804	0.0157
b	B	0.1226	<0.01	<0.004	0.1078	0.1103	0.1205	9.80	3.92	0.0762	0.0097
c	B	0.1390	<0.01	<0.004	0.1075	0.1099	0.1366	10.64	4.25	0.0720	0.0056
d	B	0.1581	<0.01	<0.004	0.1073	0.1097	0.1552	11.36	4.54	0.0680	0.0072
80.7.2a	C	0.1066	<0.01	<0.004	0.1056	0.1072	0.1032	9.01	3.60	0.0556	0.0488
b	C	0.1227	<0.01	<0.004	0.1054	0.1071	0.1186	9.80	3.92	0.0526	0.0473
c	C	0.1411	<0.01	<0.004	0.1052	0.1069	0.1363	10.64	4.25	0.0498	0.0466
d	C	0.1583	<0.01	<0.004	0.1051	0.1068	0.1528	11.36	4.54	0.0472	0.0462
2.2.3a	A	0.1282	<0.01	<0.004	<0.001	0.1139	0.0826	9.01	3.60	0.90	0.1216
b	A	0.1277	<0.01	<0.004	<0.001	0.1136	0.0806	9.80	3.92	0.98	0.1143
c	A	0.1237	<0.01	<0.004	<0.001	0.1134	0.0794	10.64	4.25	1.06	0.1112
d	A	0.1223	<0.01	<0.004	<0.001	0.1132	0.0781	11.36	4.54	1.14	0.1090
2.2.3a	B	0.1275	<0.01	<0.004	<0.001	0.1031	0.0910	9.01	3.60	0.90	0.1189
b	B	0.1218	<0.01	<0.004	<0.001	0.1031	0.0892	9.80	3.92	0.98	0.1133
c	B	0.1201	<0.01	<0.004	<0.001	0.1031	0.0877	10.64	4.25	1.06	0.1107
d	B	0.1192	<0.01	<0.004	<0.001	0.1031	0.0870	11.36	4.54	1.14	0.1088
2.2.3a	C	0.1225	<0.01	<0.004	<0.001	0.1056	0.0957	9.01	3.60	0.90	0.0651
b	C	0.1213	<0.01	<0.004	<0.001	0.1053	0.0991	9.80	3.92	0.98	0.0588
c	C	0.1196	<0.01	<0.004	<0.001	0.1052	0.0977	10.64	4.25	1.06	0.0547
d	C	0.1183	<0.01	<0.004	<0.001	0.1051	0.0967	11.36	4.54	1.14	0.0508

TABLE XV (continued)
SUMMARY OF FUSELAGE AND ROTOR NORMALIZED ACCELERATIONS FOR GROUND VIBRATIONS*

Case Number	Criterion	Fuselage Normalized Acceleration					Rotor Normalized Acceleration				
		1/rev	b/rev	2b/rev	3b/rev	4b/rev	1/rev	b/rev	2b/rev	3b/rev	4b/rev
2.4.3a**	A	-	-	-	-	-	-	-	-	-	-
b**	A	-	-	-	-	-	-	-	-	-	-
c**	A	-	-	-	-	-	-	-	-	-	-
d**	A	-	-	-	-	-	-	-	-	-	-
2.4.3a	B	0.1208	<0.01	<0.004	<0.001	0.1199	0.115	9.01	3.60	0.90	0.0683
b	B	0.1189	<0.01	<0.004	<0.001	0.1193	0.1136	9.80	3.92	0.98	0.0633
c	B	0.1175	<0.01	<0.004	<0.001	0.1187	0.1123	10.64	4.25	1.06	0.0751
d	B	0.1165	<0.01	<0.004	<0.001	0.1189	0.111	11.36	4.54	1.14	0.0835
2.4.3a**	C	-	-	-	-	-	-	-	-	-	-
b**	C	-	-	-	-	-	-	-	-	-	-
c**	C	-	-	-	-	-	-	-	-	-	-
d**	C	-	-	-	-	-	-	-	-	-	-
10.4.3a	A	0.1517	<0.01	<0.004	<0.001	0.12262	0.1461	9.01	3.60	0.90	0.0753
b	A	0.1488	<0.01	<0.004	<0.001	0.1221	0.1431	9.80	3.92	0.98	0.0883
c	A	0.1453	<0.01	<0.004	<0.001	0.1215	0.1400	10.64	4.25	1.06	0.1014
d	A	0.1432	<0.01	<0.004	<0.001	0.1212	0.1360	11.36	4.54	1.14	0.2112
10.4.3a	B	0.1512	<0.01	<0.004	<0.001	0.1129	0.1665	9.01	3.60	0.90	0.0051
b	B	0.1483	<0.01	<0.004	<0.001	0.1123	0.1333	9.80	3.92	0.98	0.0077
c	B	0.1452	<0.01	<0.004	<0.001	0.1117	0.1300	10.64	4.25	1.06	0.0132
d	B	0.1431	<0.01	<0.004	<0.001	0.1114	0.1284	11.36	4.54	1.14	0.0192
10.4.3a	C	0.1499	<0.01	<0.004	<0.001	0.1081	0.1479	9.01	3.60	0.90	0.0404
b	C	0.1470	<0.01	<0.004	<0.001	0.1080	0.1441	9.80	3.92	0.98	0.0395
c	C	0.1451	<0.01	<0.004	<0.001	0.1077	0.1412	10.64	4.25	1.06	0.0396
d	C	0.1420	<0.01	<0.004	<0.001	0.1076	0.1392	11.36	4.54	1.14	0.0406

TABLE XV (continued)
SUMMARY OF FUSELAGE AND ROTOR NORMALIZED ACCELERATIONS FOR GROUND VIBRATIONS*

Case Number	Criterion	Fuselage Normalized Acceleration					Rotor Normalized Acceleration				
		1/rev	b/rev	2b/rev	3b/rev	4b/rev	1/rev	b/rev	2b/rev	3b/rev	4b/rev
20.5.3a	A	0.1751	<0.01	<0.004	<0.001	0.1240	0.1675	9.01	3.60	0.90	0.0842
b	A	0.1748	<0.01	<0.004	<0.001	0.1234	0.1673	9.80	3.92	0.98	0.0977
c	A	0.1724	<0.01	<0.004	<0.001	0.1228	0.1651	10.64	4.25	1.06	0.1114
d	A	0.1706	<0.01	<0.004	<0.001	0.1225	0.1633	11.36	4.54	1.14	0.1241
20.5.3a	B	0.1727	<0.01	<0.004	<0.001	0.1136	0.1593	9.01	3.60	0.90	0.0089
b	B	0.1730	<0.01	<0.004	<0.001	0.1130	0.1592	9.80	3.92	0.98	0.0135
c	B	0.1709	<0.01	<0.004	<0.001	0.1125	0.1574	10.64	4.25	1.06	0.0193
d	B	0.1695	<0.01	<0.004	<0.001	0.1121	0.1557	11.36	4.54	1.14	0.0254
20.5.3a	C	0.1727	<0.01	<0.004	<0.001	0.1086	0.1689	9.01	3.60	0.90	0.0414
b	C	0.1727	<0.01	<0.004	<0.001	0.1084	0.1688	9.80	3.92	0.98	0.0380
c	C	0.1706	<0.01	<0.004	<0.001	0.1081	0.1669	10.64	4.25	1.06	0.0386
d	C	0.1689	<0.01	<0.004	<0.001	0.1081	0.1650	11.36	4.54	1.14	0.0400
40.6.3a	A	0.1667	<0.01	<0.004	<0.001	0.1216	0.1595	9.01	3.60	0.90	0.0807
b	A	0.1882	<0.01	<0.004	<0.001	0.1212	0.1730	9.80	3.92	0.98	0.0939
c	A	0.1923	<0.01	<0.004	<0.001	0.1208	0.1835	10.64	4.25	1.06	0.1072
d	A	0.1996	<0.01	<0.004	<0.001	0.1205	0.1906	11.36	4.54	1.14	0.1198
40.6.3a	B	0.1639	<0.01	<0.004	<0.001	0.1118	0.1549	9.01	3.60	0.90	0.0081
b	B	0.1782	<0.01	<0.004	<0.001	0.1113	0.1680	9.80	3.92	0.98	0.0116
c	B	0.1893	<0.01	<0.004	<0.001	0.1110	0.1782	10.64	4.25	1.06	0.0170
d	B	0.1968	<0.01	<0.004	<0.001	0.1106	0.1851	11.36	4.54	1.14	0.0230
40.6.3a	C	0.1650	<0.01	<0.004	<0.001	0.1078	0.1617	9.01	3.60	0.90	0.0390
b	C	0.1792	<0.01	<0.004	<0.001	0.1076	0.1753	9.80	3.92	0.98	0.0382
c	C	0.1901	<0.01	<0.004	<0.001	0.1075	0.1860	10.64	4.25	1.06	0.0386
d	C	0.1976	<0.01	<0.004	<0.001	0.1074	0.1932	11.36	4.54	1.14	0.0398

TABLE XV (continued)
SUMMARY OF FUSELAGE AND ROTOR NORMALIZED ACCELERATIONS FOR GROUND VIBRATIONS*

Case Number	Criterion	Fuselage Normalized Acceleration					Rotor Normalized Acceleration				
		1/rev	b/rev	2b/rev	3b/rev	4b/rev	1/rev	b/rev	2b/rev	3b/rev	4b/rev
80.6.3a	A	0.1075	<0.01	<0.004	<0.001	0.1196	0.1010	9.01	3.60	0.90	0.0540
b	A	0.1239	<0.01	<0.004	<0.001	0.1189	0.1162	9.80	3.92	0.98	0.0622
c	A	0.1426	<0.01	<0.004	<0.001	0.1182	0.1338	10.64	4.25	1.06	0.0688
d	A	0.1602	<0.01	<0.004	<0.001	0.1178	0.1501	11.36	4.54	1.14	0.0757
80.6.3a	B	0.1066	<0.01	<0.004	<0.001	0.1115	0.1042	9.01	3.60	0.90	0.0556
b	B	0.1227	<0.01	<0.004	<0.001	0.1107	0.1198	9.80	3.92	0.98	0.0515
c	B	0.1410	<0.01	<0.004	<0.001	0.1104	0.1377	10.64	4.25	1.06	0.0477
d	B	0.1582	<0.01	<0.004	<0.001	0.1101	0.1538	11.36	4.54	1.14	0.0443
80.6.3a	C	0.1071	<0.01	<0.004	<0.001	0.1070	0.1041	9.01	3.60	0.90	0.0412
b	C	0.1233	<0.01	<0.004	<0.001	0.1069	0.1197	9.80	3.92	0.98	0.0383
c	C	0.1418	<0.01	<0.004	<0.001	0.1067	0.1377	10.64	4.25	1.06	0.0359
d	C	0.1587	<0.01	<0.004	<0.001	0.1066	0.1543	11.36	4.54	1.14	0.0340
80.7.3a	A	0.1069	<0.01	<0.004	<0.001	0.1275	0.0980	9.01	3.60	0.90	0.1061
b	A	0.1231	<0.01	<0.004	<0.001	0.1264	0.1127	9.80	3.92	0.98	0.1163
c	A	0.1418	<0.01	<0.004	<0.001	0.1255	0.1297	10.64	4.25	1.06	0.1270
d	A	0.1595	<0.01	<0.004	<0.001	0.1248	0.1351	11.36	4.54	1.14	0.1373
80.7.3a	B	0.1065	<0.01	<0.004	<0.001	0.1118	0.1527	9.01	3.60	0.90	0.0562
b	B	0.1225	<0.01	<0.004	<0.001	0.1117	0.1183	9.80	3.92	0.98	0.0558
c	B	0.1408	<0.01	<0.004	<0.001	0.1109	0.1359	10.64	4.25	1.06	0.0559
d	B	0.1580	<0.01	<0.004	<0.001	0.1106	0.1523	11.36	4.54	1.14	0.0571
80.7.3a	C	0.1069	<0.01	<0.004	<0.001	0.1077	0.1027	9.01	3.60	0.90	0.0214
b	C	0.1230	<0.01	<0.004	<0.001	0.1076	0.1182	9.80	3.92	0.98	0.0197
c	C	0.1416	<0.01	<0.004	<0.001	0.1074	0.1359	10.64	4.25	1.06	0.0198
d	C	0.1590	<0.01	<0.004	<0.001	0.1074	0.1523	11.36	4.54	1.14	0.0214

TABLE XV (continued)

* Normalized acceleration values relate the levels of acceleration experienced by the isolated fuselage and rotor to the unisolated rotor excitation at the blade passage frequency. The normalized acceleration at each critical frequency is equal to the normalized rotor excitation at that frequency (Figure 1) divided by the effectiveness at that frequency (Table XII).

** Displacement feedback gain could not be reduced from the value used in Criterion B without resulting in either an unstable system or a very sluggish system response.

In-Flight Maneuvers

The excitations applied at the rotor during maneuvers are +3 g and -0.5 g ramps having a rise-time of 0.6 second. In all cases, the isolation system induces rotor and fuselage acceleration oscillations about the input acceleration. The acceleration overshoot for the rotor is greater than for the fuselage, since the control system applies the same force to both masses and, therefore, the smaller mass experiences a larger acceleration.

Table XVI shows the characteristics of the relative displacement time history for the +3 g, 0.6 second ramp input. The peak displacement is shown in each case. When the response is fast and the displacement crosses zero, the time to reach zero displacement and the amplitude of oscillation after reaching zero displacement are tabulated (Figure 26). For the cases where the system response is highly damped and reaches zero asymptotically, the time to reach a displacement equal to 5 percent of the peak displacement is tabulated. Both these times serve as a measure of the system speed of response.

Figure 34 shows the peak relative displacement during a 3 g maneuver plotted versus blade passage frequency for the two- and three-notch isolators having parameters based on the three previously mentioned criteria. The two-notch isolators give rise to smaller relative displacements due primarily to the larger relative gains required to limit the displacements during landing shock. The smallest displacements occur for Criterion B due to lower values of lead network time constant and increased relative gains.

The peak displacement due to in-flight maneuvers is independent of the rotor or fuselage masses, or their mass ratio [Equation (63)]. The rotor and fuselage acceleration overshoots are dependent on the fuselage mass [Equations (36) and (37)]. However, the overshoot does not exceed 3 percent for any of the fuselage weight changes considered in the study. Values of fuselage and rotor acceleration for the +3 g, 0.6 second ramp are shown in Table XVII.

Examination of Equations (36), (37) and (38) indicates that the system response is directly proportional to the level of the peak ramp acceleration. As previously stated, the response to a -0.5 g ramp in rotor force will be -1/6 that resulting from the +3 g ramp. Finally, an increase in the time duration of the ramp from 0.6 to 1.0 second allows the system to follow the excitation more closely. Therefore, the values of rotor and fuselage acceleration overshoot will be lower than the 3 percent value for the 0.6 second rise-time ramp. As indicated in Equation (63), the peak displacement is inversely proportional to the ramp rise-time. Values of displacement for the 0.8 and 1.0 second rise-time ramps can be obtained from those shown in Table XVI; they can be obtained from Figure 34 for the 0.6 second rise-time ramp.

TABLE XVI

SUMMARY OF SYSTEM RESPONSE TO + 3g ACCELERATION, 0.6 sec RISE TIME MANEUVER

Case Number	Criterion	Peak Displacement (in.)	Time to Reach Zero Displacement* (sec)	Oscillations After Reaching Zero Displacement (in. D.A.)	5% of Peak Displacement** (in.)	Time to Reach 5% of Peak Displacement*** (sec)
2.2.2a	A	0.03	0.80	0.0008	-	-
b	A	0.03	0.90	0.0013	-	-
c	A	0.03	0.81	0.0014	-	-
d	A	0.03	0.80	0.0014	-	-
2.2.2a	B	0.0175	0.80	0.0007	-	-
b	B	0.0175	0.90	0.0004	-	-
c	B	0.0175	0.92	0.0003	-	-
d	B	0.0175	0.98	0.0003	-	-
2.2.2a	C	0.0155	0.80	0.0005	-	-
b	C	0.0155	0.85	0.0010	-	-
c	C	0.0155	0.88	0.0006	-	-
d	C	0.0155	0.90	0.0009	-	-
2.4.2a	A	0.27	-	-	0.0135	2.00
b	A	0.27	-	-	0.0135	1.75
c	A	0.27	-	-	0.0135	1.80
d	A	0.27	-	-	0.0135	1.85
2.4.2a	B	0.0255	-	-	0.0013	0.80
b	B	0.0255	-	-	0.0013	0.80
c	B	0.0255	-	-	0.0013	0.80
d	B	0.0255	-	-	0.0013	0.78
2.4.2a	C	0.11	-	-	0.0055	1.85
b	C	0.11	-	-	0.0055	1.75
c	C	0.11	-	-	0.0055	1.80
d	C	0.11	-	-	0.0055	1.80

TABLE XVI (continued)
SUMMARY OF SYSTEM RESPONSE TO + 3g ACCELERATION, 0.6 sec RISE TIME MANEUVER

Case Number	Criterion	Peak Displacement (in.)	Time to Reach Zero Displacement* (sec)	Oscillations After Reaching Zero Displacement (in. D.A.)	5% of Peak Displacement** (in.)	Time to Reach 5% of Peak Displacement*** (sec)
10.4.2a(1)	A	0.08	-	-	0.0048	2.00
b(1)	A	0.08	-	-	0.0048	1.05
c(1)	A	0.08	-	-	0.0048	1.1
d(1)	A	0.08	-	-	0.0048	1.1
10.4.2a(1)	B	0.011	0.75	0.0003	-	-
b(1)	B	0.011	0.75	0.0006	-	-
c(1)	B	0.011	0.72	0.0007	-	-
d(1)	B	0.011	0.73	0.0006	-	-
10.4.2a(1)	C	0.048	-	-	0.0024	1.0
b(1)	C	0.048	-	-	0.0024	0.95
c(1)	C	0.048	-	-	0.0024	1.0
d(1)	C	0.048	-	-	0.0024	0.97
80.6.2a	A	0.035	0.80	0.0008	-	-
b	A	0.035	0.81	0.0008	-	-
c	A	0.035	0.80	0.0012	-	-
d	A	0.035	0.80	0.0007	-	-
80.6.2a	B	0.013	0.70	0.0008	-	-
b	B	0.013	0.80	0.0005	-	-
c	B	0.013	0.90	0.0005	-	-
d	B	0.013	0.80	0.0006	-	-
80.6.2a	C	0.0145	0.77	0.0004	-	-
b	C	0.0145	0.80	0.0004	-	-
c	C	0.0145	0.82	0.0003	-	-
d	C	0.0145	0.82	0.0003	-	-

TABLE XVI (continued)

SUMMARY OF SYSTEM RESPONSE TO + 3g ACCELERATION, 0.6 sec RISE TIME MANEUVER

Case Number	Criterion	Peak Displacement (in.)	Time to Reach Zero Displacement* (sec)	Oscillations After Reaching Zero Displacement (in. D. A.)	5% of Peak Displacement** (in.)	Time to Reach 5% of Peak Displacement*** (sec)
80.7.2a	A	0.062	-	-	0.0031	0.90
b	A	0.062	-	-	0.0031	0.95
c	A	0.062	-	-	0.0031	0.92
d	A	0.062	-	-	0.0031	0.92
80.7.2a	B	0.0105	0.80	0.0002	-	-
b	B	0.0105	0.75	0.0005	-	-
c	B	0.0105	0.75	0.0004	-	-
d	B	0.0105	0.75	0.0004	-	-
80.7.2a	C	0.025	0.90	0.0002	-	-
b	C	0.025	0.90	-	0.0011	0.90
c	C	0.025	0.90	-	0.0011	0.90
d	C	0.025	0.90	-	0.0011	0.90
2.2.3a	A	0.055	0.98	0.00075	-	-
b	A	0.055	0.98	0.00080	-	-
c	A	0.055	0.98	0.00070	-	-
d	A	0.055	0.98	0.00080	-	-
2.2.3a	B	0.0175	0.80	0.00072	-	-
b	B	0.0175	0.82	0.00060	-	-
c	B	0.0175	0.83	0.00075	-	-
d	B	0.0175	0.83	0.00075	-	-
2.2.3a	C	0.0215	0.90	0.00041	-	-
b	C	0.0215	0.90	0.00041	-	-
c	C	0.0215	0.88	0.00041	-	-
d	C	0.0215	0.91	0.00041	-	-

TABLE XVI (continued)
SUMMARY OF SYSTEM RESPONSE TO + 3g ACCELERATION, 0.6 sec RISE TIME MANEUVER

Case Number	Criterion	Peak Displacement (in.)	Time to Reach Zero Displacement* (sec)	Oscillations After Reaching Zero Displacement (in. D. A.)	5% of Peak Displacement** (in.)	Time to Reach 5% of Peak Displacement*** (sec)
2.4.3a(2)	A	-	-	-	-	-
b(2)	A	-	-	-	-	-
c(2)	A	-	-	-	-	-
d(2)	A	-	-	-	-	-
2.4.3a	B	0.080	-	-	0.0040	1.35
b	B	0.080	-	-	0.0040	1.22
c	B	0.082	-	-	0.0042	11.32
d	B	0.082	-	-	0.0042	1.23
2.4.3a(2)	C	-	-	-	-	-
b(2)	C	-	-	-	-	-
c(2)	C	-	-	-	-	-
d(2)	C	-	-	-	-	-
10.4.3a(3)	A	0.343	-	-	0.0171	2.3
b(3)	A	0.343	-	-	0.0171	2.0
c(3)	A	0.370	-	-	0.0185	2.1
d(3)	A	0.350	-	-	0.0175	2.4
10.4.3a(3)	B	0.028	-	-	0.0014	1.0
b(3)	B	0.028	-	-	0.0014	0.92
c(3)	B	0.028	-	-	0.0014	0.90
d(3)	B	0.028	-	-	0.0014	0.90
10.4.3a(3)	C	0.145	-	-	0.0078	1.75
b(3)	C	0.145	-	-	0.0078	1.70
c(3)	C	0.145	-	-	0.0078	1.6
d(3)	C	0.145	-	-	0.0078	1.5

TABLE XVI (continued)

SUMMARY OF SYSTEM RESPONSE TO + 3g ACCELERATION, 0.6 sec RISE TIME MANEUVER

Case Number	Criterion	Peak Displacement (in.)	Time to Reach Zero Displacement* (sec)	Oscillations After Reaching Zero Displacement (in. D.A.)	5% of Peak Displacement** (in.)	Time to Reach 5% of Peak Displacement*** (sec)
80.6.3a	A	0.14	-	-	0.0070	1.05
b	A	0.14	-	-	0.0070	1.05
c	A	0.14	-	-	0.0070	1.10
d	A	0.14	-	-	0.0070	1.10
80.6.3a	B	0.145	0.75	0.0004	-	-
b	B	0.145	0.75	0.0008	-	-
c	B	0.145	0.8	0.0006	-	-
d	B	0.145	0.7	0.0006	-	-
80.6.3a	C	0.06	-	-	0.0030	1.1
b	C	0.06	-	-	0.0030	1.1
c	C	0.06	-	-	0.0030	1.1
d	C	0.06	-	-	0.0030	1.1
80.7.3a	A	0.182	-	-	0.0087	1.22
b	A	0.182	-	-	0.0087	1.15
c	A	0.182	-	-	0.0088	1.18
d	A	0.182	-	-	0.0085	1.1
80.7.3a	B	0.028	0.83	0.0008	-	-
b	B	0.028	0.84	0.0005	-	-
c	B	0.028	0.90	0.0005	-	-
d	B	0.028	0.80	0.0006	-	-
80.7.3a	C	0.078	-	0.0004	0.0036	1.25
b	C	0.078	-	0.0004	0.0036	1.15
c	C	0.078	-	0.0003	0.0039	1.24
d	C	0.078	-	0.0003	0.0038	1.2

TABLE XVI (continued)

* Time at which displacement time history first crosses zero.

** For these cases the system is highly damped and the relative displacement approaches zero asymptotically. To judge the speed of response of the system, a value of 5% of the peak displacements is used instead of zero displacement.

*** Time at which the displacement equals 5% of peak value. Applicable to cases where the displacement reaches zero asymptotically.

(1) Cases 20.5.2 and 40.6.2 have response identical to case 10.4.2 since the blade passage frequency for all three cases is practically the same.

(2) Displacement feedback gain could not be reduced from the value used in Criterion B without resulting in either an unstable system or in a very sluggish system response.

(3) Cases 20.5.3 and 40.6.3 have responses identical to case 10.4.3 since the blade passage frequency for all three cases is practically the same.

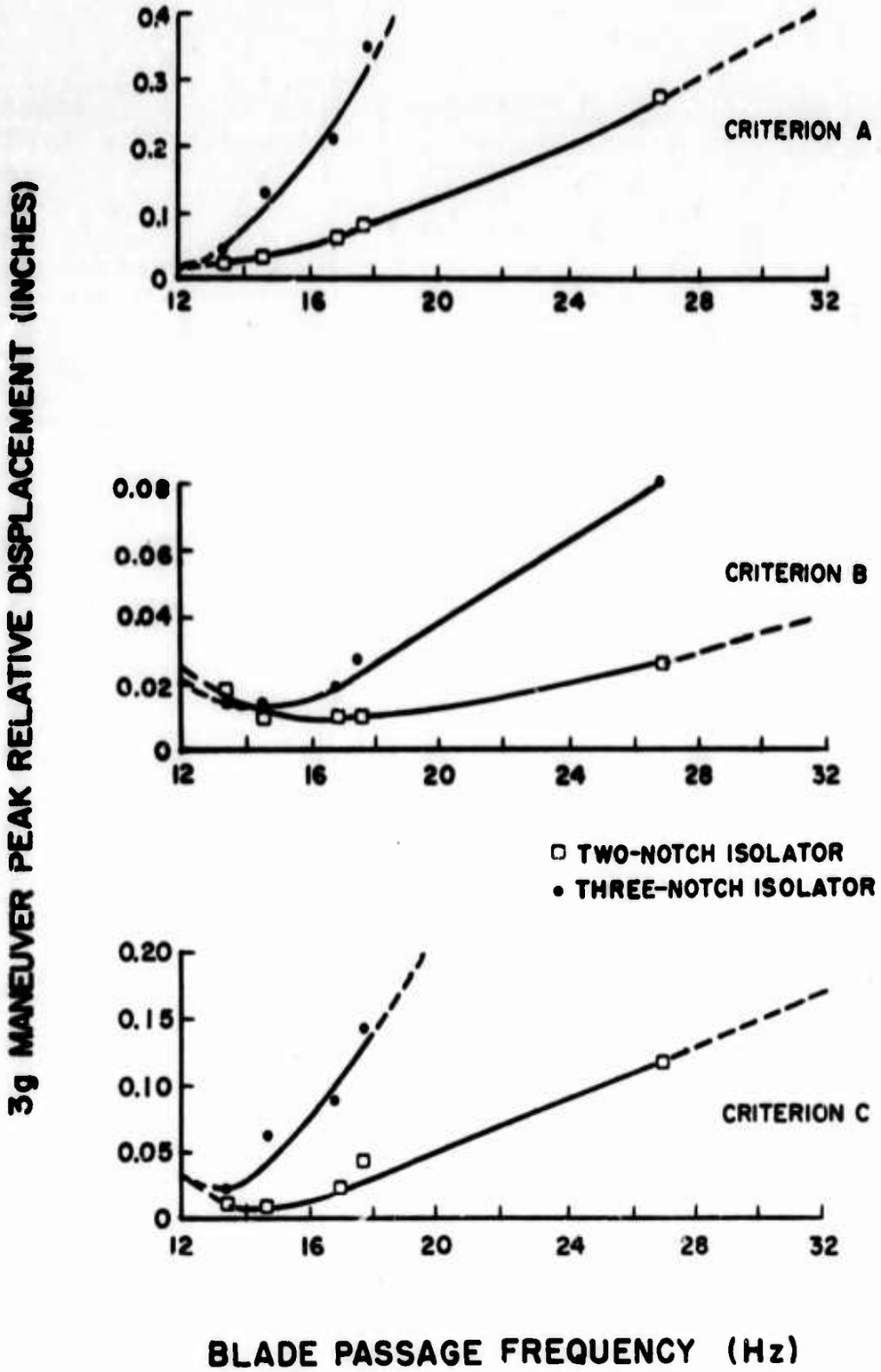

Figure 34. Relationship Between Peak Relative Displacement During +3g, 0.6 Second Maneuver, and Blade Passage Frequency for Two- and Three-Notch Isolators Having System Parameters Based on Criteria A, B, and C.

TABLE XVII

FUSELAGE AND ROTOR ACCELERATIONS FOR TRANSIENT CONDITIONS

Case Number	Criterion	Peak Acceleration			
		10 ft/sec Landing		+3 g, 0.6 sec Ramp Maneuver	
		Fuselage (g)	Rotor (g)	Fuselage (g)	Rotor (g)
2.2.2a	A	6.30	9.2	3.0	3.05
b	A	5.60	7.7	3.0	3.05
c	A	5.35	7.7	3.0	3.05
d	A	5.30	7.4	3.0	3.05
2.2.2a	B	6.0	7.0	3.0	3.05
b	B	5.5	6.2	3.0	3.05
c	B	5.3	5.6	3.0	3.05
d	B	5.3	5.8	3.0	3.05
2.2.2a	C	6.1	7.2	3.0	3.05
b	C	5.5	6.3	3.0	3.05
c	C	5.3	6.3	3.0	3.05
d	C	5.2	6.3	3.0	3.05
2.4.2a	A	6.3	8.6	3.0	3.05
b	A	5.6	7.5	3.0	3.05
c	A	5.3	7.1	3.0	3.05
d	A	5.2	6.8	3.0	3.05
2.4.2a	B	6.3	8.3	3.0	3.05
b	B	5.6	7.2	3.0	3.05
c	B	5.6	7.0	3.0	3.05
d	B	5.3	6.9	3.0	3.05
2.4.2a	C	5.7	6.8	3.0	3.05
b	C	5.5	6.3	3.0	3.05
c	C	5.5	6.1	3.0	3.05
d	C	5.0	5.8	3.0	3.05

TABLE XVII (continued)

Case Number	Criterion	Peak Acceleration			
		10 ft/sec Landing		+3 g, 0.6 sec Ramp Maneuver	
		Fuselage (g)	Rotor (g)	Fuselage (g)	Rotor (g)
10.4.2a	A	6.1	8.8	3.0	3.0
b	A	5.6	7.5	3.0	3.0
c	A	5.5	7.0	3.0	3.0
d	A	5.4	6.8	3.0	3.0
10.4.2a	B	5.8	8.4	3.0	3.0
b	B	5.7	8.4	3.0	3.0
c	B	5.5	7.4	3.0	3.0
d	B	5.2	7.0	3.0	3.0
10.4.2a	C	5.8	7.0	3.0	3.0
b	C	5.5	6.3	3.0	3.0
c	C	5.5	5.8	3.0	3.0
d	C	5.2	5.7	3.0	3.0
80.6.2a	A	6.1	9.2	3.0	3.1
b	A	5.7	8.3	3.0	3.1
c	A	5.6	7.6	3.0	3.1
d	A	5.3	7.3	3.0	3.1
80.6.2a	B	5.90	7.6	3.0	3.1
b	B	5.60	6.8	3.0	3.1
c	B	5.60	6.8	3.0	3.1
d	B	5.25	6.4	3.0	3.1
80.6.2a	C	5.8	6.70	3.0	3.1
b	C	5.6	6.95	3.0	3.1
c	C	5.4	6.20	3.0	3.1
d	C	5.1	5.80	3.0	3.1

TABLE XVII (continued)

Case Number	Criterion	Peak Acceleration			
		10 ft/sec Landing		+3 g, 0.6 sec Ramp Maneuver	
		Fuselage (g)	Rotor (g)	Fuselage (g)	Rotor (g)
80.7.2a	A	6.0	8.7	3.0	3.05
b	A	5.8	7.4	3.0	3.05
c	A	5.7	7.3	3.0	3.05
d	A	5.3	6.8	3.0	3.05
80.7.2a	B	5.9	8.4	3.0	3.05
b	B	5.7	7.6	3.0	3.05
c	B	5.5	7.2	3.0	3.05
d	B	5.5	7.2	3.0	3.05
80.7.2a	C	5.8	6.6	3.0	3.05
b	C	5.5	6.0	3.0	3.05
c	C	5.6	6.0	3.0	3.05
d	C	5.2	6.1	3.0	3.05
2.2.3a	A	5.40	7.8	3.0	3.1
b	A	5.40	8.4	3.0	3.1
c	A	5.35	8.6	3.0	3.1
d	A	5.35	8.6	3.0	3.1
2.2.3a	B	5.4	7.0	3.0	3.05
b	B	5.4	6.8	3.0	3.05
c	B	5.3	6.8	3.0	3.05
d	B	5.1	7.2	3.0	3.05
2.2.3a	C	5.4	6.2	3.0	3.02
b	C	5.4	6.0	3.0	3.02
c	C	5.2	6.3	3.0	3.02
d	C	5.3	6.3	3.0	3.02

TABLE XVII (continued)

Case Number	Criterion	Peak Acceleration			
		10 ft/sec Landing		+3g, 0.6 sec Ramp Maneuver	
		Fuselage (g)	Rotor (g)	Fuselage (g)	Rotor (g)
2.4.3a	A	-	-	-	-
b	A	-	-	-	-
c	A	-	-	-	-
d	A	-	-	-	-
2.4.3a	B	5.4	6.80	3.0	3.05
b	B	5.5	6.95	3.0	3.05
c	B	5.5	7.00	3.0	3.05
d	B	5.3	6.95	3.0	3.05
2.4.3a	C	-	-	-	-
b	C	-	-	-	-
c	C	-	-	-	-
d	C	-	-	-	-
10.4.3a	A	5.30	6.6	3.0	3.0
b	A	5.45	7.0	3.0	3.0
c	A	5.50	7.0	3.0	3.0
d	A	5.50	7.0	3.0	3.0
10.4.3a	B	5.4	6.2	3.0	3.05
b	B	5.4	6.8	3.0	3.05
c	B	5.4	7.0	3.0	3.05
d	B	5.3	6.8	3.0	3.05
10.4.3a	C	5.3	5.7	3.0	3.025
b	C	5.4	6.0	3.0	3.025
c	C	5.2	6.0	3.0	3.025
d	C	4.8	5.6	3.0	3.025

TABLE XVII (continued)

Case Number	Criterion	Peak Acceleration			
		10 ft/sec Landing		+3 g, 0.6 sec Ramp Maneuver	
		Fuselage (g)	Rotor (g)	Fuselage (g)	Rotor (g)
80.6.3a	A	5.3	7.2	3.0	3.075
b	A	5.4	7.3	3.0	3.075
c	A	5.3	6.6	3.0	3.075
d	A	4.8	6.0	3.0	3.075
80.6.3a	B	5.4	7.0	3.0	3.05
b	B	5.1	6.9	3.0	3.05
c	B	5.0	6.8	3.0	3.05
d	B	4.8	6.6	3.0	3.05
80.6.3a	C	5.2	5.8	3.0	3.03
b	C	5.3	5.8	3.0	3.03
c	C	5.0	5.4	3.0	3.03
d	C	4.8	5.2	3.0	3.03
80.7.3a	A	5.4	7.0	3.0	3.05
b	A	5.3	6.3	3.0	3.05
c	A	5.4	6.1	3.0	3.05
d	A	5.2	7.2	3.0	3.05
80.7.3a	B	5.4	7.1	3.0	3.05
b	B	5.8	7.0	3.0	3.05
c	B	5.3	6.7	3.0	3.05
d	B	5.1	6.4	3.0	3.05
80.7.3a	C	5.2	5.8	3.0	3.03
b	C	5.3	5.8	3.0	3.03
c	C	5.0	5.4	3.0	3.03
d	C	4.8	5.2	3.0	3.03

Landing Shock

The primary consideration in the selection of system parameters is to limit the peak relative displacement between rotor and fuselage during the 10 ft/sec landing shock condition. The system stability and performance under the other dynamic conditions are dependent on the same parameters, and the final design is based on a tradeoff between displacement control, vibration isolation, and stability. For the 10 ft/sec landing shock, two values of peak displacement are considered as design goals, namely 0.5 and 0.2 inch. For the smaller value of displacement, parameters are selected based on two different stability margins. In all cases the peak displacement under the most severe landing shock is equal to the value set by the performance criterion.

Values of peak fuselage and rotor accelerations are shown in Table XVII for the 10 ft/sec landing velocity. Figure 35 shows the peak acceleration experienced by the rotor during 10 ft/sec landing shock as a function of blade passage frequency for the two- and three-notch element isolators and as having parameters selected on the basis of Criteria A, B, and C. All systems having two notches of isolation yielded slightly higher rotor accelerations, due to the broader notch bandwidths. Systems having the lowest acceleration flow gains (Criterion C with three notches) resulted in the lowest rotor accelerations. A reduction in acceleration gain to satisfy stability requirements also gives rise to lower rotor accelerations with increasing blade passage frequency. For low values of b/rev, the notch bandwidths for the two- and three-notch systems are approximately the same, and the rotor experiences approximately the same acceleration in all cases.

Figure 36 shows the peak fuselage acceleration experienced by the fuselage during the 10 ft/sec landing shock as a function of blade passage frequency for the two- and three-notch element isolators with parameters selected on the basis of the three design criteria mentioned above. As in the case of rotor acceleration, the two-notch isolators resulted in higher fuselage accelerations due to broader bandwidths at each notch. However, the difference in fuselage acceleration between the two- and three-notch isolators is not very pronounced, and changes in system parameters based on the three criteria do not significantly affect the fuselage response during the landing shock, which is governed primarily by the dynamic characteristics of the landing gear. As a result of a literature survey into the typical stiffness characteristics of helicopter undercarriages, all landing gears are assumed to have a stiffness that yields a natural frequency of 3 Hz, based on the total weight of the rotor and fuselage. Therefore, the fuselage response in all cases should be approximately the same. The rotor response, however, is a function of the characteristics of the isolator interposed between the rotor and the fuselage, as indicated in the preceding paragraphs.

Table XVIII shows the characteristics of the relative displacement time history for the 10 ft/sec velocity landing shock including peak displacement, time to reach zero displacement, and displacement at the second (negative) and third (positive) peaks. The time to reach zero displacement and the displacement values of subsequent peaks give a measure of the system speed of response.

The acceleration response of each of the systems to lower velocity landing shocks is proportionately lower [Equations (39), (40), and (41)]. In the analysis, the fuselage was allowed to bounce off the ground whenever the rebounding accelerations exceeded 1 g. In all cases, the 10 ft/sec landing shock caused the fuselage to do so. For landing velocity shocks of 5 ft/sec, the fuselage did not bounce off the ground. The peak displacement and rotor and fuselage accelerations occurred during the initial response to landing prior to bouncing off the ground. Therefore, although the shape of the acceleration and displacement time histories after the bounce are different depending on whether the fuselage bounces off the ground, the peak displacement values are directly proportional to the level of velocity shock during landing.

In all cases the effect of increasing the fuselage mass changes the system response during landing. The peak rotor and fuselage accelerations decrease with increasing fuselage mass. As the fuselage mass increases, both the resonant frequency and the damping fraction of the helicopter decrease, resulting in lower values of the initial fuselage accelerations and associated reduction in rotor acceleration.

Finally, a comment is made regarding helicopters with high blade passage frequency. Examination of Figures 34, 35, and 36 indicates that no data points are shown for blade passage frequency of 26.6 Hz for the three-notch isolator having parameters selected on the basis of criteria A and C. The third notch for b/rev of 26.6 Hz occurs at approximately 80 Hz, which approaches the natural frequencies of the servovalve and actuator. The magnitude of total gain at the phase crossover frequency (Figure 15) is high; if a 20-db gain margin is to be maintained to insure system stability, a very small amount of acceleration flow gain can be introduced, and the resulting transient displacements will be less than 0.5 inch. The relative gains can be decreased and the lead time constant increased, while the acceleration gain is simultaneously increased, to result in larger displacements and satisfy the 20-db gain margin requirement. However, due to the high values of relative gains and lead time constant, the system response during in-flight maneuvers becomes very sluggish and the actuator will remain at the peak displacement position long after the in-flight ramp force has reached its final valve. Therefore, based on the desired fast system response, only the criterion of 0.2 inch maximum displacement under 10 ft/sec landing shock with a 20-db gain margin could be satisfied for the three-notch system at b/rev = 26.6 Hz.

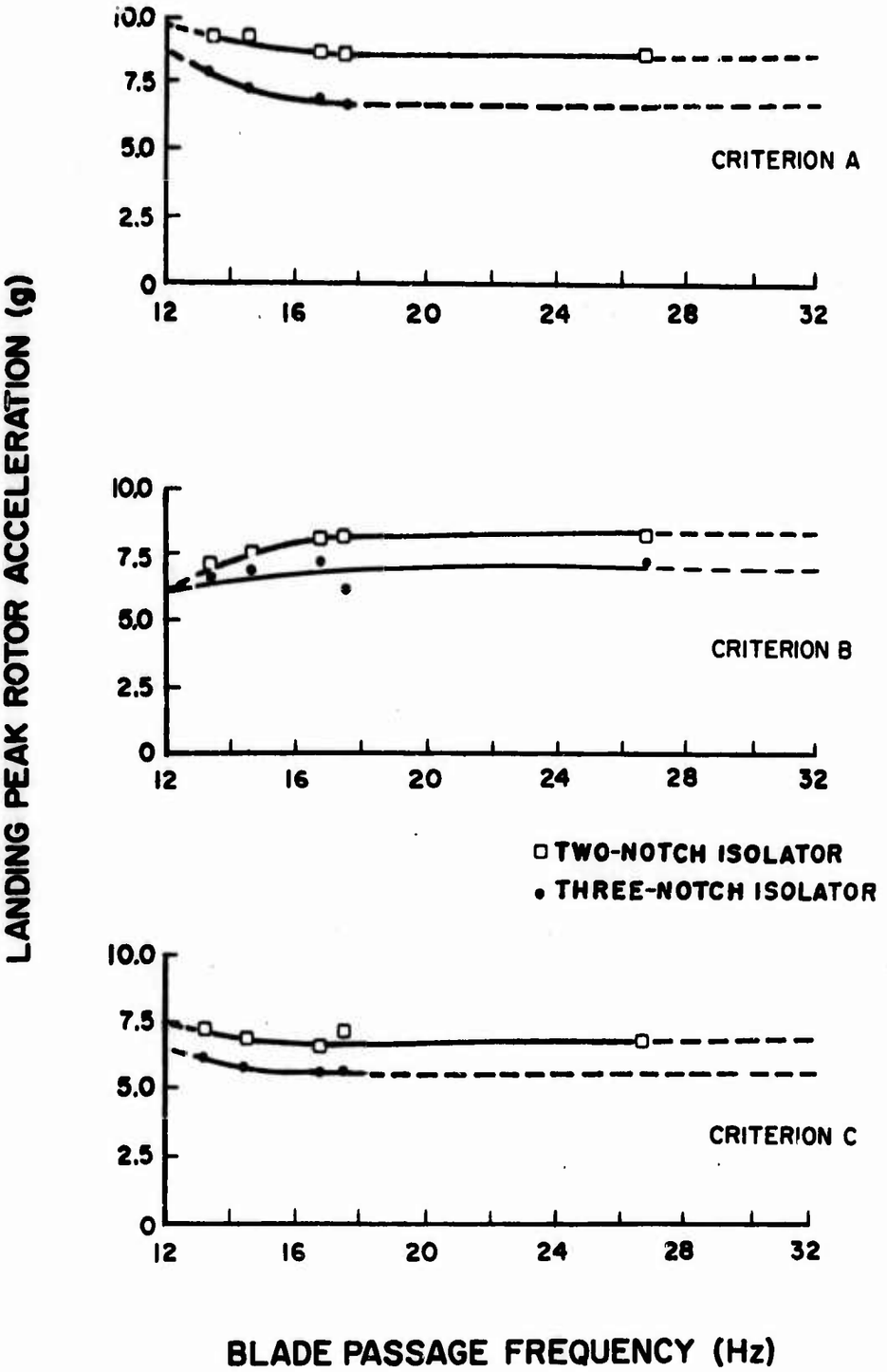

Figure 35. Relationship Between Peak Rotor Acceleration During the 10 ft/sec Landing Velocity Shock and Blade Passage Frequency for Two- and Three-Notch Isolators Having System Parameters Based on Criteria A, B, and C.

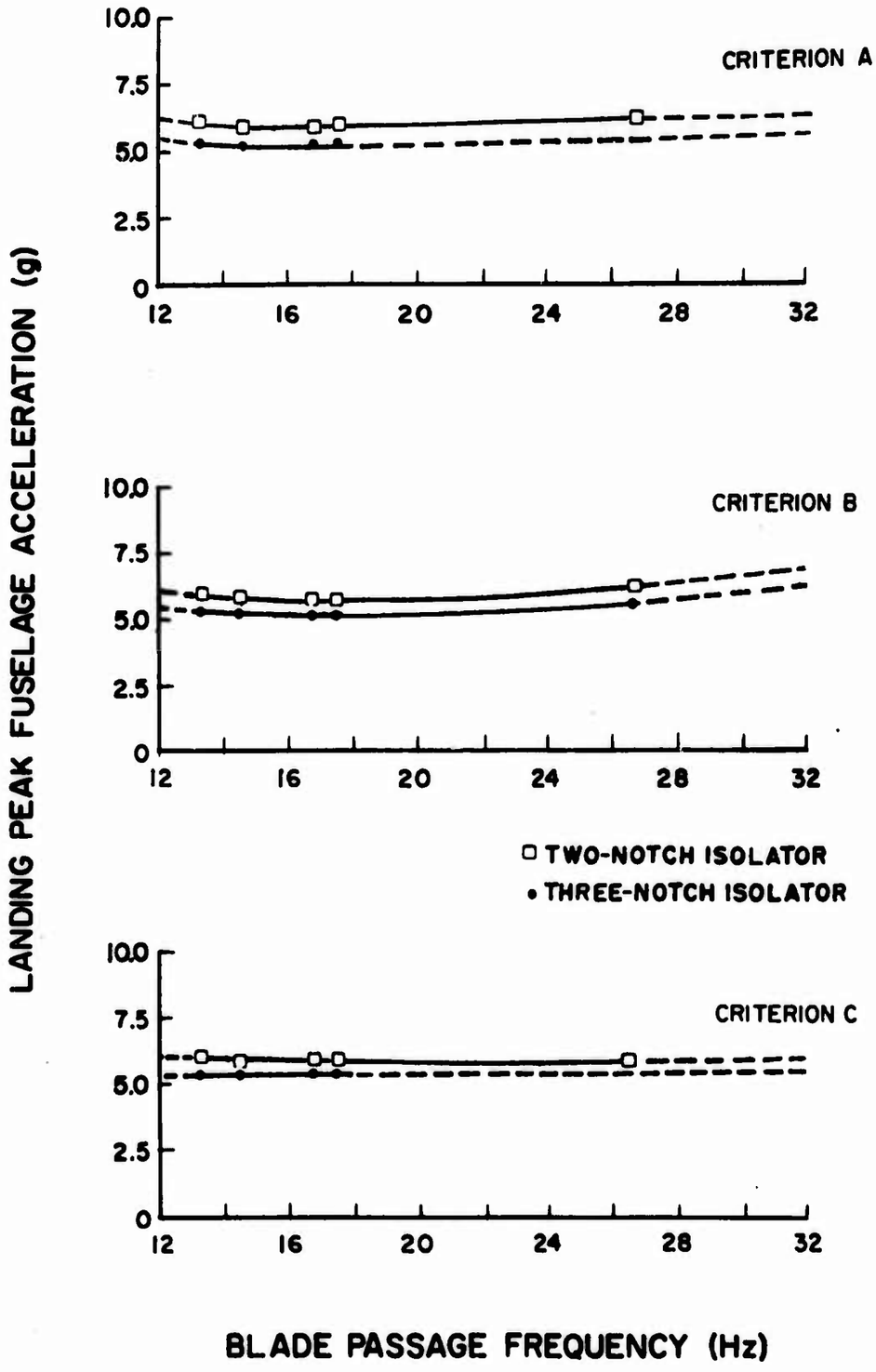

Figure 36. Relationship Between Peak Fuselage Acceleration During the 10 ft/sec Landing Velocity Shock and Blade Passage Frequency for Two- and Three-Notch Isolators Having System Parameters Based on Criteria A, B, and C.

TABLE XVIII

SUMMARY OF SYSTEM RESPONSE TO 10 ft/sec VELOCITY LANDING SHOCK

Case Number	Criterion	Maximum Displacement [First Peak] (in.)	Time to Read Zero Displacement* (sec)	Displacement at Second Peak (in.)	Displacement at Third Peak (in.)
2.2.2a	A	+0.47	0.08	-0.32	+0.10
b	A	+0.42	0.08	-0.36	+0.14
c	A	+0.41	0.08	-0.28	+0.15
d	A	+0.38	0.12	-0.36	+0.13
2.2.2a	B	+0.190	0.10	-0.14	+0.13
b	B	+0.195	0.13	-0.13	+0.095
c	B	+0.190	0.13	-0.12	+0.075
d	B	+0.185	0.14	-0.11	+0.075
2.2.2a	C	+0.190	0.09	-0.16	+0.060
b	C	+0.185	0.07	-0.16	+0.085
c	C	+0.195	0.07	-0.14	+0.085
d	C	+0.175	0.13	-0.13	+0.085
2.4.2a	A	+0.48	0.20	-0.26	+0.05
b	A	+0.43	0.20	-0.22	+0.04
c	A	+0.44	0.21	-0.20	+0.08
d	A	+0.43	0.21	-0.22	+0.06
2.4.2a	B	+0.195	0.12	-0.15	+0.050
b	B	+0.180	0.12	-0.14	+0.065
c	B	+0.180	0.13	-0.13	+0.060
d	B	+0.170	0.14	-0.12	+0.065
2.4.2a	C	+0.195	0.18	-0.12	+0.000
b	C	+0.180	0.19	-0.08	+0.025
c	C	+0.195	0.20	-0.09	+0.030
d	C	+0.180	0.20	-0.09	+0.030

TABLE XVIII (continued)
SUMMARY OF SYSTEM RESPONSE TO 10 ft/sec VELOCITY LANDING SHOCK

Case Number	Criterion	Maximum Displacement [First Peak] (in.)	Time to Read Zero Displacement* (sec)	Displacement at Second Peak (in.)	Displacement at Third Peak (in.)
10.4.2a(1)	A	+0.46	0.16	-0.26	+0.13
b(1)	A	+0.44	0.16	-0.26	+0.12
c(1)	A	+0.41	0.16	-0.24	+0.14
d(1)	A	+0.40	0.15	-0.27	+0.12
10.4.2a(1)	B	+0.190	0.09	-0.12	+0.050
b(1)	B	+0.185	0.07	-0.12	+0.055
c(1)	B	+0.185	0.10	-0.12	+0.055
d(1)	B	+0.180	0.11	-0.11	+0.050
10.4.2a(1)	C	+0.195	0.16	-0.13	+0.060
b(1)	C	+0.190	0.15	-0.13	+0.055
c(1)	C	+0.175	0.17	-0.12	+0.060
d(1)	C	+0.160	0.16	-0.12	+0.055
80.6.2a	A	+0.50	0.13	-0.30	+0.12
b	A	+0.44	0.12	-0.27	+0.12
c	A	+0.43	0.12	-0.24	+0.13
d	A	+0.38	0.13	-0.24	+0.10
80.6.2a	B	+0.180	0.07	-0.16	+0.035
b	B	+0.175	0.08	-0.13	+0.065
c	B	+0.175	0.07	-0.12	+0.070
d	B	+0.160	0.12	-0.11	+0.065
80.6.2a	C	+0.195	0.12	-0.14	+0.055
b	C	+0.195	0.08	-0.13	+0.065
c	C	+0.175	0.13	-0.11	+0.065
d	C	+0.160	0.12	-0.12	+0.060

TABLE XVIII (continued)

SUMMARY OF SYSTEM RESPONSE TO 10 ft/sec VELOCITY LANDING SHOCK

Case Number	Criterion	Maximum Displacement [First Peak] (in.)	Time to Read Zero Displacement* (sec)	Displacement at Second Peak (in.)	Displacement at Third Peak (in.)
80.7.2a	A	+0.48	0.12	-0.30	+0.13
b	A	+0.40	0.12	-0.26	+0.10
c	A	+0.38	0.13	-0.25	+0.14
d	A	+0.35	0.14	-0.24	+0.13
80.7.2a	B	+0.195	0.11	-0.15	+0.035
b	B	+0.170	0.07	-0.11	+0.040
c	B	+0.165	0.06	-0.10	+0.050
d	B	+0.155	0.06	-0.10	+0.060
80.7.2a	C	+0.181	0.06	-0.17	+0.055
b	C	+0.170	0.13	-0.12	+0.060
c	C	+0.165	0.12	-0.12	+0.060
d	C	+0.150	0.14	-0.11	+0.065
2.2.3a	A	+0.440	0.13	-0.32	+0.13
b	A	+0.435	0.13	-0.32	+0.15
c	A	+0.433	0.14	-0.32	+0.14
d	A	+0.432	0.13	-0.30	+0.17
2.2.3a	B	+0.20	0.08	-0.17	+0.065
b	B	+0.22	0.09	-0.14	+0.080
c	B	+0.21	0.08	-0.16	+0.070
d	B	+0.20	0.08	-0.15	+0.065
2.2.3a	C	+0.190	0.14	-0.13	+0.050
b	C	+0.195	0.13	-0.13	+0.060
c	C	+0.200	0.15	-0.13	+0.075
d	C	+0.190	0.14	-0.12	+0.075

TABLE XVIII(continued)

SUMMARY OF SYSTEM RESPONSE TO 10 ft/sec VELOCITY LANDING SHOCK

Case Number	Criterion	Maximum Displacement [First Peak] (in.)	Time to Read Zero Displacement* (sec)	Displacement at Second Peak (in.)	Displacement at Third Peak (in.)
2.4.3a(2)	A	-	-	-	-
b(2)	A	-	-	-	-
c(2)	A	-	-	-	-
d(2)	A	-	-	-	-
2.4.3a	B	+0.2	0.18	-0.11	+0.020
b	B	+0.2	0.17	-0.12	+0.025
c	B	+0.2	0.18	-0.13	+0.030
d	B	+0.2	0.18	-0.12	+0.060
2.4.3a(2)	C	-	-	-	-
b(2)	C	-	-	-	-
c(2)	C	-	-	-	-
d(2)	C	-	-	-	-
10.4.3a(3)	A	+0.455	0.24	-0.23	+0.04
b(3)	A	+0.460	0.24	-0.24	+0.00
c(3)	A	+0.480	0.25	-0.23	+0.06
d(3)	A	+0.495	0.25	-0.23	+0.09
10.4.3a(3)	B	+0.190	0.13	-0.12	+0.045
b(3)	B	+0.195	0.14	-0.12	+0.050
c(3)	B	+0.195	0.15	-0.12	+0.060
d(3)	B	+0.195	0.15	-0.12	+0.060
10.4.3a(3)	C	+0.195	0.24	-0.09	+0.005
b(3)	C	+0.195	0.23	-0.11	+0.000
c(3)	C	+0.195	0.24	-0.10	+0.010
d(3)	C	+0.185	0.26	-0.10	+0.020

TABLE XVIII (continued)

SUMMARY OF SYSTEM RESPONSE TO 10 ft/sec VELOCITY LANDING SHOCK

Case Number	Criterion	Maximum Displacement [First Peak] (in.)	Time to Read Zero Displacement* (sec)	Displacement at Second Peak (in.)	Displacement at Third Peak (in.)
80.6.3a	A	+0.470	0.16	-0.29	+0.09
b	A	+0.475	0.16	-0.27	+0.12
c	A	+0.420	0.17	-0.28	+0.12
d	A	+0.410	0.15	-0.27	+0.13
80.6.3a	B	+0.205	0.12	-0.14	+0.055
b	B	+0.180	0.12	-0.13	+0.055
c	B	+0.170	0.13	-0.11	+0.050
d	B	+0.140	0.12	-0.09	+0.055
80.6.3a	C	+0.195	0.16	-0.13	+0.045
b	C	+0.195	0.17	-0.12	+0.055
c	C	+0.195	0.18	-0.13	+0.060
d	C	+0.170	0.18	-0.11	+0.065
80.7.3a	A	+0.450	0.18	-0.30	+0.08
b	A	+0.395	0.19	-0.24	+0.08
c	A	+0.380	0.20	-0.26	+0.07
d	A	+0.375	0.20	-0.24	+0.10
80.7.3a	B	+0.19	0.12	-0.12	+0.050
b	B	+0.19	0.12	-0.12	+0.065
c	B	+0.19	0.12	-0.12	+0.060
d	B	+0.19	0.11	-0.11	+0.070
80.7.3a	C	+0.200	0.18	-0.12	+0.035
b	C	+0.180	0.17	-0.10	+0.035
c	C	+0.175	0.18	-0.11	+0.035
d	C	+0.170	0.18	-0.12	+0.035

TABLE XVIII (continued)

* Time at which displacement time history first crosses zero.

(1) Case 20.5.2 and 40.6.2 have response identical to case 10.4.2 since the blade passage frequency for all three cases is practically the same.

(2) Displacement feedback could not be reduced from the value used in Criterion B without resulting in either an unstable system or a very sluggish system response.

(3) Cases 20.5.3 and 40.6.3 have response identical to case 10.4.3 since the blade passage frequency for all three cases is practically the same.

FLOW AND POWER REQUIREMENTS

Figure 37 shows the instantaneous peak flow requirements for all systems considered as a function of the ratio of total helicopter weight to blade passage frequency. The required peak flow is proportional to the total weight of the helicopter and inversely proportional to the blade passage frequency [Equation (77)]. In order to minimize the flow requirements, the actuator is assumed to have unequal areas for the upper and lower chambers and is able to generate forces corresponding to +3g and -0.5g, respectively, based on a 500 psi supply pressure drop across each servovalve land and a 4,000 psi supply pressure. The curve shown on Figure 37 applies to peak flow values for both the two- and three-notch isolators. The flow requirements for the two-notch systems are approximately 3 percent lower than for the three-notch systems. Differences in system parameters based on the three performance criteria do not affect the flow requirements. As indicated in Figure 37, the peak flow requirements increase with increasing helicopter weight and decrease with increasing blade passage frequency.

In order to size the hydraulic power supply, the pump flow requirements are based on the rectified average of the instantaneous flow [Equation (79)]. Pump flow and power requirements are presented in Table XIX. The rectified average flow, identified as the maximum pump flow in Figure 38, is plotted versus gross weight and blade passage frequency. This equating of the rectified average flow to the maximum flow is justified since accumulators in hydraulic power units can account for instantaneous flow requirements exceeding the average. In the case of the servovalve, however, components must be selected on the basis of peak flow values, since the servovalve must be able to perform when the peak flow is required for proper operation.

Figure 39 shows the hydraulic power requirements as a function of helicopter weight and blade passage frequency for all systems considered, based on average pump flow. Comparing Equations (82) and (83), it can be seen that the two-notch isolator power requirements are only slightly lower than those for the three-notch isolator (less than 0.5 percent). As in the case of flow requirements, values shown on Figure 39 are based on nominal fuselage weights for each blade passage frequency. Increases in fuselage weight for a given blade passage frequency would result in proportionately larger values of both flow and power.

The operational amplifiers in the servoamplifier and the acceleration and relative displacements transducers require electrical power. The servoamplifier has built within it a dual tracking power supply of $\pm$ 15 volts and a maximum current output of 300 milliamps, which is sufficient to power all the electrical components of the isolation system. Electrical power must be supplied to the electronics power supply in the servoamplifier. This unit requires 115 volts $\pm$ 10% volts AC, 50 to 400 Hz at a power level of 28 watts (250 milliamps).

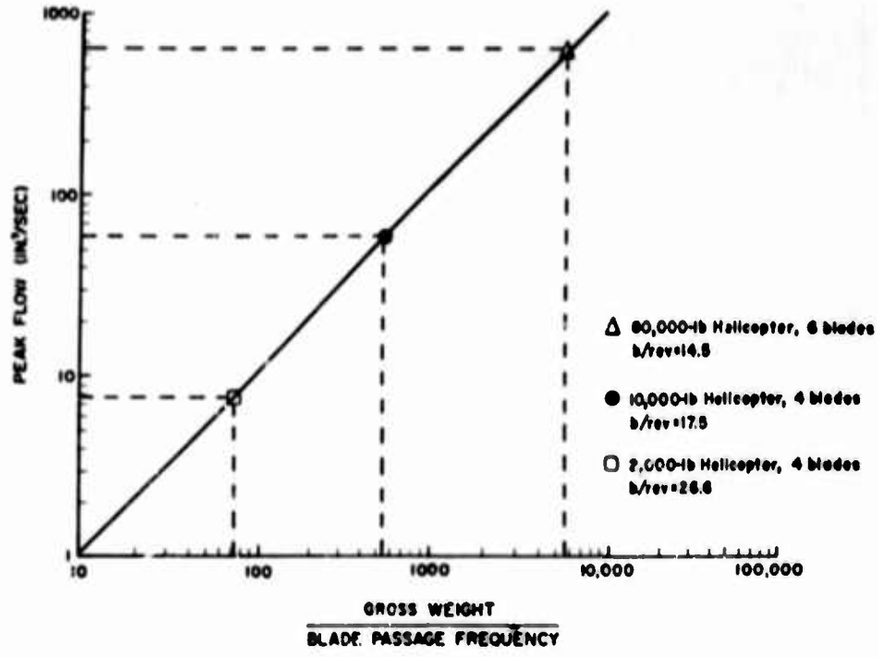

Figure 37. Relationship Between Instantaneous Peak Flow, Helicopter Gross Weight, and Blade Passage Frequency for Two- and Three-Notch Isolators.

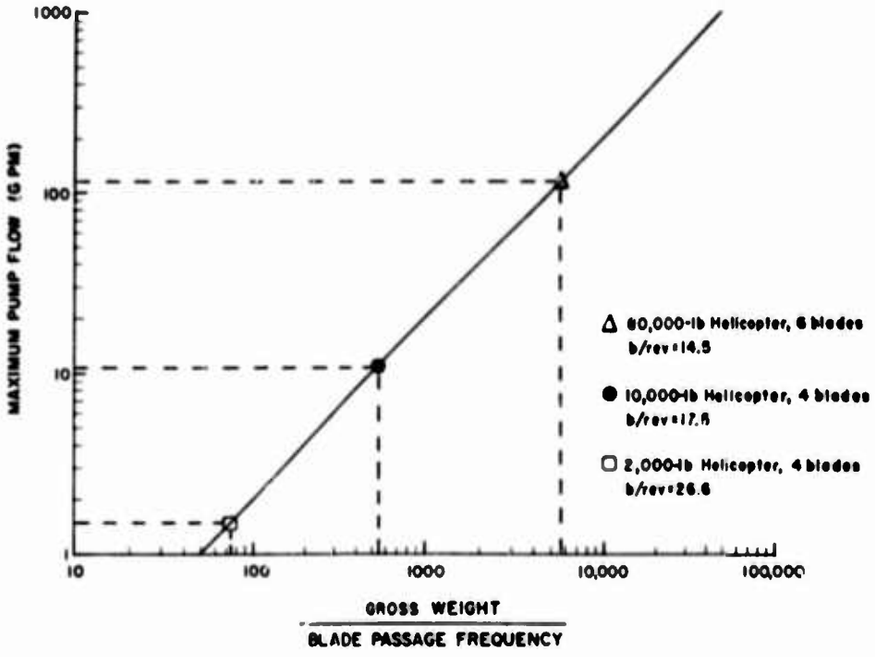

Figure 38. Relationship Between Maximum Pump Flow, Helicopter Gross Weight, and Blade Passage Frequency.

TABLE XIX

SUMMARY OF PUMP FLOW AND POWER REQUIREMENTS

Nominal Helicopter Gross Weight (lb)	Number of Blades b	Maximum Pump Flow*		Maximum Pump Power*	
		2-Notch System (gpm)	3-Notch System	2-Notch System (hp)	3-Notch System
2,000	2	3.94	3.94	9.18	9.19
2,000	4	1.96	1.96	4.59	4.59
10,000	4	14.95	14.96	34.88	34.92
20,000	5	29.67	29.95	69.22	69.64
40,000	6	59.84	59.88	139.62	139.75
80,000	6	144.51	144.81	337.18	337.40
80,000	7	124.74	124.81	291.03	291.21

* Based on 30% fuselage weight increase from nominal helicopter gross weight, and 4,000 psi supply pressure.

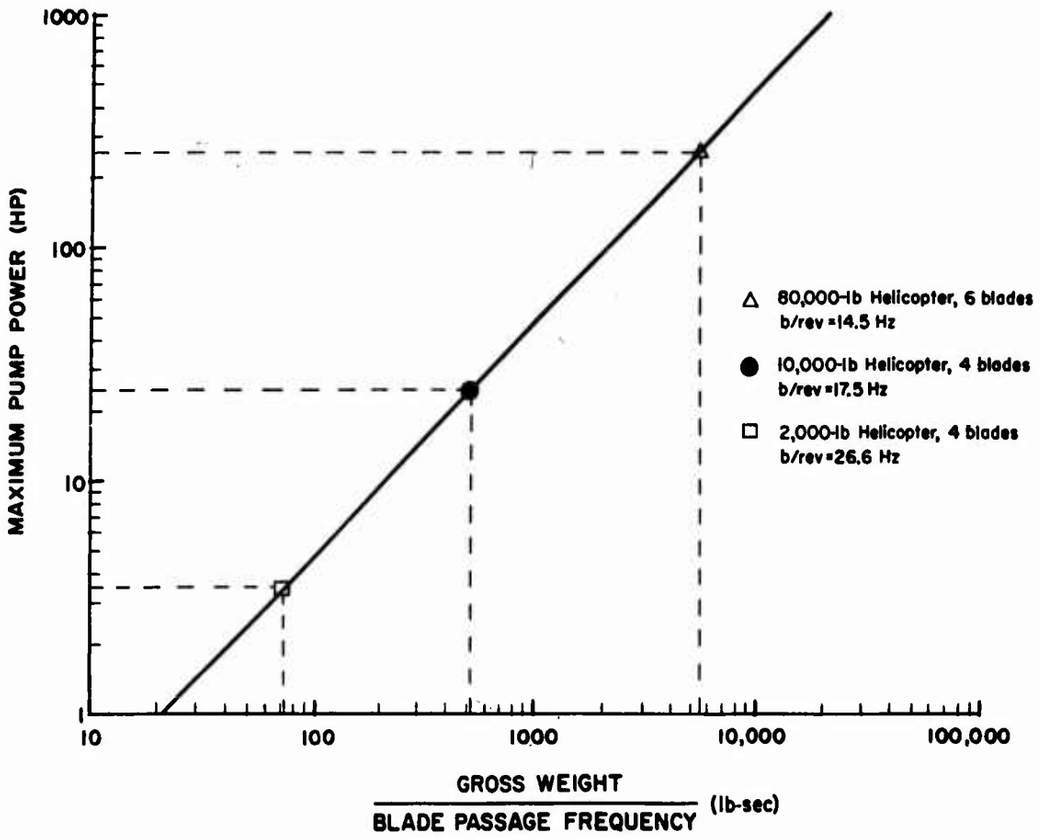

Figure 39. Relationship Between Maximum Pump Power, Helicopter Gross Weight, and Blade Passage Frequency.

ISOLATION SYSTEM WEIGHT

A conceptual design is shown in Figure 40 for incorporation of a two-notch isolator with a maximum relative displacement of 0.2 inch in the OH-6A helicopter. Estimates of isolation system weights are based on the isolator weight calculated for this aircraft. The rotor mast is hollow and the rotor shaft passes through it. The actuator is incorporated as part of the mast assembly. The rotor mast is attached to the hollow piston rod which in turn is connected to the helicopter fuselage by the hydrostatic pressures in the cylinder. In this manner the vertical vibratory forces normally transmitted to the fuselage through the rotor mast are isolated. The actuator shown has a stroke of $\pm$ 0.2 inch. The rotor shaft passes through the mast and hollow actuator rod, and is attached to the transmission by a spline that is assumed to transmit torque while allowing relative motion between the rotor and fuselage.

The gross weight of the OH-6A helicopter is 2,300 pounds. The blade passage frequency, based on a rotor speed of 470 rpm and four blades, is 31.3 Hz. For a two-notch isolator, the approximate system parameters are obtained from Figures 33 through 39 and are shown below.

Peak relative displacement during 3 g maneuver	0.04 in.
Peak rotor acceleration during landing (10 ft/sec)	6.5 g
Peak fuselage acceleration during landing (10 ft/sec)	5.8 g
Peak relative displacement during landing (10 ft/sec)	0.2 in.
Peak servovalve flow	7.5 $in.^3$/sec
Pump flow	1.6 gpm
Hydraulic power	3.5 HP
Notch bandwidth	4%

Table XX shows the estimated weights of the actuator and hydraulic and electronic components. The estimated total weight of the isolation system for the OH-6A helicopter is 87.45 pounds, or approximately 3.8 percent of the gross fuselage weight.

It is evident that each helicopter would require a different design for the incorporation of the type of isolation system discussed in this study, and that Figure 40 depicts only one of many possible approaches. However, in order to approximate the isolation system weight for the range of helicopters considered in the investigation, it is assumed that, having estimated the weight of the various components for one type of helicopter, the weight of other isolation systems can be calculated in terms of the characteristics and requirements defined in the investigation for each case.

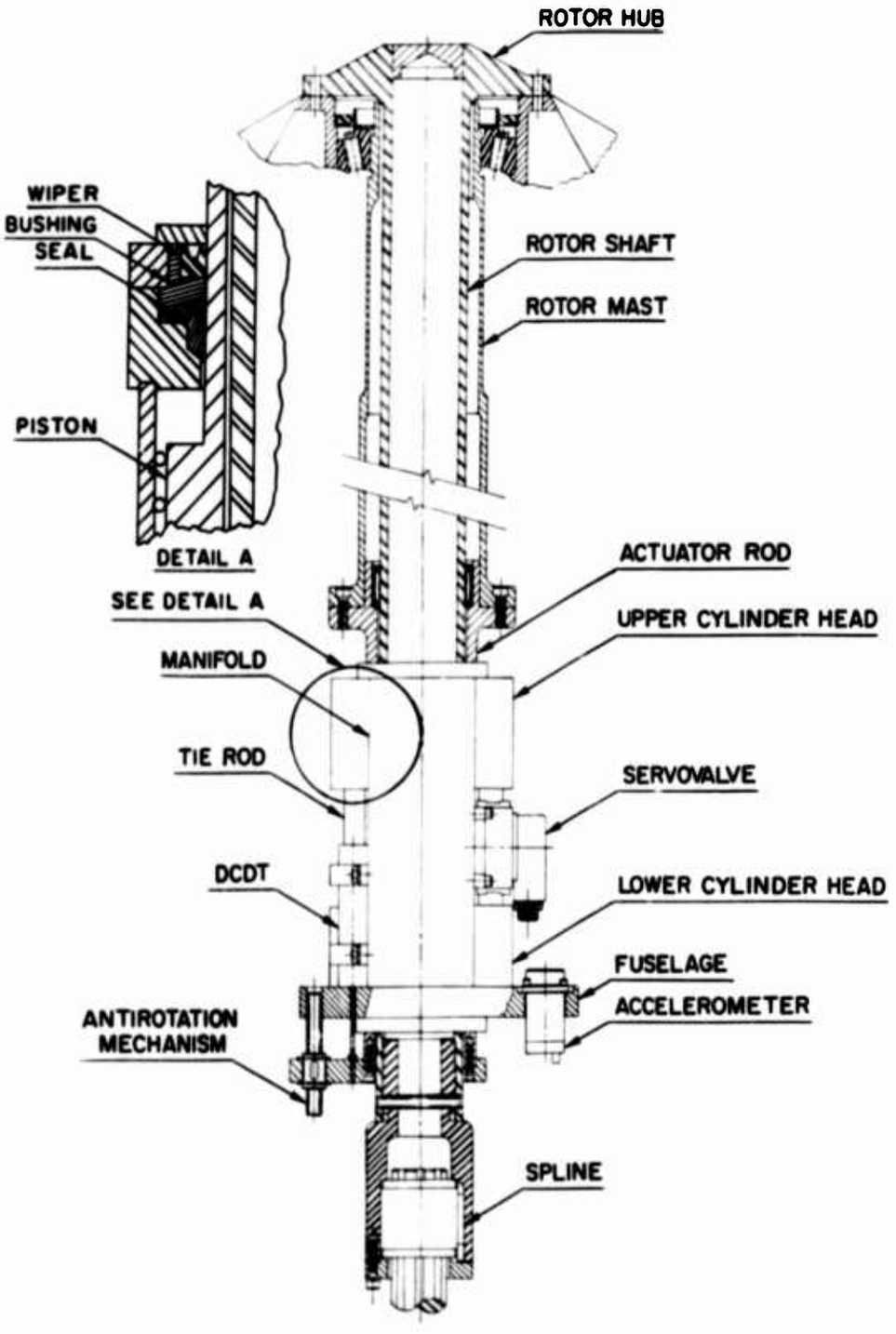

Figure 40. Conceptual Design For The Incorporation of Electrohydraulic Isolation System in OH-6A Helicopter.

TABLE XX

ISOLATOR WEIGHT FOR OH-6A

Component	Material	Weight (lb)
Actuator Rod	Steel	9.5
Top Cylinder Plate	Aluminum	1.7
Tie Rods	Steel	0.9
Top Cylinder Cap	Aluminum	2.8
Cylinder Tube	Steel	1.5
Piston	Aluminum	0.9
Bottom Cylinder Cap	Aluminum	2.8
Bottom Cylinder Plate	Steel	12.8
Servovalve Manifold	Aluminum	3.0
Servovalve		0.75
Accelerometer		0.5
Displacement Transducer		0.2
Antirotation Mechanism	Steel	1.0
Accumulator	Fiberglass	5.0
Oil in Cylinder		0.1
0.5 Gallon Oil		5.0
Hydraulic Tubing	Steel	7.0
Hydraulic Pump		20.0
Oil Filter		2.0
Heat Exchanger		5.0
Servoamplifier		5.0
Total Actuator Weight		37.75
Total Hydraulic Power Supply Weight		44.0
Total Weight of Electronics		5.7
	TOTAL WEIGHT	87.45

In order to estimate the weight of isolation systems for helicopters of different gross weights, it was assumed that the weight of the system components was a function of the following parameters:

Components	Weight Proportional To
Accelerometer	Constant
Displacement Transducer	Constant
Servoamplifier	Constant
Heat Exchanger	Power
Filter	Flow
Pump	Flow
Oil in Reservoir	Flow
Accumulator	Flow
Tubing	Flow
Servovalve	Number and Type of Valves
Manifold	Flow
Actuator and Rod	Average Actuator Area
Antirotation Mechanism	Average Actuator Area

Based on these assumptions and the estimated weight for the OH-6A helicopter, isolation system weights for the various helicopters considered in the investigation were calculated and are shown in Table XXI. Figure 41 shows the estimated isolation system weight, in percent of helicopter gross weight, plotted against blade passage frequency.

These weight estimates do not necessarily represent the net increase in total helicopter gross weight associated with the introduction of electrohydraulic systems for the isolation of rotor-induced forces. In most instances, the linkages required to operate the rotor collective and cyclic pitch controls may have to be redesigned, and could introduce an additional weight increase. However, reduction of the vertical vibratory acceleration transmitted to the fuselage would generally eliminate the need of vibration isolators inside the fuselage used at the present time to protect critical equipment and/or crew. A considerable reduction in weight would be achieved by eliminating the present practice of using dynamic vibration absorbers. For example, four 175-lb dynamic absorbers are used to reduce the high level of acceleration experienced at the pilot and copilot stations of the CH-46A helicopter (gross weight 20,000 lbs) (Reference 3). Therefore, it is possible that the use of active notch isolation systems could result in no net increase or even a net decrease in gross fuselage weight, depending on the particular design.

TABLE XXI
SUMMARY OF ESTIMATED ISOLATION SYSTEM WEIGHT

Helicopter Gross Weight (lb):	2,000	2,000	10,000	20,000	40,000	80,000	80,000
Blade Passage Frequency (Hz):	13.3	26.6	17.5	17.9	17.7	14.5	16.9
Accelerometer	0.5	0.5	0.5	0.5	0.5	0.5	0.5
DCDT	0.2	0.2	0.2	0.2	0.2	0.2	0.2
Servoamplifier	5	5	5	5	5	5	5
Heat Exchanger	10	5	19	38	71	173.5	158
Filter	4	2	7.5	15	30	72	62
Pump	20	20	75	150	300	700	600
Oil Reservoir	10	5	37.5	75	150	360	312
Accumulator	10	5	37.5	75	150	360	312
Tubing	14	7	26.25	52.5	105	255	217.5
Servovalve	0.75	0.75	2.25	4.5	10	22.5	20.5
Manifold	6	3	11.25	22.5	45	108	93.5
Actuator and Rod	33	33	248	495	990	2,060	2,060
Antirotation	1	1	5	10	20	40	40
ISOLATION SYSTEM WEIGHT (lb):	114.45	87.45	474.95	943.2	1,876.7	4,156.7	3,881.2
% GROSS WEIGHT:	5.72	4.37	4.75	4.71	4.69	5.39	4.85

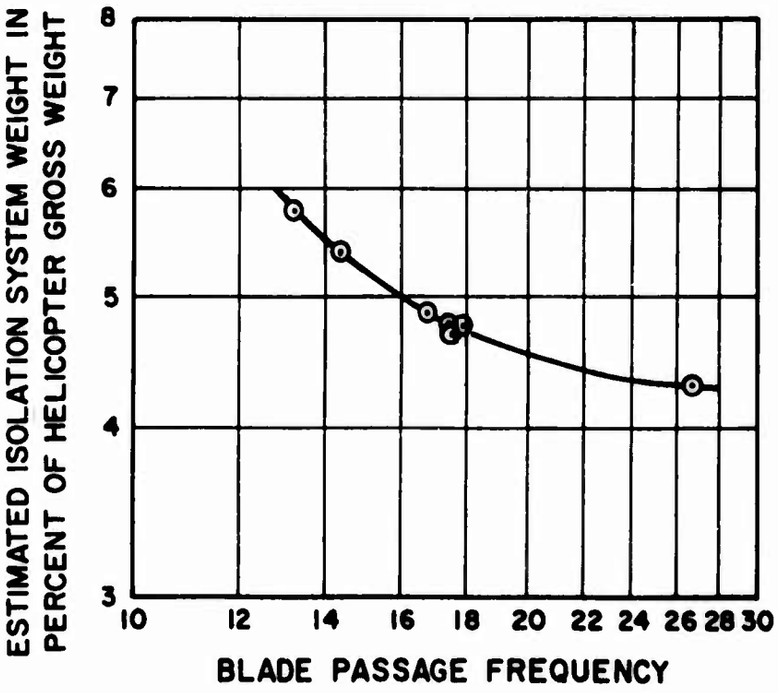

Figure 41. Relationship Between Estimated Isolation System Weight and Blade Passage Frequency.

RELIABILITY, FAIL-SAFE AND CRASH LOAD CONSIDERATIONS

RELIABILITY AND MAINTAINABILITY

The solid-state operational amplifiers within the servoamplifier are protected inst overload, supply voltages other than specified, and reversed supply tage polarity. The interconnecting electrical components such as wiring, resistors and capacitors are mounted on circuit boards and potted to provide protection from moisture. dirt and mechanical vibration. Thus, the reliability of the components within the servoamplifier is high. Based on Barry Controls' experience, such systems have been tested under vibratory excitation conditions for periods as long as 1,500 hours without any electrical failures. The only maintenance required for the servoamplifier is an occasional calibration to compensate for a gradual change of component characteristics with age. Such a calibration normally would entail the readjustment of a few potentiometers and should not be required more frequently than every 1,000 hours of operation.

The relative displacement transducer is a linear variable differential transformer with built-in exciter carrier oscillator and phase sensitive demodulator systems. A unit of this type manufactured by Sanborn and known as a DCDT has been used in one of Barry Controls active isolation systems. The unit was subjected to long periods of vibration at levels of 10 g or more. At no time was there any indication of a malfunction or failure of the system. However, it was observed that exposure of the unit to strong magnetic fields did result in output error, but without permanent damage.

The acceleration transducer can be either a servoaccelerometer or a piezoelectric accelerometer. The servoaccelerometer has better sensitivity and resolution and would lead to a slightly higher effectiveness of the system than the piezoelectric accelerometer. However, Barry Controls' experience with servoaccelerometers has encountered several failures due to both mechanical overload and internal electrical failures of the unit. It is desirable to use the very reliable piezoelectric accelerometer and sacrifice a small amount of peak notch effectiveness. Normally, maintenance should not be required for the displacement and acceleration transducers.

The hydraulic power supply consists of a variable flow-pressure compensated pump, oil reservoir, heat exchanger, filter, and accumulator. Power supply systems are very reliable and have service time intervals of about 1,500 hours. The normal maintenance of the power supply is the changing of the hydraulic oil and filter and the replacement of worn parts of the pump.

The actuator and servovalve should not require major maintenance for at least 1,000 hours of operation. However, because of the continuous rapid motion of the actuator, the rod seals will require more frequent maintenance.

FAIL-SAFE REQUIREMENTS

The failure characteristics of the various components are discussed in the following paragraphs. Failure of components can result in an unstable condition for the control system, causing severe oscillations of the actuator at one of the notch frequencies; either damage to the isolation system or loss of aircraft control would occur. Since failure of the system would result in larger fuselage vibration levels at the notch frequencies, a fail-safe circuit is incorporated in the isolator design to detect the increase in fuselage acceleration and activate a relay such that the power to the servoamplifier and the hydraulic fluid supply are automatically shut down.

The fail-safe circuit consists of a separate accelerometer to detect the fuselage vibration, a high-pass filter to filter out the large amplitude low-frequency accelerations resulting from transient excitations, a rectifier and passive integrator to determine the time-averaged vibration level, and a relay to shut down the isolation system. The rectified acceleration signal would be integrated over a time constant of a few seconds, thereby giving a voltage proportional to the time-averaged acceleration level on the fuselage. Therefore, since the integrator operates on a time-averaged basis, the presence of a large high frequency vibration level will quickly activate the shut down relay. Lower acceleration levels will require a longer time to actuate the relay. Consequently, acceleration levels near those of normal system operation will not activate the fail-safe circuit.

The following paragraphs discuss the effect on system performance caused by failure of various components and the manner in which the fail-safe circuit is activated in each instance.

Hydraulic Power Failure

The loss of hydraulic pressure will stop the system from functioning. The actuator will move slowly until it bottoms wherein the weight of the fuselage will be carried by the piston in contact with the upper cylinder block. This condition will remain as long as the rotor acceleration, based on the total helicopter gross weight, does not exceed -1 g. The system in this state will be operating without vibration isolation and with a sustained relative deflection equal to one-half the total stroke of the actuator. This condition, however, should not constitute any serious hazard since helicopters operate today without vibration isolation, and the sustained relative deflection would be within the design limits of linkages controlling the rotor cyclic and collective pitch.

Accelerometer Failure

The failure of the accelerometer in the acceleration feedback loop will remove the acceleration feedback signal from the loop. Thus, the only remaining feedback signal will be that from the relative displacement transducer. With only displacement feedback the system becomes a displacement servo offering no vibration isolation and positioning the actuator at its null position regardless of the forces acting on the rotor.

Displacement Transducer Failure

The loss of the displacement feedback signal would result in a system having acceleration feedback only. Such a system configuration leads to drifting of the actuator until the piston engages either the top or bottom cylinder block. The system would then chatter and bounce off the stroke limit position. Continued operation under these conditions could result in permanent damage to the actuator. However, such a condition will activate the automatic fail-safe circuit described above.

Failure of Electronics in Acceleration Loop

Failure of the electronics in the acceleration loop can occur in one of two possible modes. The first is the loss of gain resulting from a failure of an operational amplifier, resistor or capacitor. A failure of this type would be similar to that described above for the loss of the acceleration feedback signal. The second mode of failure is that of an increased gain in the acceleration feedback loop. This change, if not too large, would result in a system offering broader bandwidth of isolation and excessive transient relative deflections. Very large increases of gain could cause the system to become unstable and oscillate at a frequency near that of the highest notch frequency. Oscillations of this nature are generally not too severe, but would be very noticeable and would activate the fail-safe circuit described above.

Failure of Electronics in Displacement Loop

Failure of the electronics in the displacement loop can occur in one of two possible modes. The first is the loss of gain resulting from a failure of an operational amplifier or a resistor. This type of failure would be similar to the loss of the acceleration signal described above. The second mode is that of an increased gain in the displacement feedback loop. This type of failure would result in a system response having narrower bandwidths of isolation and decreased transient relative deflections. If the gain increase is extremely large, the system can become unstable and oscillate at a frequency near the first notch frequency. The magnitudes of such oscillations are generally large, and the servovalve will saturate. Such oscillations would activate the fail-safe circuit previously described.

Failure of the Electronics in the Frequency Tracking Network

The failure of the tracking network would mean that the notch frequency does not equal the blade passage frequency. Under these conditions the fuselage acceleration will increase, and thereby the fail-safe circuit will be activated.

Electronic Power Supply Failure

The failure of the electronic power supply would essentially shut down the system and would be similar to the loss of hydraulic power described above.

Servovalve Failure

There are three possible modes of servovalve failure. The first mode of failure results from normal wear of the servovalve spool and flapper nozzles. This condition will lower the valve gain and frequency response, resulting in a system having narrower notch bandwidths and a smaller gain margin. This type of failure is difficult to detect during normal operation and would generally be indicated only by a frequency response test performed on the system.

The second mode of failure results when one of the pilot valve nozzles becomes clogged with dirt because of improper system maintenance. Under this condition the valve will not operate properly and the system will perform erratically, sometimes operating well and at other times not operating at all, resulting in excessive fuselage accelerations.

The third mode of failure of the servovalve results from the opening of one of the two coils of the torque motor in the first stage of the valve. For this condition the valve spool will open fully in one direction, causing the actuator to move to one of its extreme positions and remain there.

Whenever any of these failure modes result in excessive fuselage acceleration, the fail-safe circuit will be activated and the system will automatically shut down.

CRASH LOAD CONSIDERATIONS

There are two primary design recommendations for the crash safety of a helicopter having an electrohydraulic vibration isolation system. The first is to rapidly reduce the hydraulic pressure of the system so that, in the event of pressure buildup, high pressure oil is dumped into the reservoir. An acceleration actuated mechanical pressure relief valve is inserted in the oil supply line just after the hydraulic pump, such that upon extremely severe impact the resulting large acceleration values would open the relief valve and very rapidly dump the high pressure oil into the reservoir.

The second concern is to insure that the actuator does not fail, such that the rotor becomes detached and crashes down upon the fuselage. During severe crash landings the rotor mass will tend to drive the actuator rod down toward the fuselage. The hydraulic oil in the actuator will initially resist this movement. However, accelerations of the rotor greater than 30 g will cause the servovalve and manifold to rupture due to the extreme buildup of pressure above 8,000 psi. The actuator rod, however, is still retained by the upper and lower cylinder blocks, and the piston and upper flange on the actuator rod will prevent further travel of the rotor shaft into the fuselage.

CONCLUSIONS

Based on the results of the analyses and parametric study for the two- and three-notch isolation systems involving helicopters ranging in weight from 2,000 to 8,000 pounds, the following conclusions are made:

1. Stable active isolation systems can be designed to provide virtually 100 percent isolation from the helicopter rotor-induced vertical vibrations at the blade passage frequency and higher harmonics. Vibration isolation is also provided during combined vibratory and transient excitations, such as can be expected during transition from one flight mode to another.

2. The number of notches of isolation that can be provided at the blade passage frequency and harmonics thereof is limited by system stability requirements. For helicopters having blade passage frequencies higher than 20 Hz only up to 3 notches can be provided. However, for lower blade passage frequencies a larger number of notches could be incorporated in the system.

3. System parameters can be selected such that the relative displacement between rotor and fuselage under 10 ft/sec landing velocity is 0.2 inch or less in all cases. For lower values of sink speeds, the relative displacements would be proportionately reduced.

4. During in-flight maneuvers, the maximum relative displacements between rotor and fuselage are functions of the number of g's experienced, the weight of the helicopter, and the blade passage frequency. For system parameters yielding a maximum relative displacement of 0.2 inch under 10 ft/sec landing velocity, the relative displacement under the maximum expected maneuver loads of 3 g's is less than 0.15 inch for all cases. For maneuvers involving a lower number of g's, displacements would be less.

5. For the range of helicopter gross weights and blade passage frequencies considered, estimated isolator system weights are 4 to 6 percent of vehicle gross weight.

6. Based on power requirements, number of servovalves, and isolation system weight, the selected approach appears to be feasible for single-rotor helicopters weighing up to 40,000 pounds.

7. The two- and three-notch active isolation systems described in this investigation can best be incorporated into new helicopter rotor configurations since undoubtedly design problems would be encountered in adapting the approach to an existing rotor. Nevertheless, the results of the analysis indicate that the vertical vibration and displacement control provided by a multinotch electrohydraulic isolation system may surpass those attained with any other type of system reported on to date.

RECOMMENDATIONS

In order to prove experimentally the ability to design a system which would encompass the various components described in this study, and eventually to investigate rotor-induced forces in other directions, it is recommended that an experimental laboratory model study be undertaken.

The proposed isolation system requires that a hydraulic cylinder be introduced in series with the rotor shaft. Although various schemes can be devised to incorporate the cylinder in an existing rotor assembly (schemes which must consider space and functional requirements of rotor assembly components), a common requirement is that the actuator must be capable of transmitting torque from the engine and transmission to the rotor and allowing relative displacements between the rotor and fuselage, while rotating at the required rotor speed. Conventional actuators are not normally subjected to this type of loading, and the effects of the combined translational and rotational motions on the actuator performance should be determined.

In addition, the compensation and notch-generating circuits have been defined on the basis of analog and digital computer studies. The simulation employed in the parametric feasibility study does not include the exact dynamic characteristics of components such as servovalve, accelerometers, cylinder resonances, etc. Primarily, low frequency dynamic characteristics of the various components were simulated since the active hydraulic isolation system basically responds as a low frequency device. In general, it is not practical to attempt to exactly simulate the higher frequency characteristics in an analog computer since they can only be defined by testing of actual hardware. As in all control applications, final definition of the required compensations must be based on the experimentally defined dynamic characteristics of the hardware to be used.

Consequently, the next logical step in the development of a practical hardware solution to the rotor isolation problem should involve the performance of laboratory model experiments in preparation for eventual full-scale performance evaluation of the isolation technique.

In addition, further analytical consideration should be given to isolation of in-plane rotor excitations. Although in-plane excitations are generally lower in magnitude than the vertical, they are nevertheless present, and would become the more significant ones, and perhaps even increase, once the vertical vibration levels are reduced as shown. Finally, future analyses should include isolation of combined vertical and in-plane rotor-induced vibrations and the effects of fuselage and rotor impedance on system response.

REFERENCES

1. Brandt, D. E., "Vibration Control in Rotary-Winged Aircraft," Proceedings of AGARD Technical Meeting, January 10-14, 1966, Paris, France, AD 805752.

2. Payne, P. R., Helicopter Dynamics and Aerodynamics, MacMillan, 1959.

3. Anon., "CH-46 A Marine Assault Helicopter Vibration Study, "Boeing Report 107 M-D-09, Contract NOw 62-0177f, Boeing, Vertol Division, Morton, Pa., April 1965.

4. Shaw, J., "A Feasibility Study of Helicopter Vibration Reduction by Self-Optimizing Higher Harmonic Blade Pitch Control," Master of Science Thesis, Massachusetts Institute of Technology, June 1967.

5. Schuett, E. P., "Helicopter Excitation Criteria, "Research Note 67-3, Kaman Aircraft, Bloomfield, Conn., March 1967.

6. Theobald, C. E., Jr., and Jones, R., "Isolation of Helicopter Rotor Vibratory Forces from the Fuselage," Air Force Report WADC TR 57-104, September 1957, AD 130991.

7. Crede, C. E., Cavanaugh, R. D., and Abramson, H. N., "Feasibility Study on Active Vibration Isolator for a Helicopter Rotor," Air Force Report WADC TR 58-103, March 1958.

8. Smollen, L. E., Marshal, P., and Gabel, R., "A Servo Controlled Rotor Vibration Isolation System for the Reduction of Helicopter Vibration," Institute of Aerospace Sciences, IAS Paper No. 62-34, 1962.

9. Calcaterra, P. C., "Performance Characteristics of Active Systems for Low Frequency Vibration Isolation," SM Thesis, MIT, May 1967.

10. Pepi, J. S., "Vibration Isolation of Optical Aerial Reconnaissance Sensors, "Air Force Report AFAL-TR-67-277, October 1967.

11. Ruzicka, J. E., "Active Vibration and Shock Isolation," SAE Paper No. 680747, 1968.

12. Calcaterra, P. C., and Schubert, D. W., "Research on Active Vibration Isolation Techniques for Aircraft Pilot Protection," Air Force Report AMRL-TR-67-138, October 1967.

13. D'Azzo, T. T., and Houpis, C. H., Feedback Control System Analysis and Synthesis, Second Edition, McGraw Hill, 1966.

14. Hildebrand, F. B., Advanced Calculus for Applications, Chapter 5, Prentice-Hall, 1963.

15. Scheiman, J., "A Tabulation of Helicopter Rotor Blade Differential Pressure, Stresses, and Motions as Measured in Flight," NASA TMX-952, Langley Field, March 1964.

16. Edenborough, H. K., "Control and Maneuver Requirements for Armed Helicopters," Twentietn Annual Forum, American Helicopter Society, Washington, D. C., May 1964.

APPENDIX

FREQUENCY TRACKING CIRCUITS

The active hydraulic isolation system with the notch-producing compensators can provide virtually 100 percent isolation at the notch frequencies, and at the same time limit the transient relative deflections to tolerable values. However, the isolation system can only be effective in reducing the fuselage vibration levels if the system notch frequencies are equal to the frequencies of excitation induced by the rotor.

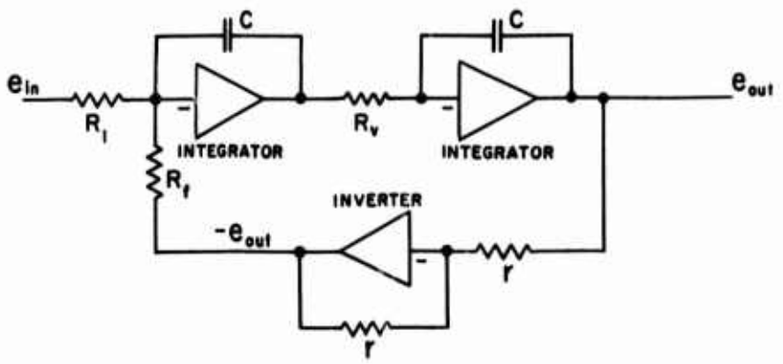

Figure 42. Active Electronic Notch Oscillator Circuit.

Figure 42 shows a notch compensator circuit without any provisions for tracking. The circuit consists of two active integrators utilizing operational amplifiers with capacitive feedback and one inverting operational amplifier having a gain of unity. The transfer function of this circuit is the ratio of the transform of the output voltage to the transform of the input voltage, and is given by

$$\frac{e_{out}(s)}{e_{IN}(s)} = \frac{R_f / R_i}{1 + R_f R_i (Cs)^2} \tag{87}$$

Symbols used in this appendix are defined in the nomenclature.

The resonant frequency of the circuit and the resulting system notch frequency is given by the relation

$$\omega_n = \sqrt{\frac{1}{R_f R_v C^2}} \tag{88}$$

The function of a tracking network is to change one of the parameters governing the circuit resonant frequency ω_n. However, the parameter change must be such that the static gain of the circuit R_f/R_i remains unchanged, since it is primarily this gain value that determines the transient behavior of the system. Examination of the circuit transfer function and resonant frequency equations indicates that the only circuit parameter that will change the frequency, and not the gain, is the resistance value R_v.

The most direct manner to construct the tracking circuit is to sense the excitation frequency using a tachometer or a frequency discriminator that gives a DC voltage proportional to the excitation frequency (blade passage frequency). Then the effective value of R_v may be changed in a manner proportional to the square of the voltage from the frequency detector by using two multipliers as shown on Figure 43.

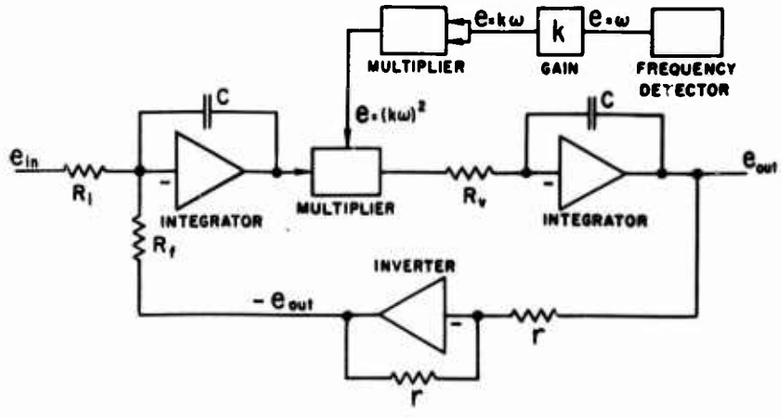

Figure 43. Active Electronic Notch Oscillator Circuit With Frequency Tracking Element.

The transfer function of the circuit of Figure 43 is shown below, where the value of the resistance R_v is a function of $(k\omega_n)^2$:

$$\frac{e_{out}(s)}{e_{in}(s)} = \frac{\frac{R_f}{R_i}}{1 + \frac{R_v}{(k\omega)^2} R_f (Cs)^2} \qquad (89)$$

The resonant frequency of the circuit is determined from Equation (89).

$$\omega_n = \omega \sqrt{\frac{K^2}{R_v R_f C^2}} \qquad (90)$$

Then, if the gain k is adjusted such that $k^2 = R_v R_f C^2$, the notch frequency ω_n will equal the excitation frequency ω. Thus, the isolator will track the excitation frequency and the resulting transmissibility will always be near zero regardless of the frequency of the excitation. The range over which the network tracks the rotor speed should be limited to a low frequency ω_L and to a high frequency ω_H, in order to prevent possible unstable conditions where the notch frequencies become either too high or too low.

Applying this tracking technique to the helicopter notch isolation system requires the use of two multipliers in each notch circuit and a single frequency detector, such as a tachometer, to sense the blade passage frequency and set the notch frequency of each oscillator.

The function of a tracking network is to change one of the parameters governing the circuit resonant frequency ω_n. However, the parameter change must be such that the static gain of the circuit R_f / R_i remains unchanged, since it is primarily this gain value that determines the transient behavior of the system. Examination of the circuit transfer function and resonant frequency equations indicates that the only circuit parameter that will change the frequency, and not the gain, is the resistance value R_v.

The most direct manner to construct the tracking circuit is to sense the excitation frequency using a tachometer or a frequency discriminator that gives a DC voltage proportional to the excitation frequency (blade passage frequency). Then the effective value of R_v may be changed in a manner proportional to the square of the voltage from the frequency detector by using two multipliers as shown on Figure 43.

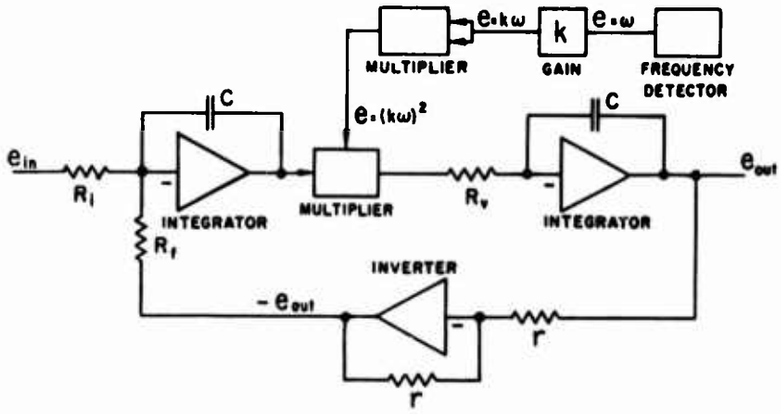

Figure 43. Active Electronic Notch Oscillator Circuit With Frequency Tracking Element.

The transfer function of the circuit of Figure 43 is shown below, where the value of the resistance R_v is a function of $(k\omega_n)^2$:

$$\frac{e_{out}(s)}{e_{in}(s)} = \frac{\frac{R_f}{R_i}}{1 + \frac{R_v}{(K\omega)^2} R_f (Cs)^2} \tag{89}$$

The resonant frequency of the circuit is determined from Equation (89).

$$\omega_n = \omega \sqrt{\frac{K^2}{R_v R_f C^2}} \tag{90}$$

Then, if the gain k is adjusted such that $k^2 = R_v R_f C^2$, the notch frequency ω_n will equal the excitation frequency ω. Thus, the isolator will track the excitation frequency and the resulting transmissibility will always be near zero regardless of the frequency of the excitation. The range over which the network tracks the rotor speed should be limited to a low frequency ω_L and to a high frequency ω_H, in order to prevent possible unstable conditions where the notch frequencies become either too high or too low.

Applying this tracking technique to the helicopter notch isolation system requires the use of two multipliers in each notch circuit and a single frequency detector, such as a tachometer, to sense the blade passage frequency and set the notch frequency of each oscillator.

Unclassified

Security Classification

DOCUMENT CONTROL DATA - R & D

(Security classification of title, body of abstract and indexing annotation must be entered when the overall report is classified)

1. ORIGINATING ACTIVITY (Corporate author)	2a. REPORT SECURITY CLASSIFICATION
Barry Controls Division Barry Wright Corporation Watertown, Massachusetts	Unclassified 2b. GROUP

3. REPORT TITLE

ISOLATION OF HELICOPTER ROTOR-INDUCED VIBRATIONS USING ACTIVE ELEMENTS

4. DESCRIPTIVE NOTES (Type of report and inclusive dates)

Final Report

5. AUTHOR(S) (First name, middle initial, last name)

Peter C. Calcaterra
Dale W. Schubert

6. REPORT DATE	7a. TOTAL NO. OF PAGES	7b. NO. OF REFS
June 1969	170	16

8a. CONTRACT OR GRANT NO.	9a. ORIGINATOR'S REPORT NUMBER(S)
DA 44-177-AMC-472(T) b. PROJECT NO. Task 1F125901A13903 c. d.	USAAVLABS Technical Report 69-8 9b. OTHER REPORT NO(S) (Any other numbers that may be assigned this report) R&D Report No. 128

10. DISTRIBUTION STATEMENT

This document is subject to special export controls and each transmittal to foreign governments or foreign nationals may be made only with prior approval of US Army Aviation Materiel Laboratories, Fort Eustis, Virginia 23604.

11. SUPPLEMENTARY NOTES	12. SPONSORING MILITARY ACTIVITY
	US Army Aviation Materiel Laboratories Fort Eustis, Virginia

13. ABSTRACT

Results of an analytical investigation of the feasibility of isolating helicopter fuselages from rotor-induced vertical vibratory forces while limiting the relative displacements during transient maneuvers and landing are presented. Electrohydraulic elements are combined to provide better than 90 percent isolation at the critical rotor frequencies. System parameters are selected for single-rotor helicopters ranging in weight from 2,000 to 80,000 pounds. Results of the parametric study show the response of the electrohydraulic notch isolation systems to the various types of dynamic excitations in terms of rotor and fuselage transmitted accelerations, relative displacement between the rotor and fuselage, stability margin, power requirements, and estimated isolation system weight. System performance and requirements are evaluated as a function of helicopter weight, blade passage frequency, number of notches of isolation, stability, changes in fuselage weight and rotor speed, and maximum allowable relative displacement during landing. Recommendations are made regarding experimental verification of system performance, incorporation of approach into practical hardware, and isolation of combined vertical and in-plane rotor-induced vibrations.

DD FORM 1 NOV 68 1473 REPLACES DD FORM 1473, 1 JAN 64, WHICH IS OBSOLETE FOR ARMY USE.

Unclassified

Security Classification

14. KEY WORDS	LINK A		LINK B		LINK C	
	ROLE	WT	ROLE	WT	ROLE	WT
Rotor-Induced Vibrations						
Active Systems						
Vibration Isolation						
Helicopter						